Doctoral degree dissertation

Biological methane production from electricity without organic substrates

(無機環境下での電気エネルギーからの生物学的メタン生成)

by

DINH THI THU HA

in partial fulfilment of the requirements for the degree of Doctor of Engineering
in Civil and Environmental Engineering

Environmental Preservation Engineering Laboratory
Department of Civil and Environmental Engineering
Graduate School of and Engineering, Hiroshima University

Hiroshima Japan, September 2021

Biological methane production from electricity without organic substrates

Promotor: Professor Akiyoshi OHASHI
Graduate School of Engineering, Hiroshima University

Committee: Professor Akiyoshi OHASHI
Graduate School of Engineering, Hiroshima University

Professor Toshirou HATA
Graduate School of Engineering, Hiroshima University

Associate Professor Noriatsu OZAKI
Graduate School of Engineering, Hiroshima University

Associate Professor Tomonori KINDAICHI
Graduate School of Engineering, Hiroshima University

Associate Professor Yoshiteru AOI
Graduate School of Integrated Sciences for Life, Hiroshima University

Acknowledgements

Throughout the writing of this dissertation, I have received a great deal of support and assistance.

I would first like to sincerely thank my supervisor, Professor Akiyoshi Ohashi, who gave me support through each stage of the research process. Your strict guidance and insightful feedback pushed me to sharpen my thinking and brough my study to a higher level.

I would also like to thank Associate Professor Noriatsu Ozaki, Associate Professor Tomonori Kindaichi, Associate Professor Yoshiteru Aoi and Assistant Professor Amin Mojiri for their advices and valuable comments. I want also to thank all lab mates and Ms. Oyama from Environmental Preservation Engineering, who provided me wonderful collaboration and inspirations.

I would like to acknowledge Ministry of Education, Culture, Sports, Science and Technology (MEXT) of Japan for providing PhD scholarships. I thank to all staff from Engineering Student Support Group for their guidance and support during my Ph.D. program course.

In addition, I would like to thank my Vietnamese and foreign friends for their kindness and moral support during my study in Hiroshima University. Thank you so much for the friendship and memories. All the best for a bright future!

I would particularly like to thank my big family from Vietnam: my parents for their wise counsel and sympathetic ear; my siblings for their support and motivation. You are always there for me. Finally, I could not have completed this dissertation without the big support of my husband and my cutest daughter, who provided happy distractions to rest my mind outside of my research.

Contents

Chapter

1

General Introduction

1. Background

Recently, global energy consumption significantly grew, spurred by the sustained economic and population growth. Although we have added more clean energy sources in the past 45 years, more than 80% of global energy supply relies on depletable fossil fuel (Vinson *et al.*, 2017). The resources of fossil fuel are being unevenly distributed across world regions, and new reserves are becoming harder to find, creating significant energy security challenges. Methane, the main component of natural gas, is utilized as an efficient energy source in home and industries. On contrary, methane is also a toxic greenhouse gas. Studies show that methane is 84 times more dangerous compared to carbon dioxide in short term, negatively contributing to the climate change (Myhre *et al.*, 2014). Beside of methane production from human sources such as fossil fuel production or livestock farming, methane is released into the atmosphere by natural process (Bousquet *et al.*, 2006). Until now, the main natural sources mainly include wetlands, terminates and the oceans, significantly contributing for the total methane emission. To add the globe energy sources and decrease the environmental impacts of methane, one of most important things is to find the pathways for the methane production in natural environment.

Methane may be classified based on how it is produced, by either thermogenic or microbial processes, together contributing to 20%–80% of natural gas reserves (Rice and Claypool, 1981). Thermogenic methane is formed when organic matter is buried and heated, usually at considerable depths over long periods of time, and includes methane associated with coal, gas, and oil formations (Schoell, 1988). Thermogenesis also produces longer chain hydrocarbon gases such as ethane, propane, butane, and pentane, and the methane is heavier isotopically because of the extended time, heat, and pressure hydrocarbons undergo in the thermogenic process. Conversely, biological methane forms at shallower depths by the actions of methanogenic bacteria on organic matter in anoxic environments that include wetlands, landfills, and some aquifer sediments (Zinder, 1993; Stams *et al.*, 2006; Deppenmeier and Müller, 2008). Methanogens use substrates such as acetate, formate, and hydrogen gas produced from organic matter during fermentation. Such methane fermentation occurs in nature but has also been applied as an eco-friendly wastewater treatment technology (Onodera, 2013; Townsend-Small *et al.*, 2016). The artificially produced biogas, mainly composed of methane, can also be utilized as an energy source after purification.

Organic loading is clearly critical factor in the above two dominant processes that generate methane in nature. Likewise, natural gas and methane hydrate-submarine source that has been attracting attention in recent years, are also due to the decomposition of fossil derived organic matter by methanogens (Alexei *et al.*, 2005). However, Christner *et al.* (2014) confirmed that aquatic environments beneath the Antarctic ice sheet support viable microbial ecosystems, they contain globally relevant pools of carbon and microbes. It leads to the possibility of methane production under no organic matter condition, which is different from the conventional methanogenesis. Additionally, based on thermodynamic calculations, methane could be produced through carbon dioxide reduction at a voltage of 0.169 V under standard conditions, or −0.244 V under more biologically relevant conditions at a pH=7. A methane-producing microbial electrosynthesis system (MES) is a technology to convert CO_2 into methane, using electricity as an energy source and microorganisms as the catalyst (Cheng *et al.*, 2009; Zhen *et al.*, 2015; Gomez Vidales *et al.*, 2019). Therefore, methanogens may be catalyzed to produce methane from CO_2 by using electrical energy without organic matter.

Deep-sea hydrothermal vents are hot springs on the seafloor. In recent years, electricity generation in deep-sea hydrothermal vents has been reported (Nakamura *et al.*, 2010; Ang *et al.*, 2015, Yamamoto *et al.*, 2017, 2018). Ang *et al.*, 2015 provided definitive evidence that thermoelectricity can be directly generated by natural sulfide minerals (chalcopyrite), $Cu_{1+x}Fe_{1-x}S_2$ (Takai *et al.*, 2008), obtained from a deep-sea hydrothermal vent. These sulfide mineral can function as thermoelectric materials that convert temperature gradient into electricity (Seeback effect). Indeed, the measurements of the electrical resistivity of the three examined natural samples ($Cu_{1+x}Fe_{1-x}S_2$: x=0.17, 0.08, and 0.02) showed that they exhibited excellent conductive behavior with semiconductive characteristics. To further examine the evolution of electronic state in $Cu_{1+x}Fe_{1-x}S_2$, the thermoelectric power (S) of three samples were also conducted. For x=0.17, the sign of S is mostly positive and reaches the maximum value was 215 $\mu V\ K^{-1}$, which indicates that the majority of charge carriers are of the hole type (p-type). Conversely, for x=0.02, S displays highly negative values and reaches remarkable values of −713 $\mu V\ K^{-1}$, thereby demonstrating that the majority of charge carriers are of the electron type (n-type). Based on these thermoelectric properties, a difference of 305℃ through the chimney minerals between a hydrothermal fluid and seawater can produce approximately 217 mV of electricity (Ooka *et al.*, 2019).

This discovery provides the feasibility of thermoelectricity generation and electron/hole carrier modulation with natural materials that are abundant in the Earth's crust.

1.2 Objectives

The physical phenomena of generating electricity from natural minerals and the catalytic ability of microbes to bio-electrochemically produce methane through CO_2 reduction, may establish a new hypothesis about the possibility of methane production in natural environment. According to **Fig. 1-1**, the small electric current could be generated through the natural minerals obtained from the Earth's curt, and these minerals can convert heat energy from the geothermal gradient into electric power. This small electric power could drive redox, which is mainly based on the activity of related microbes. For instance, with abundant inorganic sources such as HS^- and CO_2 in nature, as well as the ecosystems which surround them, methane production from CO_2 could be coupled with HS^- oxidation with the assistance of methanogens and sulfur bacteria, respectively.

To evaluate this hypothesis, a two-chamber microbial electrosynthesis system (MES), in which no organic substrate was supplied, was applied at very low voltages. Initially, two electrodes of an MES were connected to a DC power supply; After that, the electric power will be developed due to the Seeback effect, which converts temperature gradients to electricity. In MES, the voltage applied to produce methane depends not only on the biocathode potential but also on the anode potential. When coupled with the oxidation of inorganic compounds such as NH_4^+ and HS^- with low potential at the anode, MES for methane production at very low applied voltage can be theoretically established without organic substrates. However, many MES studies have not provided sufficient information about the oxidation reaction on the anode, with experiments conducted at higher applied voltages (>1.0 V). To the best of our knowledge, this study is also the first to report the coupling of NH_4^+ and/or HS^- oxidation on the abiotic and/or biotic anode in a methane-producing MES. In addition, microbial community analysis of the biomass collected from bio-electrodes on the last day of MES operation, revealed the interactions between microbes and bio-electrodes as well as interspecies in bioelectrical methane production.

The more specific objectives corresponding to different experimental conditions of this study were:

a. To investigate the possibility of bioelectrical methane production coupled with abiotic NH_4^+ oxidation in an applied voltage range of 0.05–3.0 V

b. To investigate the possibility of bioelectrical methane production coupled with abiotic HS^- oxidation (MES; abiotic anode) at a low applied voltage.

c. To investigate the possibility of bioelectrical methane production coupled with biotic HS^- oxidation (MES; biotic anode) at a low applied voltage.

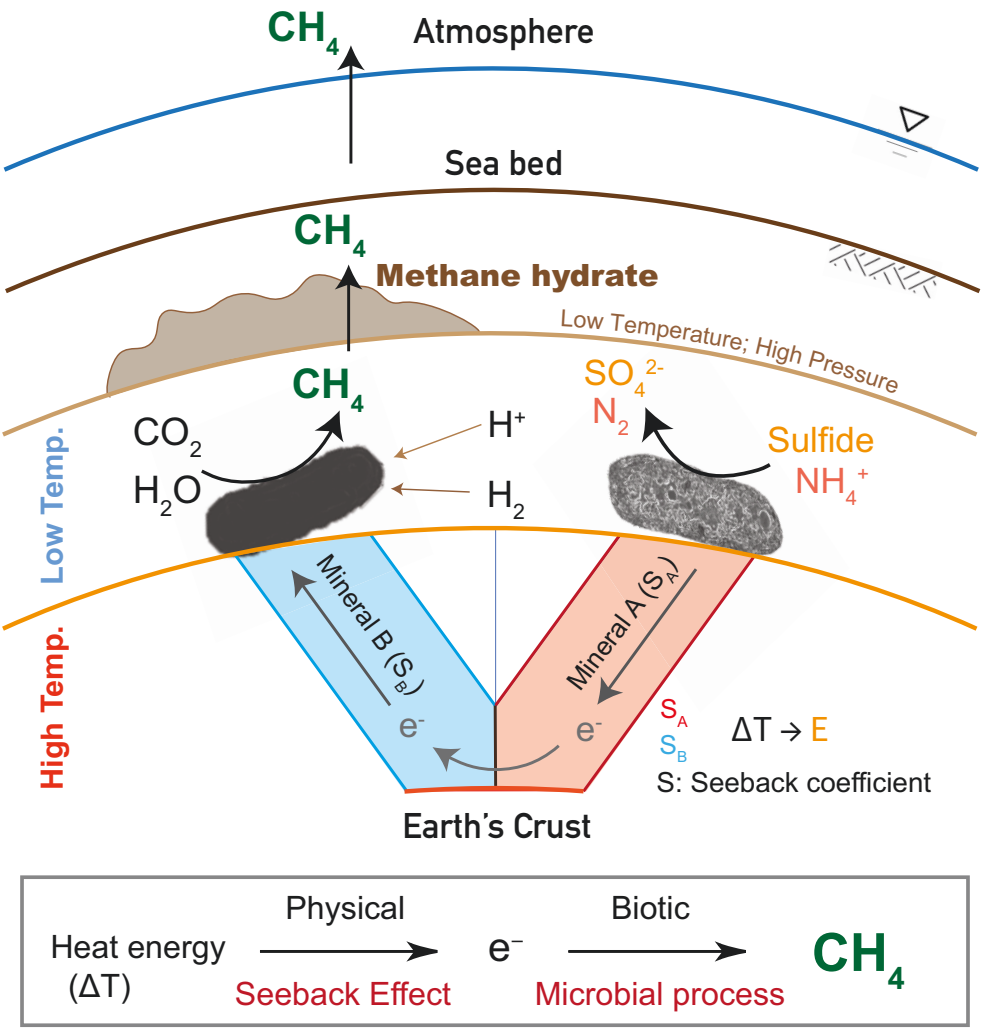

Fig. 1-1 A hypothesis of methane production in natural environments

1.3 Outline of dissertation

This dissertation is based on the research design (**Fig. 1-2**) and can be detailly outlined as follows:

Chapter 1: presents the general background of this study, including problem statement, research purpose and the outline of this dissertation.

Chapter 2: covers a literature review of related topics including :1) origin of methane in subseafloor geofluid systems; 2) microbes regarding the process of methane production; 3) biological methane production using MES.

Chapter 3: investigated the possibility of bioelectrical methane production in MES with abiotic NH_4^+ oxidation in an applied voltage range of 0.05–3.0 V. MES, in which no organic was supplied, was operated in batch processing mode. It consisted of biocathode and anode, which were connected to a salt bridge (2% agar and 20% KCl). A small amount of anaerobic sludge taken from a laboratory-scale upflow anaerobic sludge blanket (UASB) reactor was inoculated on the electrode, which worked as a biocathode. Platinum powder coated on the surface of the anode was used as anodic catalyst to enhance the NH_4^+ oxidative reaction. In the biocathode, microbial community at the biocathode was analyzed to identify the microbes involved in bio-electrical methane production at the biocathode.

Chapter 4: investigated the possibility of bioelectrical methane production at the biocathode coupled with HS^- oxidation at a low applied voltage. The results obtained in chapter 3 showed that besides methane production at the biocathode, biological denitrification also occurred at a higher rate. NO_3^- for this denitrification was produced by chemical NH_4^+ oxidation at the anode and transferred to the biocathode chamber via the salt bridge. In this chapter, instead of the salt bridge, a cation exchange membrane (CEM) thus placed between the anode and biocathode chamber. Abiotic sulfur oxidation on the anode was catalyzed by platinum powder coated on the surface of the anode. In addition, we propose the scheme of electron flow in methane production at the biocathode based on the microbial community analysis of biomass enriched on the electrode.

Chapter 5: investigated the possibility of bioelectrical methane production coupled with biotic HS^- oxidation at bioanode at a low applied voltage. In chapters 3 and 4, platinum (Pt)

effectively played the role of the anodic catalyst for the oxidative reaction on the anode. However, Pt is a precious metal catalyst. Thus, using the microbial anode as an alternative anode catalyst for sulfur oxidation was considered. The MES used in this chapter as well as the experimental conditions were almost the same as in chapter 4; the only difference point is the HS^- oxidation with the assistance of microbes enriched on the bioanode. The analysis of two microbial communities collected from biocathode and bioanode revealed the most probable pathways of methane production and sulfur oxidation from electrons.

Chapter 6: presents the main findings and conclusions of overall this study, after which recommendations for future works are also proposed in this chapter.

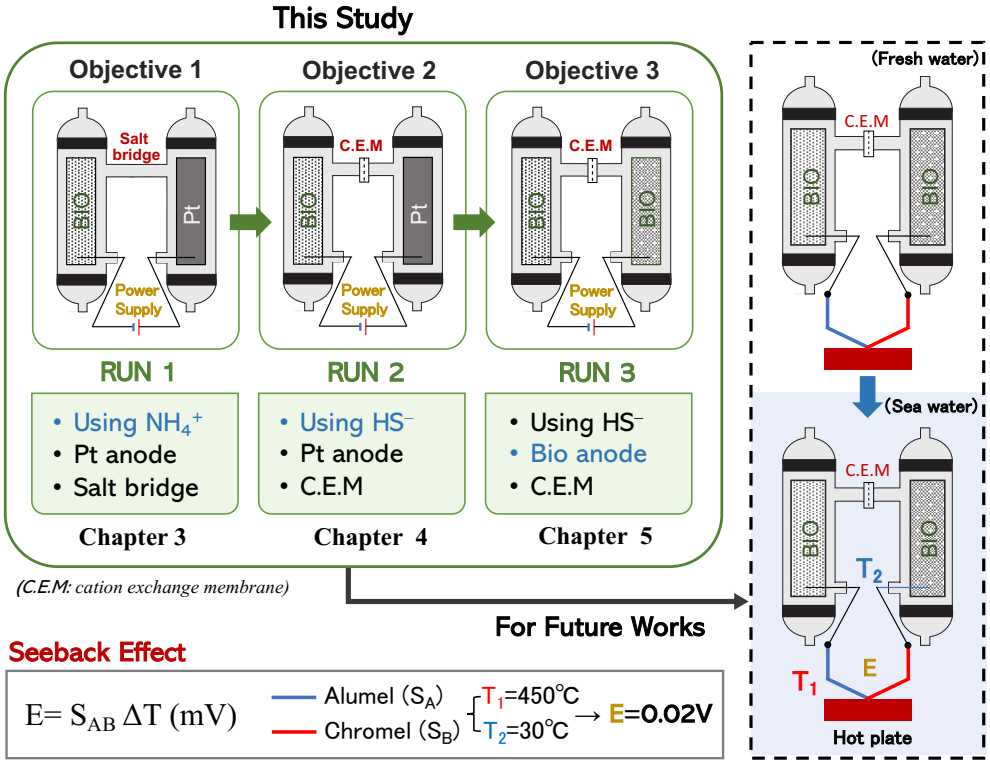

Fig. 1-2 Research design of the study

References

Ang, R., Khan, A.U., Tsujii, N., Takai, K., Nakamura, R., and Mori, T. (2015) Thermoelectricity Generation and Electron–Magnon Scattering in a Natural Chalcopyrite Mineral from a Deep-Sea Hydrothermal Vent. *Angewandte Chemie International Edition* **54**: 12909–12913.

Bousquet, P., Ciais, P., Miller, J.B., Dlugokencky, E.J., Hauglustaine, D.A., Prigent, C., et al. (2006) Contribution of anthropogenic and natural sources to atmospheric methane variability. *Nature* **443**: 439–443.

Cheng, S., Xing, D., Call, D.F., and Logan, B.E. (2009) Direct Biological Conversion of Electrical Current into Methane by Electromethanogenesis. *Environmental Science & Technology* **43**: 3953–3958.

Deppenmeier, U. and Müller, V. (2008) Life Close to the Thermodynamic Limit: How Methanogenic Archaea Conserve Energy. In *Bioenergetics: Energy Conservation and Conversion*. Results and Problems in Cell Differentiation. Schäfer, G. and Penefsky, H.S. (eds). Berlin, Heidelberg: Springer, pp. 123–152.

Gomez Vidales, A., Omanovic, S., and Tartakovsky, B. (2019) Combined energy storage and methane bioelectrosynthesis from carbon dioxide in a microbial electrosynthesis system. *Bioresource Technology Reports* **8**: 100302.

Myhre, G., Shindell, D., and Pongratz, J. (2014) Anthropogenic and Natural Radiative Forcing. In *Climate change 2013 : the physical science basis; Working Group I contribution to the fifth assessment report of the Intergovernmental Panel on Climate Change*. Stocker, T. (ed). Cambridge: Ludwig-Maximilians-Universität München, pp. 659–740.

Nakamura, R., Takashima, T., Kato, S., Takai, K., Yamamoto, M., and Hashimoto, K. (2010) Electrical Current Generation across a Black Smoker Chimney. *Angewandte Chemie International Edition* **49**: 7692–7694.

Onodera, I. (2013) Development of Methane Fermentation Technology for Wastewater Treatment. *Japan Tappi Journal* **67**: 82–85.

Ooka, H., McGlynn, S.E., and Nakamura, R. (2019) Electrochemistry at Deep-Sea Hydrothermal Vents: Utilization of the Thermodynamic Driving Force towards the Autotrophic Origin of Life. *ChemElectroChem* **6**: 1316–1323.

Stams, A.J.M., Bok, F.A.M.D., Plugge, C.M., Eekert, M.H.A.V., Dolfing, J., and Schraa, G. (2006) Exocellular electron transfer in anaerobic microbial communities. *Environmental Microbiology* **8**: 371–382.

Takai, K., Nunoura, T., Ishibashi, J., Lupton, J., Suzuki, R., Hamasaki, H., et al. (2008) Variability in the microbial communities and hydrothermal fluid chemistry at the newly discovered Mariner hydrothermal field, southern Lau Basin. *Journal of Geophysical Research: Biogeosciences* **113**:.

Townsend-Small, A., Disbennett, D., Fernandez, J.M., Ransohoff, R.W., Mackay, R., and Bourbonniere, R.A. (2016) Quantifying emissions of methane derived from anaerobic organic matter respiration and natural gas extraction in Lake Erie. *Limnology and Oceanography* **61**: S356–S366.

Vinson, D.S., Blair, N.E., Martini, A.M., Larter, S., Orem, W.H., and McIntosh, J.C. (2017) Microbial methane from in situ biodegradation of coal and shale: A review and reevaluation of hydrogen and carbon isotope signatures. *Chemical Geology* **453**: 128–145.

Yamamoto, M., Nakamura, R., Kasaya, T., Kumagai, H., Suzuki, K., and Takai, K. (2017) Spontaneous and Widespread Electricity Generation in Natural Deep-Sea Hydrothermal Fields. *Angewandte Chemie International Edition* **56**: 5725–5728.

Yamamoto, M., Nakamura, R., and Takai, K. (2018) Deep-Sea Hydrothermal Fields as Natural Power Plants. *ChemElectroChem* **5**: 2162–2166.

Zhen, G., Kobayashi, T., Lu, X., and Xu, K. (2015) Understanding methane bioelectrosynthesis from carbon dioxide in a two-chamber microbial electrolysis cells (MECs) containing a carbon biocathode. *Bioresource Technology* **186**: 141–148.

Zinder, S.H. (1993) Physiological Ecology of Methanogens. In *Methanogenesis: Ecology, Physiology, Biochemistry & Genetics*. Chapman & Hall Microbiology Series. Ferry, J.G. (ed). Boston, MA: Springer US, pp. 128–206.

Chapter

2

Literature Review

2.1 Origin of methane in subsea floor and geofluid

Methane gas is a reduced form of carbon and is distinguished by its origin, as methane derived from organic matter, or methane derived from processes that do not involve organic matter (Kulongoski *et al.*, 2018). The expected methane production in the crustal environment was summarized in **Fig. 2-1**.

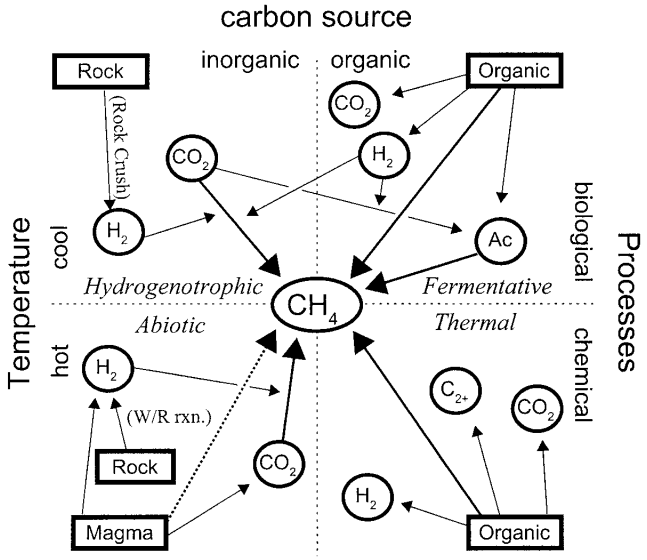

Fig. 2-1 A schematic drawing illustrating the methanogenic pathways in subseafloor geofluid systems with the processes effecting methanogenesis. Terms of "Ac" and "C2." respectively mean acetate and hydrocarbons with carbon numbers more than 2 (Kawaguchi and Toki, 2010).

2.1.1 Methane derived from organic matter

Methane in this section, is classified two types based on how it is produced, by either thermogenic or microbial processes.

a) Thermogenic methane

Thermogenic methane is formed when organic matter is buried and heated, usually at considerable depths over long periods of time, and includes methane associated with coal, gas, and oil formations (Schoell, 1983, 1988). Thermogenesis also produces longer chain hydrocarbon gases such as ethane, propane, butane, and pentane, and the methane is heavier isotopically because of the extended time, heat, and pressure hydrocarbons undergo. In the

thermogenic process, it is predicted that most natural gases form at temperatures greater than 150°C (Mackenzie and Quigley, 1988).

Some recent advances in science and technology, particular in extremophile, suggests that a part of the phenomena derived from thermogenesis may be due to the microbial activity. (Takai *et al.*, 2008) found that the growth possible temperature of methanogens has been updated to 122 ℃, which exceeds the autoclave temperature of about 121℃. This shows that the activity of methanogens can't be ignored in the temperature range of the thermal decomposition. Indeed, in the experiments in which submarine sediments were cultured at 90℃, the concentration of metal and hydrogen were measured and then compared to the sterile control (Parkes *et al.*, 2007). The results indicated that the rate of produced methane by methanogen was higher than that of the thermogenic methane.

b) Biological methane (fermentative methanogenesis)

Biological methane forms at shallower depths by the actions of methanogenic bacteria on organic matter in anoxic environments that include wetlands, landfills, and some aquifer sediments (Zinder, 1993; Stams *et al.*, 2006; Deppenmeier and Müller, 2008a). These methanogens produce primarily methane, rather than longer chain hydrocarbon gases, and the methane is isotopically lighter because the organic material that microbes convert to methane is isotopically light to start with (Jenden and Kaplan, 1986; Whiticar, 1999)

Methanogenesis is the terminal decomposition of organic matter in those environments which generally lack inorganic electron acceptors except for protons and CO_2, namely fermentative methanogenesis. In general, microbial methane formation follows two pathways: via CO_2 reduction or acetate fermentation. It has been suggested that fermentation dominates in recent sediments and is characterized by a depletion in deuterium in methane, while methane formed by CO_2 reduction is more common in older sediments (Whiticar *et al.*, 1986; Schoell, 1988; Whiticar, 1999). Seasonal control of methanogenic processes in the near-surface environment can occur where acetate fermentation dominates in warm, summer conditions, while in winter with cooler sediment temperatures, CO_2 reduction is the predominant process (e.g., Burke et al., 1988; Martens et al., 1986; Schoell, 1988).

2.1.2 Methane derived from inorganic mater

Similarly to section 2.1.1, methane is also classified two types based on how it is produced, by either chemical reaction at high temperature or microbial processes.

a) Abiotic methane

Abiotic methane forms in different geologic environments by chemical reactions that do not include organic matter and is produced in smaller amounts than methane derived from organic, primarily in magmatic process or through gas-water-rock interactions (Etiope & Sherwood Lollar, 2013; Potter & Konnerup-Madsen, 2003; Welhan, 1988). Production mechanisms include both high-temperature (volcanic and hydrothermal) settings and lower-temperature (<100°C) postmagmatic processes. The isotopic composition of abiotic methane is typically ^{2}H enriched and ^{13}C enriched ($\delta^{2}H$ > -200‰ and $\delta^{13}C$ > -20‰) or depleted ($\delta^{2}H$ < -200‰ and $\delta^{13}C$ between -30 and -47‰), due to variation in carbon feedstock and fractionation between CO2 and methane (Etiope & Sherwood Lollar, 2013).

The production of abiotic methane is typically represented as follow:

$$CO_2 + 4H_2 \rightarrow CH_4 + 2H_2O \qquad (2\text{-}1)$$

There are two main chemical reactions for the abiotic methane production as folows

i) Fischer Tropsch Type reaction:

This reaction involves the reduction of carbon atoms on the catalyst surface and the formation of jointing C-C which continuously occur. The catalyst for this reaction was invented in 1920s.

ii) Sabatier reaction reaction:

According to the catalyst such as Ni, Al_2O_3 methane can be produced through CO_2 reduction.

b) Biological methane

CO_2 is the only carbon sources for the proceess of the methane production based on the activity of microorganism. H_2 is used as electron acceptor together with CO_2 reduction to produce methane. In the subseafloor environment, inorganic carbonic acid is usually abundant, so that H_2 for methane production is limited. However, H_2 is supplied by rock crushing which especially occurs around the active layer zone (Wakita *et at.*, 1980). With

ecosystem diversity in the subseafloor environment, H_2 is also produce by microbial fermentation using organic matter close to thermodynamic limits (Jackson *et al.*, 2002). It leads to the thinking whether microbes could be catalyzed H_2 production by the other factors such as electricity instead of organic matter in nature.

Deep-sea hydrothermal vents and the ecosystem which surround them, provide insight into this question. Electricity can be generated through the sulfide minerals that form in seafloor hydrothermal deposits, and these minerals can convert the redox and heat energy between hydrothermal fluids and seawater into electric power (Nakamura *et al.*, 2010; Ang *et al.*, 2015; Yamamoto *et al.*, 2017, 2018; Ooka *et al.*, 2019). Thermoelectricity can be directly generated by sulfide minerals obtained from a deep-sea hydrothermal vent (Ang *et al.*, 2015). These sulfide mineral can function as thermoelectric metherials that convert temperature gradient into electricity (Seeback effect). Indeed, the measurements of the electrical resistivity of the three examined natural samples ($Cu_{1+x}Fe_{1-x}S_2$: x=0.17, 0.08, and 0.02) showed that they exhibited excellent conductive behavior with semiconductive characteristics. To further examine the evolution of electronic state in $Cu_{1+x}Fe_{1-x}S_2$, the thermoelectric power (S) of three samples were also conducted. For x=0.17, the sign of S is mostly positive and reaches the maximum value was 215 μV K^{-1}, which indicates that the majority of charge carriers are of the hole type (p-type). Conversely, for x=0.02, S displays highly negative values and reaches remarkable values of −713 μV K^{-1}, thereby demonstrating that the majority of charge carriers are of the electron type (n-type). Based on these thermoelectric properties, a difference of 305°C through the chimney minerals between a hydrothermal fluid and seawater can produce approximately 217 mV of electricity (Ooka *et al.*, 2019).

2.1.3 Methane hydrate

Gas hydrates are crystalline solids that form from mixtures of water and light natural gases such as methane, carbon dioxide, ethane, propane and butane. Methane was the dominant component among other hydrocarbon gases in the sediments. Methane hydrates are ice-like crystalline solids formed from a mixture of water and methane gas. They occur where high pressure, and low temperature combined with gas saturation, and local chemical conditions combine to make them stable. However, methane hydrates are metastable, changes in pressure and temperature affect their stability. Destabilized gas hydrates beneath the seafloor

lead to geologic hazards, and may also affect climate through the release of methane (Kvenvolden, 1993). Although the existence of methane hydrate has been widely known since the latter half of the 19th century, the studies in using methane hydrate as natural gas have been just started from the middle of the 20th century.

Methane hydrate occurs worldwide, but, because of the pressure-temperature and gas volume requirements, they are restricted to two regions: polar and deep oceanic (Potential Tas Committee, 1981) **(Fig. 2-2)**. In most methane hydrate, methane has molecular and isotopic characteristics that are diagnostic of a microbial origin. According to the criteria of Bernard *et al.*, (1976), who used hydrocarbon gas composition of methane to establish the origin of the methane: microbial, thermal, and mixed (Kvenvolden, 1995a). In case of microbial process, where methane is being microbially generated within a sedimentary section, there is a carbon-isotopic relationship between the methane and CO_2. This relationship is evident in sediment of the Blake Outer (Galimov and Kvenvolden, 1983). However, molecular and isotopic compositions of gas associated with gas hydrate found from Guatemela support either a microbial or thermal source for the methane (Kvenvolden, 1984). Only in the Gulf of Mexico and the Caspian Sea has methane hydrate been found in which methane is mainly thermogenic (Brooks *et al.*, 1986; Ginsburg *et al.*, 1992; Sassen and MacDonald. 1994).

The very large accumulations of methane, in the form of gas hydrate make this substance attractive as a potential energy resource for the future. Uncertainties about the mode of occurrence and the lack of applicable production techniques, however, augur that wide-scale exploitation, if proven feasible, could take place sometime in the 21st century when conventional natural gas deposits have been depleted.

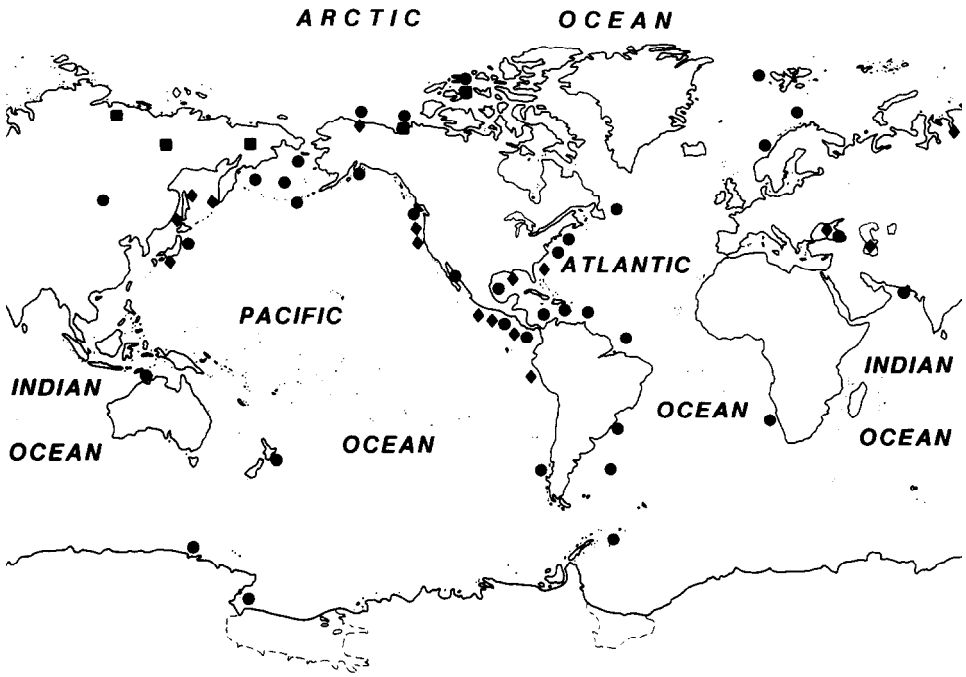

Fig. 2-2 Worldwide locations of known and inferred gas hydrate in oceanic (aquatic) sediment (circles) and in continental (permafrost) regions (squares), and locations where gas hydrates have been observed (diamonds). Modified from Kvenvolden (1993).(Kvenvolden, 1995)

2.2 Methanogen

2.2.1 Methanogen in nature

There are over 50 described species of methanogens, which do not form a monophyletic group, although all known methanogens belong to Archaea. They are mostly anaerobic organisms that cannot function under aerobic conditions. They are common in wetlands, where they are responsible for marsh gas, and in the digestive tracts of animals such as ruminants and many humans, where they are responsible for the methane content of belching in ruminants and flatulence in humans (Joseph W. Lengeler, 1999). In marine sediments, the biological production of methane, also termed methanogenesis, is generally confined to where sulfates are depleted, below the top layers (Kristjansson *et al.*, 1982). Moreover, methanogenic archaea populations play an indispensable role in anaerobic wastewater treatments (Tabatabaei *et al.*, 2010). Others are extremophiles, found in environments such as hot springs and submarine hydrothermal vents as well as in the "solid" rock of Earth's crust, kilometers below the surface.

Methanogens are key agents of remineralization of organic carbon in continental margin sediments and other aquatic sediments with high rates of sedimentation and high sediment organic matter (Yoshioka *et al.*, 2015). Under the correct conditions of pressure and temperature, biogenic methane can accumulate in massive deposits of methane clathrates (Kvenvolden, 1995b) which account for a significant fraction of organic carbon in continental margin sediments and represent a key reservoir of a potent greenhouse gas (Milkov, 2004). Methanogens have been found in several extreme environments on Earth – buried under kilometers of ice in Greenland and living in hot, dry desert soil. They are known to be the most common archaebacteria in deep subterranean habitats. Live microbes making methane were found in a glacial ice core sample retrieved from about three kilometers under Greenland by researchers from the University of California, Berkeley. They also found a constant metabolism able to repair macromolecular damage, at temperatures of 145 to 40 °C. For instance, thermophilic *Methanothermococcus* and hyperthermophilic *Methanocaldococcus species* are among the most common high-temperature methanogens found globally in hydrothermal vents and hot subsurface petroleum reservoirs (Takai *et al.*, 2004; Stewart *et al.*, 2019) (**Fig. 2-3**).

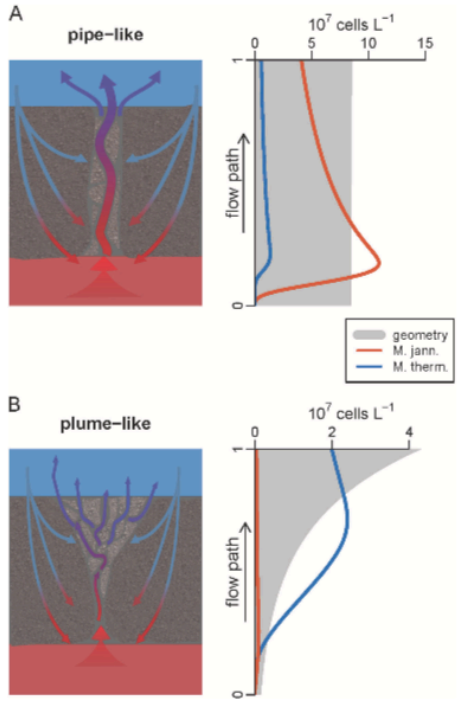

Fig. 2-3 General reactive transport model results for straight-pipe (a) and expanding-plume
(b) models. Lateral cross- sections depicting each model are shown on the left. The estimated concentration of *M. jannaschii* and M. *thermolithotrophicus* cells and the geometry of the flow path are shown on the right. The fluid temperatures at steps 0 and 1 are 84.6 and 26.7 °C, respectively

2.2.2 Methanogenesis

Methanogenesis was once considered a special type of fermentation. However, in some respects a very unique biochemistry is involved, which distinguishes methanogenesis from fermentation as well as from respiration. The process is carried out by strictly anaerobic bacteria all of which belong to the phylum Euryarchaeota in five orders that include mesophiles to thermophiles: *Methanobacteriales, Methanococcales, Methanomicrobiales, Methanopyrales, and Methanosarcinales* (Naomochi,1992). Methanogens occur in freshwater and marine environments, cold sediments and hydrothermal vents, as free-living cells and as symbionts with protists and animals that facilitate methane production and as symbionts with bacteria that promote anaerobic methane oxidation.

Acetoclastic methanogens could reduce acetate to produce CH4 according to:

$CH_3COOH \rightarrow CO_2 + CH_4$ $\Delta G^{0'} = -31$ kJ/reactor (2-2)

Diversity of acetoclastic methanogens that are important for conversion of acetate to methane is very limited. The reported acetoclastic methanogens are only *Methanosarcina* and *Methanosaeta spp. Methanosarcina* can consume a relatively high concentration of acetate and have the ability in using methyl compounds such as methanol (Kurade *et al.*, 2019; Conrad, 2020). Although *Methanosaeta* can consume a lower concentration of acetate and play a role in decreasing chemical oxygen demand (COD) in anaerobic digestion, since their growth rate is significantly low, the amount of *Methanosaeta* cells significantly affects the performance of anaerobic digestion.

Hydrogenotrophic methanogenesis, which occurs in all five orders above use H_2 for the reduction of CO_2 (or CO or formate) according to:

$4H_2 + CO_2 \rightarrow CH_4 + 2H_2O$ $\Delta G^{0'} = 136$ kJ/reactor (2-3)

This process is formally a type of respiration, and the organisms that use it can grow autotrophically (Schoell, 1980; Xu *et al.*, 2019). The energetics of the hydrogenotrophic methanogenesis seem to be relatively favourable theoretically, but in practice cell growth rates and yields are lower than predicted from thermodynamic considerations. This is in part due to that autotrophic growth requires use of some of the substrate for C-assimilation, including a significant amount of ATP.

The energetics of acetoclastic methanogenesis is less favourable than that of hydrogenotrophic methanogenesis, resulting in even slower growth rates and lower cell yields (Li *et al.*, 2019; Conrad, 2020). Relative to sulfate reducers, methanogens are inferior competitors for substrates they both use: H_2 and acetate (Thauer and Shima, 2006). Thus, when sulfate is present, methanogenesis is typically low. However, in sulfate-depleted, anaerobic habitats – especially in freshwater sediments, sewage digesters, in the rumen and at some depth in marine sediments-methanogens play a central role as H_2-scavengers and in the terminal mineralization of acetate. As such, they contribute significantly to the carbon cycle.

Table 2-1 Methanogens for producing methane

Specices	Function	Reference
Acetoclastic methanogens (using acetate for growth)		
Methanosarcina	High concentration of acetate	Kurude *et al.*, 2010 Conrad *et al.*, 2020
	DIET vs *Geobacter* (GAC)	Liu *et al.*, 2012
Methanosaeta	Low concentration of acetate	Fey and Conrad, 2000 Hua *et al.,* 2020
	DIET vs *Geobacter* (GAC)	Rotaru *et al.*, 2014 Zhao *et al.*, 2015
Hydrogenotrophic methanogens (using H_2/CO_2 for growth)		
Methanococcus maripaludis	Direct electron uptake from Fe^0	Uchiyama *et al.*, 2010
Methanospirillum hungatei	Electrically conductive	Walker *et al.*, 2019
Methanolinea	DIET vs *Geobacter* (GAC)	Salvador *et al.*, 2017
Methanobrevibacter	Co-culture with H_2-producing bacteria	Sasaki *et al.*, 2011
Methanocorpusculum	in MES	Jiang *et al.*, 2014
MEthanoculleus		Siegert *et al.*, 2015
Methanobacterium	In MES:	
	Indirect: with intermediate production of hydrogen	Villano *et al.*, 2010 Zhen *et al.*, 2015a; 2018b
	Direct: electron uptake from cathode	Cheng *et al.*, 2009

2.3 Electron transfer

2.3.1 Methanogen vs other species

In general, methane is formed via interspecies electron transfer (IET) between fermenting bacteria and methanogenic archaea. Fermenting bacteria fermenting bacteria degrade sugars, long chain fatty acids and amino acids into VFAs, and produce diffusive electron carriers (e.g., hydrogen and formate) (Kokko *et al.*, 2018). Methanogenic archaea, namely hydrogenotrophic methanogen can utilizes diffusive electron carriers to produce methane (Giovannini *et al.*, 2016). However, (Rotaru *et al.*, 2013) found that a new model for electron flow during anaerobic digestion (**Fig. 2-4**). *Methanosaeta species* can make direct electrical connections with *Geobacter species*, accepting electrons for the reduction of carbon dioxide to methane, and that direct interspecies electron transfer (DIET) is an alternative to interspecies H_2/ formate transfer. Additionally, Holmes *et al.* (2017) also provided provided metatranscriptomic evidence for DIET in mthanogenic rice paddy aoils, in which *Geobacter* species were providing electrons to *Methanothrix* species for methane production through electrical connections of e-pili. *Methanosaeta* species are also ubiquitous in methanogenic soils and sediments, suggesting that a substantial portion of global methane production could be derived from DIET.

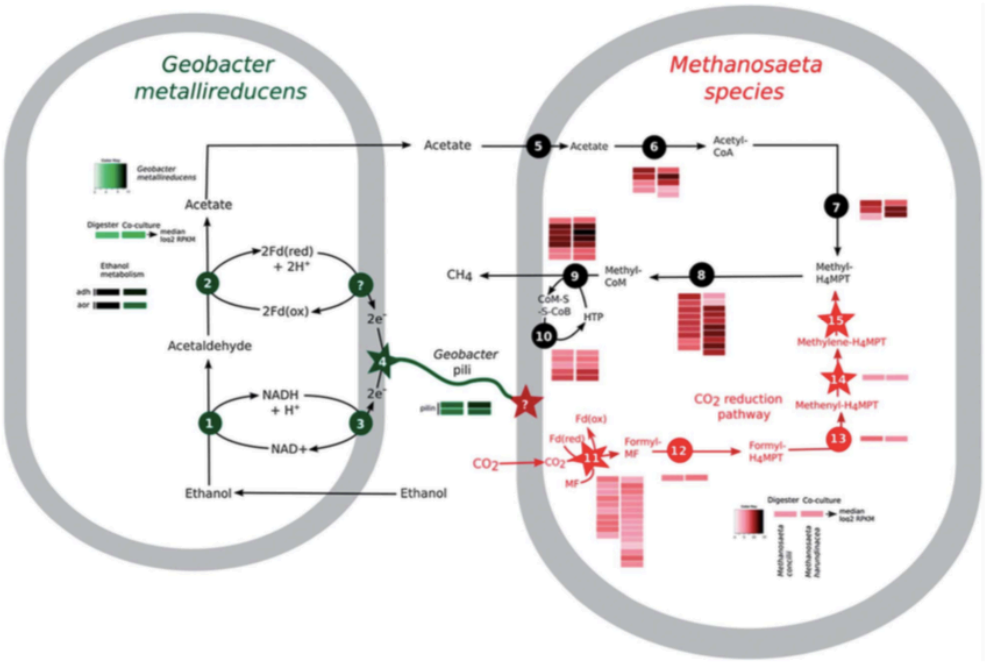

Fig. 2-4 DIET-based on metabolism in digester samples and defined co-cultures of *Geobater metallireducens* and *Methanosaeta harundinacea* as revealed metatranscriptomics. (Rotaru *et al.*, 2013)

Recently, several studies revealed that adding conductive materials (e.g., granular activated carbon (GAC) and iron oxides) to methanogenic anaerobic reactors facilitates DIET between the two groups of microorganisms (i.e., exoelectrogenic bacteria and methanogenic archaea) without mediating diffusive electron carriers (Kato *et al.*, 2012; Zhao, Zhang, Yu, Dang, *et al.*, 2016). In DIET, conductive materials play a role as electrodes to accept electrons from exoelectrogenic bacteria and donate the electrons to methanogenic archaea (Zhao *et al.*, 2015). DIET via conductive materials is reported to be more efficient than that via IET in terms of rate and amount of methane production (Lee *et al.*, 2016). This is due to the obviation of several steps involved in the production and consumption of diffusive electron carriers (Lovley, 2011). *Methanosaeta harundinacea*, *Methanosarcina barkeri* (Liu *et al.*, 2012) and *M. acetivorans* (Salvador *et al.*, 2017) are representative methanogens capable of this function. *Geobacter sulfurreducens* with features: extracellular c-Cyts (Marsili *et al.*, 2010); extracellular polysaccharides (Rollefson *et al.*, 2011); and conductive pili (Reguera *et al.*, 2005; Malvankar *et al.*, 2011), are the most well-known exoelectrogens. Interestingly, Walker *et al.* (2019) reported that the archaellum of *Methanospirillum hungatei* is electrically conductive. The availability of the M.hungatei archaellum structure is expected to substantially advance mechanistic evaluation of long-range electron transport in microbially produced electrically conductive filaments and to aid in the design of "green" electronic materials that can be microbially produced with renewable feedstocks.

2.3.2 Methanogen vs electron donor such as Fe^0, electrode

Currently, methanogenic archaea are the only microorganisms known to produce methane as the major end product of their metabolism from a limited source of substrates like H_2 + CO_2, formate, methanol and acetate. It is commonly recognized, that under environmental conditions, methanogenic archaea operate close to the thermodynamic limit, demanding elaborate mechanisms of energy conservation (Deppenmeier and Müller, 2008b). For instance, certain methanogenic archaea have been isolated that are able to utilize elemental iron (Fe^0) as the sole electron donor for the production of methane, which has a redox potential close to the thermodynamic equilibrium for CO_2 reduction (Daniels *et al.*, 1987; Dinh *et al.*, 2004; Uchiyama *et al.*, 2010). Especially the *Methanobacterium*-like archaeon strain IM1 (Dinh *et al.*, 2004) and the *Methanococcus maripaludis* strain KA1 (Uchiyama *et al.*, 2010) were shown to corrode iron by direct electron uptake coupled to metabolic

activity; i.e. a mechanism recently termed electrical microbially influenced corrosion (Enning *et al.*, 2012; Venzlaff *et al.*, 2013; Enning and Garrelfs, 2014).

Methanogens could accept electrons from iron without the need for hydrogen evolution. However, it is possible that the microbe enhanced corrosion rates (and thus hydrogen evolution rates), and there was no further electrochemical analysis of the corrosion or examination of the growth of this microorganism on an electrode. The ability of microorganisms to donate electrons to iron does not necessarily mean they can use a carbon electrode as an electron acceptor. While thermodynamic data and these experiments suggest that direct electron transfer to methanogens is possible, it has not been previously demonstrated using electrodes in a bioelectrochemical system. However, Cheng *et al.*, (2009) demonstrated that *Methanobacterium palust*re used on the cathode in an MEC to produce methane gas from electrical current at rates much greater than those possible via hydrogen gas evolution from a noncatalyzed electrode. Furthermore, Beese-Vasbender *et al.* (2015) reported for the first time on selective microbial electro- synthesis of methane by a pure culture of the marine litho- autotrophic *Methanobacterium*-like archaeon strain IM1(**Fig. 2-5**). This investigation is of crucial fundamental interest to confirm and elucidate

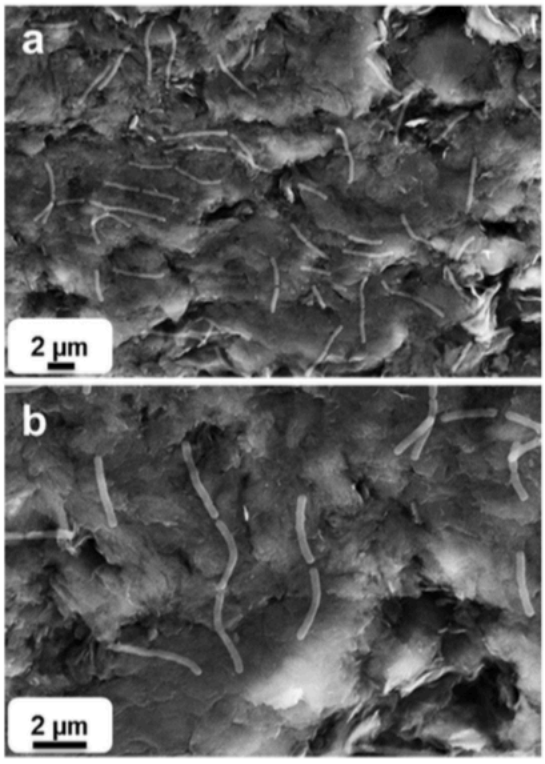

Fig. 2-5 Scanning electron micrographs of strain IM1. Cells of strain IM1 attached to a graphite surface that served as the sole electron donor for microbial electrosynthesis of methane. Scanning electron micrographs shown in (a) 5000× and (b) 10,000× magnification. (Beese-Vasbender *et al.*, 2015)

the relevant electron transfer mechanisms, as well as to resolve the individual contribution to the microbial electrosynthesis of methane to confirm and elucidate the relevant electron transfer mechanisms, as well as to resolve the individual contribution to the microbial electrosynthesis of methane.

Table 2-2 Electron transfer between microorganism and electrodes as well as interspecies

Phylum	Specices	Reference
1) Electrogenic microorganism in MFC		
γ-Proteobacteria	*Shewanella oneidensis*	Ringeisen *et al*., 2006
	Shewanella putrefaciens	Kim *et al.*, 2002
	Pseudomonas aeruginosa	Liu *et al.*, 2012
δ-Proteobacteria	*Geobacter sulfurreducens*	Ishii *et al.*, 2008 Bond and Lovley, 2003 Lovley *et al.*, 2011)
	Desulfobulbus propionicus	Holmes *et al.*, 2004b
Acidobacteria	*Geothrix fermentans*	Bond and Lovley, 2005
Chloroflexi	*Anaerolineaece*	Cabezas *et al.*, 2015 Wang *et al.*, 2021
Enriched microorganism in MFCs (syntrophic bacteria)		
γ-Proteobacteria	*Rhodocyclaceae*	Sun *et al.*, 2009
Bacteroides	*SB1*	Yu *et al.*, 2016)
Acidobacteria	*Aminicenantales*	Salgado-Dávalos *et al.*, 2021
Caldiserica	*Caldisericum*	Wang *et al.*, 2021
2) DIET involved bacteria		
δ-Proteobacteria	*Geobacter*	(Park *et al.*, 2018)
	Syntrophorhabdus	Mostafa *et al.,* 2020
	Syntrophus	(Park *et al.*, 2018)

2.4 Biological methane production using microbial electrosynthesis system

2.4.1 MFCs and MECs

Two new methods of bioenergy production from biomass include electricity production using microbial fuel cells (MFCs) and hydrogen production by electrohydrogenesis using microbial electrolysis cells (MECs) (Logan *et al.*, 2006, 2008) (**Fig. 2-6**).

Electricity generation in an MFC is spontaneous with oxidation of organic matter such as acetate by electrogenic bacteria on the anode (E_{An} = –0.2 V vs standard hydrogen electrode) and oxygen reduction at the cathode (E_{Cat} = 0.2 V), with a working cell potential of approximately 0.4 V and a theoretical potential as high as 1.1 V under neutral pH

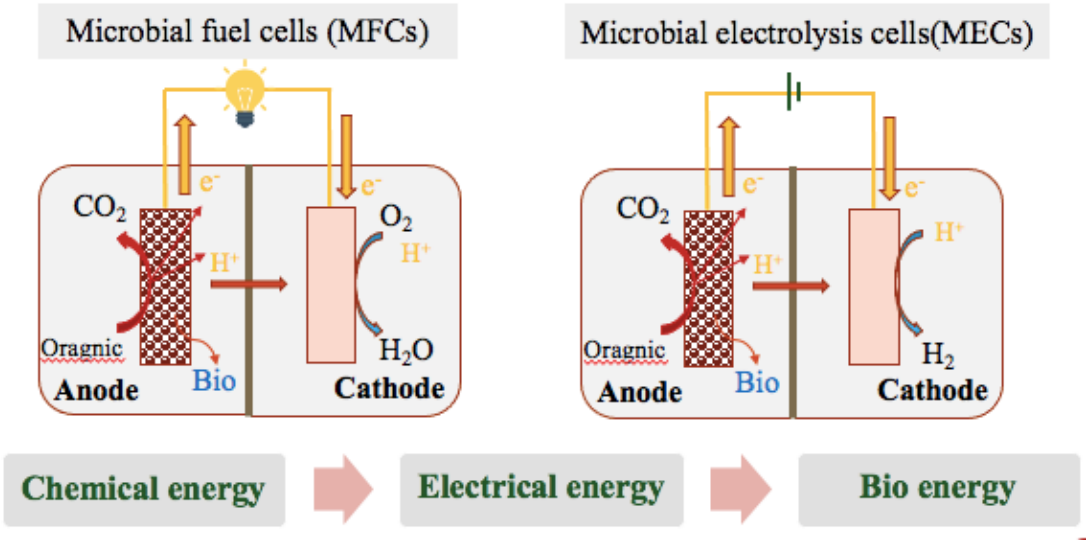

Fig. 2-6 Scheme of microbial fuel cell and microbial electrolysis fuels

conditions (Logan *et al.*, 2006). MFCs operated using cultures achieve substantially power densities. Community analysis of the microorganisms that exist in MFCs has so far revealed a great diversity in composition. Some recent MFC studies discovered many new types of bacteria that are capable of anodophilic electron transfer (electron transfer to an anode) or even interspecies electron transfer (electrons transferred between bacteria in any form) (Cabezas *et al.*, 2015; Sarmin *et al.*, 2019; Salgado-Dávalos *et al.*, 2021). Among of them, *Geobacter sulfurreducens* can attach to electrodes and remain viable for long periods of time while completely oxidizing organic substrates with quantitative transfer of electrons to an electrode (Bond and Lovley, 2003; Li *et al.*, 2018).

The MEC is a type of modified MFC that has been used to efficiently store electrical energy as a biofuel (hydrogen gas) (Logan *et al.*, 2008). Hydrogen gas evolution from the cathode, however, is not spontaneous (Rozendal *et al.*, 2008). The voltage produced by electrogenic bacteria on the anode using a substrate such as acetate (E_{An} = –0.2 V) is insufficient to evolve hydrogen gas at the cathode (E_{cell} = –0.414 V, pH = 7). By adding a small voltage, hydrogen gas can be produced using MECs at very high energy efficiencies evaluated in terms of just electrical energy alone (200 – 400%) or both electrical energy and substrate heat of combustion energy (82%) (Liu *et al.*, 2005; Tartakovsky *et al.*, 2009). Therefore, the main advantage of MEC versus abiotic water electrolysis is that the oxidation

of water is replaced by the oxidation of organic compounds, which can occur at significantly lower redox potentials. The thermodynamic cell voltage of an MEC is thus considerably reduced with respect to the famous 1.23 V threshold of water electrolysis in standard conditions (Rozendal *et al.*, 2006).

2.4.2 Methane production using MES

Currently, one of the main disadvantages of MEC, is the requirement of expensive materials, such as platinum, as cathodic catalysts. The choice for platinum in MEC is due to its excellent electrocatalytic activity towards hydrogen evolution, even though its performance is negatively affected by several different components often present in waste streams. The need for cheaper and more sustainable cathodes, to be employed for bioenergy generation in MEC, has prompted research into the development of alternative cathode catalysts, such as microbial biocathodes (Clauwaert, van der Ha, *et al.*, 2007; Rozendal *et al.*, 2008). Recently, microbial biocathodes are being explored also for other applications, such as the biological reduction of oxidized pollutants in bioremediation systems (Aulenta *et al.*, 2009), or the biological reduction of nitrate to nitrogen gas (Clauwaert, Rabaey, *et al.*, 2007).

Another possible application is the electrochemical reduction of carbon dioxide to methane according to the following reaction:

$$CO_2 + 8H^+ + 8e^- \rightarrow CH_4 + 2H_2O \qquad (2\text{-}4)$$

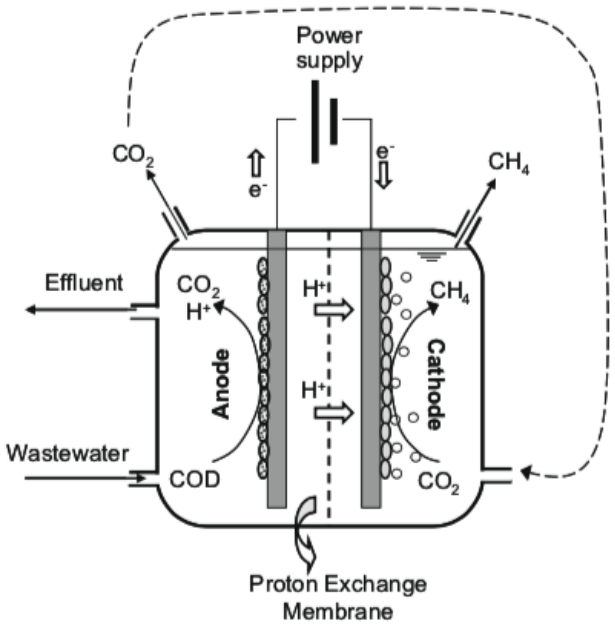

Fig. 2-7 Schematic drawing of a bioelectrochemical system for wastewater treatment and simultaneous CH_4 production based on bioelectrochemical CO_2 reduction

Indeed, both the electrons and the carbon dioxide released at the anode during the microbial oxidation of the organic matter contained in a waste stream can be in principle exploited for the cathodic generation of methane, according to the schematic drawing reported in **Fig. 2-7**. At standard conditions, this reaction requires a theoretical voltage of –0.244 V (vs. SHE) at pH = 7, but it is usually affected by quite large overpotentials. However, it could be possibly reduced by using a microbial biocathode. In summary, self-regenerating methanogenic archaea that are able to accept electrons from cathodes for their metabolism, are advantageous over chemical catalysts due to their high efficiency and selectivity. The system for methane production through CO_2 reduction, in which use electricity as an energy source and microorganisms as the catalyst, is widely called Microbial Electrosynthesis System (MES).

MES has a wide range of applications in wastewater treatment and other energy recycling fields. (Clauwaert and Verstraete, 2009; Zhao, Zhang, Yu, Ma, *et al.*, 2016; Zakaria and Dhar, 2021). Cathodic reduction of CO_2 and anodic oxidation of organic matters are crucial to MES (**Fig. 2-7**). Compared to conventional anaerobic digestion, this process could offer some specific advantages, such as the physical separation of the waste organic matter oxidation stage from the methane production one. This would allow to protect the methanogenic consortia against inhibitory compounds possibly present in the waste streams and to produce methane with lower content in carbon dioxide and other impurities. Moreover, since the wastewater only flows through the anodic chamber (which can even be operated at ambient temperature), less energy is required to maintain the cathode at the desired temperature (e.g., 35 °C). Higher methane production can be expected in MES than in conventional methane fermentation reactors for wastewater. It can be due to the combination of methane production from organic substrates and conversion of CO_2 to methane through electricity by microorganism (Clauwaert and Verstraete, 2009; Peng *et al.*, 2019). Ding *et al.* (2016) found 0.8 V to be the optimal applied voltage for appropriate wastewater treatment and maximum methane production using an MES. Information provided will be useful to design reactor and maintain industry practice.

2.4.3 Methane production using MES without organic substrates

Bio-electrical methane production controlled by MES is performed without organic substrates (Villano *et al.*, 2010; Aryal *et al.*, 2017; Schlager *et al.*, 2017; Zhen *et al.*, 2018).

In this case, the microbial oxidation of organic matter was replaced by the oxidation of H_2O without biocatalyst on the anode (abiotic anode). Gomez Vidales *et al.* (2019) found that carbon dioxide was reduced to methane at an applied voltage of 2.6 V, which is higher than the required voltage in range of 0.8–1.2 V when using organic-based wastewater as a substrate for the anode chamber (Ding *et al.*, 2016; Flores-Rodriguez *et al.*, 2019). These studies mainly focused on better understanding the underlying mechanisms for microbial electrosynthesis of methane in a two-chamber MECs containing a carbon biocathode. Although the complex interactions between microorganisms and cathode as well as interspecies have not been fully explored, two mechanisms have been proposed in electron follow. First, certain methanogens directly accept electrons from the electrode to generate methane with CO_2 reduction (Cheng *et al.*, 2009). Second, once H_2 is abiotically or biologically produced by proton reduction with electrons, methane is produced by hydrogenotrophic methanogens using the generated H_2 with CO_2 uptake (Villano *et al.*, 2010; Zhen *et al.*, 2018).

The standard reduction potential $E^{0\prime}$ of CO_2 to methane at pH = 7 is −0.24 V (vs. standard hydrogen potential [SHE]). The voltage applied to produce methane in MES depends not only on the biocathode potential but also on the anode potential. When coupling of H_2O oxidation ($E^{0\prime}$ = 0.81 V vs. SHE) at the anode and CO_2 reduction at the cathode takes place in an MES, more than 1.05 V is thermodynamically required in the applied voltage under the standard condition for methane production. However, when coupled with oxidation of NH_4^+ to NO_3^- ($E^{0\prime}$ = 0.36 V vs. SHE) instead of H_2O oxidation, methane can be produced a lower applied voltage of 0.6 V. If oxidation of HS^- to SO_4^{2-} ($E^{0\prime}$ = −0.22 V vs. SHE) occurs at the anode, an MES for methane production at a very low applied voltage (0.02 V) can be theoretically established without organic substrates. Pt is commonly accepted as the most promising catalyst in the electrochemical oxidation of ammonia and /or sulfur. However, considering the development of alternative anode catalysts, such as microbial bioanodes are required. Recently, microbial bioanodes are widely known in MFC. Electricity generation is spontaneous with the oxidation of organic matter such as acetate by electrogenic bacteria on the anode. In the absence of organic matter, Sun *et al.* (2009) demonstrated that both electrochemical reactions and microbial catalysis were involved in such a complex sulfide oxidation process in the bioanode of an MFC. Not only in MFC, but the highly detected microorganism in the bioanode can mainly drive the complete anoxic conversion of ammonium to N_2 in MEC (Vilajeliu-Pons *et al.*, 2018).

Table 2-3 Microorganims for sulfur oxdation

Genus (Family)	Characteristics in HS- oxidation Enzyme	S oxidation	Electron acceptors	Reference
S disproportionation		Disproportionation of		
+ *Dissulfurimicrobium*		S^0, $S_2O_3^{2-}$, SO_3^{2-} to SO_4^{2-} and sulfide	None	(Slobodkin *et al.*, 2016; Slobodkin and
+ *Desulfomonile*		$S_2O_3^{2-}$ to SO_4^{2-} and sulfide	SO_4^{2-}	Slobodkina, 2019)
+ *Desulfobulbus propionacus*		S^0, $S_2O_3^{2-}$, SO_3^{2-} to SO_4^{2-} and sulfide	Fe (III), electrode	(Holmes et al. - 2004)
S oxidation (SOM)				
+ *uncultured* (SB-5)				(Phelps *et al.*, 1998)
+*uncultured* (SB1)		Sulfide → S^0, ($S_2O_3^{2-}$, SO_3^{2-})	MFC	(Yu *et al.*, 2016;)
+ *Spirochaeta2, uncultured*			O_2,	
(Spirochaetaceae)		Sulfide → S^0, ($S_2O_3^{2-}$, SO_3^{2-})	Fe_3O_4	(Dubinina *et al.,* 2011*;* Jung *et al.*, 2020)
+ *Thiobacillus, uncultured*	SoxYZ, SoxXA	Sulfide, S^0, $S_2O_3^{2-}$ → SO_4^{2-}	O_2, NO_3^-	(Wasmund *et al.*, 2017; Lin *et al.*, 2018)
(Hydrogenophilaceae)	SoxCD			(Friedrich *et al.*, 2001)
+*blank, uncultured*		Sulfide, S^0, $S_2O_3^{2-}$ → SO_4^{2-}	NO_3^- → NO_2^-	(Bell *et al.*, 2020)
(Rhodocyclaceae)	Sat-AprBA DsrAB, dsrEFH		Anode (MFC)	(Sun *et al.*, 2009)
+ *Longilinea,*		Sulfide → S^0, $S_2O_3^{2-}$	SO_4^{2-}, NO_3^-	(Xia *et al.*, 2017; Bell *et al.*, 2020;
Leptolinea		(heterotrophic bacteria)	Anode (MFC)	Wang *et al.*, 2021)
(Anaerolineaceae)	sqr	Filamentous-keystone species in MFC		
+ *Sulfuricurvum, uncultured*		Sulfide, S^0, $S_2O_3^{2-}$ → SO_4^{2-}	O_2, NO_3^-	(Kodama and Watanabe, 2004)
(Thiovulaceae)				
		Syntrophic between SOM and methanogen		(Jung *et al.*, 2020)
S reduction (SRM)		Filamentous-keystone species in MFC;		
+ *Caldisericum*		Associated with SOM and EAM to produce current in MFC	S^0, $S_2O_3^{2-}$ (from HS^- oxidation)	(Sun *et al.*, 2009; Wang *et al.*, 2021)
+ *Desulfatirhabdium*		Electron donor: acetate, H2, formate	SO_4^{2-}	(Wasmund *et al.*, 2017)
+ *Syntrophobacter*		Electron donor: propionate	SO_4^{2-}	(Wallrabenstein, 1995)

References

Ang, R., Khan, A.U., Tsujii, N., Takai, K., Nakamura, R., and Mori, T. (2015) Thermoelectricity Generation and Electron–Magnon Scattering in a Natural Chalcopyrite Mineral from a Deep-Sea Hydrothermal Vent. *Angewandte Chemie International Edition* **54**: 12909–12913.

Aryal, N., Ammam, F., Patil, S.A., and Pant, D. (2017) An overview of cathode materials for microbial electrosynthesis of chemicals from carbon dioxide. *Green Chem* **19**: 5748–5760.

Aulenta, F., Canosa, A., Roma, L.D., Reale, P., Panero, S., Rossetti, S., and Majone, M. (2009) Influence of mediator immobilization on the electrochemically assisted microbial dechlorination of trichloroethene (TCE) and cis-dichloroethene (cis-DCE). *Journal of Chemical Technology & Biotechnology* **84**: 864–870.

Bernard B. B., Brooks J. M. and Sackett W. M. (1976) Natural gas seepage in the Gulf of Mexico. Earth Planet. Sci. Left. 31, 48-54.

Beese-Vasbender, P.F., Grote, J.-P., Garrelfs, J., Stratmann, M., and Mayrhofer, K.J.J. (2015) Selective microbial electrosynthesis of methane by a pure culture of a marine lithoautotrophic archaeon. *Bioelectrochemistry* **102**: 50–55.

Bond, D.R. and Lovley, D.R. (2003) Electricity Production by Geobacter sulfurreducens Attached to Electrodes. *Appl Environ Microbiol* **69**: 1548–1555.

Brooks J. M. Cox B. H. Brvant W. R. Kennicutt M. C. III, Mann R. G.and McDonald T. J. (1986) Association of gas hydrates and oil seepage in the Gulf of Mexico. Org. Geochem. 10, 221-234.

Burke, R. A., Martens, C. S., & Sackett, W. M. (1988). Seasonal variations of D/H and 13C12C ratios of microbial methane in surface sediments. Nature, 332(6167), 829–831. https://doi.org/10.1038/332829a0

Cabezas, A., Pommerenke, B., Boon, N., and Friedrich, M.W. (2015) Geobacter, Anaeromyxobacter and Anaerolineae populations are enriched on anodes of root exudate-driven microbial fuel cells in rice field soil. *Environmental Microbiology Reports* **7**: 489–497.

Cheng, S., Xing, D., Call, D.F., and Logan, B.E. (2009) Direct Biological Conversion of Electrical Current into Methane by Electromethanogenesis. *Environmental Science & Technology* **43**: 3953–3958.

Clauwaert, P., van der Ha, D., Boon, N., Verbeken, K., Verhaege, M., Rabaey, K., and Verstraete, W. (2007) Open Air Biocathode Enables Effective Electricity Generation with Microbial Fuel Cells. *Environ Sci Technol* **41**: 7564–7569.

Clauwaert, P., Rabaey, K., Aelterman, P., De Schamphelaire, L., Pham, H.T., Boeckx, P., et al. (2007) Biological denitrification in microbial fuel cells. *ENVIRONMENTAL SCIENCE & TECHNOLOGY* **41**: 3354–3360.

Clauwaert, P. and Verstraete, W. (2009) Methanogenesis in membraneless microbial electrolysis cells. *Appl Microbiol Biotechnol* **82**: 829–836.

Conrad, R. (2020) Importance of hydrogenotrophic, aceticlastic and methylotrophic methanogenesis for methane production in terrestrial, aquatic and other anoxic environments: A mini review. *Pedosphere* **30**: 25–39.

Daniels, L., Belay, N., Rajagopal, B.S., and Weimer, P.J. (1987) Bacterial Methanogenesis and Growth from CO2 with Elemental Iron as the Sole Source of Electrons. *Science* **237**: 509–511.

Deppenmeier, U. and Müller, V. (2008a) Life Close to the Thermodynamic Limit: How Methanogenic Archaea Conserve Energy. In *Bioenergetics: Energy Conservation and*

Conversion. Results and Problems in Cell Differentiation. Schäfer, G. and Penefsky, H.S. (eds). Berlin, Heidelberg: Springer, pp. 123–152.

Deppenmeier, U. and Müller, V. (2008b) Life Close to the Thermodynamic Limit: How Methanogenic Archaea Conserve Energy. In *Bioenergetics: Energy Conservation and Conversion*. Results and Problems in Cell Differentiation. Schäfer, G. and Penefsky, H.S. (eds). Berlin, Heidelberg: Springer, pp. 123–152.

Ding, A., Yang, Y., Sun, G., and Wu, D. (2016) Impact of applied voltage on methane generation and microbial activities in an anaerobic microbial electrolysis cell (MEC). *Chemical Engineering Journal* **283**: 260–265.

Dinh, H.T., Kuever, J., Mußmann, M., Hassel, A.W., Stratmann, M., and Widdel, F. (2004) Iron corrosion by novel anaerobic microorganisms. *Nature* **427**: 829–832.

Enning, D. and Garrelfs, J. (2014) Corrosion of iron by sulfate-reducing bacteria: new views of an old problem. *Appl Environ Microbiol* **80**: 1226–1236.

Enning, D., Venzlaff, H., Garrelfs, J., Dinh, H.T., Meyer, V., Mayrhofer, K., et al. (2012) Marine sulfate-reducing bacteria cause serious corrosion of iron under electroconductive biogenic mineral crust. *Environmental Microbiology* **14**: 1772–1787.

Etiope, G., & Sherwood Lollar, B. (2013). Abiotic methane on Earth. Reviews of Geophysics, 51, 276–299. https://doi.org/10.1002/rog.20011

Flores-Rodriguez, C., Nagendranatha Reddy, C., and Min, B. (2019) Enhanced methane production from acetate intermediate by bioelectrochemical anaerobic digestion at optimal applied voltages. *Biomass and Bioenergy* **127**: 105261.

Galimov E. M. and Kvenvolden K. A. (1983) Concentrations and carbon isotopic compositions of CH_4 and CO_2 in gas from sediments of the Blake Outer Ridge, Deep Sea Drilling Project Leg 76, In Initial Reports, Deep Sea Drilling Project 76 (Edited by Sheridan R.E., Gradstein F. M. et al.), pp. 403407. U.S. Government Printing Office, Washington, D.C.

Ginsburg G., Guseynov R.A., Dadashev A.A., Ivanova G.A., Kazantsev S.A., Soloviev V.A., Telepnev E.V., Askeri-Nasirov P.Ye., Yesikov A.A., Mal'tseva V.I., Mashirov Yu.G., Shabayeva I.Yu. Gas hydrates of the southern Caspian Int. Geol. Rev., 43 (1992), pp. 765-782

Giovannini, G., Donoso-Bravo, A., Jeison, D., Chamy, R., Ruíz-Filippi, G., and Vande Wouwer, A. (2016) A review of the role of hydrogen in past and current modelling approaches to anaerobic digestion processes. *International Journal of Hydrogen Energy* **41**: 17713–17722.

Gomez Vidales, A., Omanovic, S., and Tartakovsky, B. (2019) Combined energy storage and methane bioelectrosynthesis from carbon dioxide in a microbial electrosynthesis system. *Bioresource Technology Reports* **8**: 100302.

Holmes, D.E., Shrestha, P.M., Walker, D.J.F., Dang, Y., Nevin, K.P., Woodard, T.L., and Lovley, D.R. (2017) Metatranscriptomic Evidence for Direct Interspecies Electron Transfer between Geobacter and Methanothrix Species in Methanogenic Rice Paddy Soils. *Appl Environ Microbiol* **83**:.

Jackson, B. E. and McInerney, M. J. (2002) Anaerbic microbial metabolism can procedd close to thermodynamic limits. Nature, 415, 454-456

Joseph W. Lengeler (1999). *Biology of the Prokaryotes*. Stuttgart: Thieme. p. 796. ISBN 978-0-632-05357-5.

Jenden, P.D. and Kaplan, I.R. (1986) Comparison of microbial* gases from the Middle America Trench and Scripps Submarine Canyon: implications for the origin of natural gas. *Applied Geochemistry* **1**: 631–646.

Kato, S., Hashimoto, K., and Watanabe, K. (2012) Methanogenesis facilitated by electric syntrophy via (semi)conductive iron-oxide minerals. *Environmental Microbiology* **14**: 1646–1654.

Kokko, M., Epple, S., Gescher, J., and Kerzenmacher, S. (2018) Effects of wastewater constituents and operational conditions on the composition and dynamics of anodic microbial communities in bioelectrochemical systems. *Bioresource Technology* **258**: 376–389.

Kristjansson, J.K., Schönheit, P., and Thauer, R.K. (1982) Different Ks values for hydrogen of methanogenic bacteria and sulfate reducing bacteria: An explanation for the apparent inhibition of methanogenesis by sulfate. *Arch Microbiol* **131**: 278–282.

Kulongoski, J.T., McMahon, P.B., Land, M., Wright, M.T., Johnson, T.A., and Landon, M.K. (2018) Origin of Methane and Sources of High Concentrations in Los Angeles Groundwater. *Journal of Geophysical Research: Biogeosciences* **123**: 818–831.

Kurade, M.B., Saha, S., Salama, E.-S., Patil, S.M., Govindwar, S.P., and Jeon, B.-H. (2019) Acetoclastic methanogenesis led by Methanosarcina in anaerobic co-digestion of fats, oil and grease for enhanced production of methane. *Bioresource Technology* **272**: 351–359.

Kvenvolden, K.A. (1995) A review of the geochemistry of methane in natural gas hydrate. *Organic Geochemistry* **23**: 997–1008.

Kvenvolden, K.A. (1993) Gas hydrates—geological perspective and global change. *Reviews of Geophysics* **31**: 173–187.

Lee, J.-Y., Lee, S.-H., and Park, H.-D. (2016) Enrichment of specific electro-active microorganisms and enhancement of methane production by adding granular activated carbon in anaerobic reactors. *Bioresource Technology* **205**: 205–212.

Li, M., Zhou, M., Tian, X., Tan, C., McDaniel, C.T., Hassett, D.J., and Gu, T. (2018) Microbial fuel cell (MFC) power performance improvement through enhanced microbial electrogenicity. *Biotechnology Advances* **36**: 1316–1327.

Li, Y., Chen, Y., and Wu, J. (2019) Enhancement of methane production in anaerobic digestion process: A review. *Applied Energy* **240**: 120–137.

Liu, F., Rotaru, A.-E., Shrestha, P.M., Malvankar, N.S., Nevin, K.P., and Lovley, D.R. (2012) Promoting direct interspecies electron transfer with activated carbon. *Energy Environ Sci* **5**: 8982–8989.

Liu, H., Grot, S., and Logan, B.E. (2005) Electrochemically Assisted Microbial Production of Hydrogen from Acetate. *Environ Sci Technol* **39**: 4317–4320.

Logan, B.E., Call, D., Cheng, S., Hamelers, H.V.M., Sleutels, T.H.J.A., Jeremiasse, A.W., and Rozendal, R.A. (2008) Microbial Electrolysis Cells for High Yield Hydrogen Gas Production from Organic Matter. *Environ Sci Technol* **42**: 8630–8640.

Logan, B.E., Hamelers, B., Rozendal, R., Schröder, U., Keller, J., Freguia, S., et al. (2006) Microbial Fuel Cells: Methodology and Technology. *Environ Sci Technol* **40**: 5181–5192.

Lovley, D.R. (2011) Live wires: direct extracellular electron exchange for bioenergy and the bioremediation of energy-related contamination. *Energy Environ Sci* **4**: 4896–4906.

Mackenzie, A.S. and Quigley, T.M. (1988) Principles of Geochemical Prospect Appraisal. *AAPG Bulletin* **72**: 399–415.

Malvankar, N.S., Vargas, M., Nevin, K.P., Franks, A.E., Leang, C., Kim, B.-C., et al. (2011) Tunable metallic-like conductivity in microbial nanowire networks. *Nature Nanotechnology* **6**: 573–579.

Marsili, E., Sun, J., and Bond, D.R. (2010) Voltammetry and Growth Physiology of Geobacter sulfurreducens Biofilms as a Function of Growth Stage and Imposed Electrode Potential. *Electroanalysis* **22**: 865–874.

Martens, C. S., Blair, N. E., Green, C. D., & Des Marais, D. J. (1986). Seasonal variations in the stable carbon isotopic signature of biogenic methane in coastal sediment. Science, 233(4770), 1300–1303.

Milkov, A.V. (2004) Global estimates of hydrate-bound gas in marine sediments: how much is really out there? *Earth-Science Reviews* **66**: 183–197.

Nakamura, R., Takashima, T., Kato, S., Takai, K., Yamamoto, M., and Hashimoto, K. (2010) Electrical Current Generation across a Black Smoker Chimney. *Angewandte Chemie International Edition* **49**: 7692–7694.

Naomichi Nishio, Physiology and Utilization of Methanogens, Chemistry and Biology, Vol. 30, No. 8, pp.537-542, 1992

西尾尚道, メタン生成菌の生理と利用, 化学と生物, Vol. 30, No. 8, pp.537-542, 1992

Ooka, H., McGlynn, S.E., and Nakamura, R. (2019) Electrochemistry at Deep-Sea Hydrothermal Vents: Utilization of the Thermodynamic Driving Force towards the Autotrophic Origin of Life. *ChemElectroChem* **6**: 1316–1323.

Parkes, M., Barrett, J.C., Prescott, N.J., Tremelling, M., Anderson, C.A., Fisher, S.A., et al. (2007) Sequence variants in the autophagy gene IRGM and multiple other replicating loci contribute to Crohn's disease susceptibility. *Nat Genet* **39**: 830–832.

Potter, J., & Konnerup-Madsen, J. (2003). A review of the occurrence and origin of abiogenic hydrocarbons in igneous rocks. Geological Society, London, Special Publications, 214(1), 151–173. https://doi.org/10.1144/gsl.sp.2003.214.01.10

Peng, H., Zhao, Z., Xiao, H., Yang, Y., Zhao, H., and Zhang, Y. (2019) A strategy for enhancing anaerobic digestion of waste activated sludge: Driving anodic oxidation by adding nitrate into microbial electrolysis cell. *Journal of Environmental Sciences* **81**: 34–42.

Reguera, G., McCarthy, K.D., Mehta, T., Nicoll, J.S., Tuominen, M.T., and Lovley, D.R. (2005) Extracellular electron transfer via microbial nanowires. *Nature* **435**: 1098–1101.

Rollefson, J.B., Stephen, C.S., Tien, M., and Bond, D.R. (2011) Identification of an Extracellular Polysaccharide Network Essential for Cytochrome Anchoring and Biofilm Formation in Geobacter sulfurreducens. *Journal of Bacteriology* **193**: 1023–1033.

Rotaru, A.-E., Shrestha, P.M., Liu, F., Shrestha, M., Shrestha, D., Embree, M., et al. (2013) A new model for electron flow during anaerobic digestion: direct interspecies electron transfer to Methanosaeta for the reduction of carbon dioxide to methane. *Energy Environ Sci* **7**: 408–415.

Rozendal, R.A., Hamelers, H.V.M., Euverink, G.J.W., Metz, S.J., and Buisman, C.J.N. (2006) Principle and perspectives of hydrogen production through biocatalyzed electrolysis. *International Journal of Hydrogen Energy* **31**: 1632–1640.

Rozendal, R.A., Jeremiasse, A.W., Hamelers, H.V.M., and Buisman, C.J.N. (2008) Hydrogen Production with a Microbial Biocathode. *Environ Sci Technol* **42**: 629–634.

Sassen R., MacDonald I.R.. Evidence of structure H hydrate, Gulf of Mexico continental slope Org. Geochem., 22 (1994), pp. 1029-1032

Salgado-Dávalos, V., Osorio-Avilés, S., Kamaraj, S.K., Vega-Alvarado, L., Juárez, K., Silva-Martínez, S., and Alvarez-Gallegos, A. (2021) Sediment Microbial Fuel Cell Power Boosted by Natural Chitin Degradation and Oxygen Reduction Electrocatalysts. *CLEAN – Soil, Air, Water* **49**: 2000465.

Salvador, A.F., Martins, G., Melle-Franco, M., Serpa, R., Stams, A.J.M., Cavaleiro, A.J., et al. (2017) Carbon nanotubes accelerate methane production in pure cultures of methanogens and in a syntrophic coculture. *Environ Microbiol* **19**: 2727–2739.

Sarmin, S., Ethiraj, B., Islam, M.A., Ideris, A., Yee, C.S., and Khan, Md.M.R. (2019) Bio-electrochemical power generation in petrochemical wastewater fed microbial fuel cell. *Science of The Total Environment* **695**: 133820.

Schlager, S., Haberbauer, M., Fuchsbauer, A., Hemmelmair, C., Dumitru, L.M., Hinterberger, G., et al. (2017) Bio-Electrocatalytic Application of Microorganisms for Carbon Dioxide Reduction to Methane. *ChemSusChem* **10**: 226–233.

Schoell, M. (1980) The hydrogen and carbon isotopic composition of methane from natural gases of various origins. *Geochimica et Cosmochimica Acta* **44**: 649–661.

Schoell, M. (1983) Genetic Characterization of Natural Gases. *AAPG Bulletin* **67**: 2225–2238.

Schoell, M. (1988) Multiple origins of methane in the Earth. *Chemical Geology* **71**: 1–10.

Stams, A.J.M., Bok, F.A.M.D., Plugge, C.M., Eekert, M.H.A.V., Dolfing, J., and Schraa, G. (2006) Exocellular electron transfer in anaerobic microbial communities. *Environmental Microbiology* **8**: 371–382.

Stewart, L.C., Algar, C.K., Fortunato, C.S., Larson, B.I., Vallino, J.J., Huber, J.A., et al. (2019) Fluid geochemistry, local hydrology, and metabolic activity define methanogen community size and composition in deep-sea hydrothermal vents. *The ISME Journal* **13**: 1711–1721.

Tabatabaei, M., Rahim, R.A., Abdullah, N., Wright, A.-D.G., Shirai, Y., Sakai, K., et al. (2010) Importance of the methanogenic archaea populations in anaerobic wastewater treatments. *Process Biochemistry* **45**: 1214–1225.

Takai, K., Gamo, T., Tsunogai, U., Nakayama, N., Hirayama, H., Nealson, K.H., and Horikoshi, K. (2004) Geochemical and microbiological evidence for a hydrogen-based, hyperthermophilic subsurface lithoautotrophic microbial ecosystem (HyperSLiME) beneath an active deep-sea hydrothermal field. *Extremophiles* **8**: 269–282.

Takai, K., Nakamura, K., Toki, T., Tsunogai, U., Miyazaki, M., Miyazaki, J., et al. (2008) Cell proliferation at 122°C and isotopically heavy CH4 production by a hyperthermophilic methanogen under high-pressure cultivation. *PNAS* **105**: 10949–10954.

Tartakovsky, B., Manuel, M.-F., Wang, H., and Guiot, S.R. (2009) High rate membrane-less microbial electrolysis cell for continuous hydrogen production. *International Journal of Hydrogen Energy* **34**: 672–677.

Thauer, R.K. and Shima, S. (2006) Methane and microbes. *Nature* **440**: 878–879.

Uchiyama, T., Ito, K., Mori, K., Tsurumaru, H., and Harayama, S. (2010) Iron-Corroding Methanogen Isolated from a Crude-Oil Storage Tank. *Appl Environ Microbiol* **76**: 1783–1788.

Venzlaff, H., Enning, D., Srinivasan, J., Mayrhofer, K.J.J., Hassel, A.W., Widdel, F., and Stratmann, M. (2013) Accelerated cathodic reaction in microbial corrosion of iron due to direct electron uptake by sulfate-reducing bacteria. *Corrosion Science* **66**: 88–96.

Villano, M., Aulenta, F., Ciucci, C., Ferri, T., Giuliano, A., and Majone, M. (2010) Bioelectrochemical reduction of CO2 to CH4 via direct and indirect extracellular electron transfer by a hydrogenophilic methanogenic culture. *Bioresource Technology* **101**: 3085–3090.

Walker, D.J.F., Martz, E., Holmes, D.E., Zhou, Z., Nonnenmann, S.S., and Lovley, D.R. (2019) The Archaellum of Methanospirillum hungatei Is Electrically Conductive. *mBio* **10**:.

Wakita H., Nakamura Y., Notsu K., Noguchi M., Asada Radon T. anomaly: a possible precursor of the 1978 Izu-Oshima-Kinkai earthquake. Science, 207 (1980), pp. 882-883

Welhan, J. A. (1988). Origins of methane in hydrothermal systems. Chemical Geology, 71(1-3), 183–198. https://doi.org/10.1016/0009- 2541(88)90114-3

Whiticar, M.J. (1999) Carbon and hydrogen isotope systematics of bacterial formation and oxidation of methane. *Chemical Geology* **161**: 291–314.

Whiticar, M.J., Faber, E., and Schoell, M. (1986) Biogenic methane formation in marine and freshwater environments: CO2 reduction vs. acetate fermentation—Isotope evidence. *Geochimica et Cosmochimica Acta* **50**: 693–709.

Xu, R., Xu, S., Florentino, A.P., Zhang, L., Yang, Z., and Liu, Y. (2019) Enhancing blackwater methane production by enriching hydrogenotrophic methanogens through hydrogen supplementation. *Bioresource Technology* **278**: 481–485.

Yamamoto, M., Nakamura, R., Kasaya, T., Kumagai, H., Suzuki, K., and Takai, K. (2017) Spontaneous and Widespread Electricity Generation in Natural Deep-Sea Hydrothermal Fields. *Angewandte Chemie International Edition* **56**: 5725–5728.

Yamamoto, M., Nakamura, R., and Takai, K. (2018) Deep-Sea Hydrothermal Fields as Natural Power Plants. *ChemElectroChem* **5**: 2162–2166.

Yoshioka, H., Mochimaru, H., Sakata, S., Takeda, H., and Yoshida, S. (2015) Methane production potential of subsurface microbes in Pleistocene sediments from a natural gas field of the dissolved-in-water type, central Japan. *Chemical Geology* **419**: 92–101.

Zakaria, B.S. and Dhar, B.R. (2021) Characterization and significance of extracellular polymeric substances, reactive oxygen species, and extracellular electron transfer in methanogenic biocathode. *Sci Rep* **11**: 1–13.

Zhao, Z., Zhang, Y., Wang, L., and Quan, X. (2015) Potential for direct interspecies electron transfer in an electric-anaerobic system to increase methane production from sludge digestion. *Scientific Reports* **5**: 11094.

Zhao, Z., Zhang, Y., Yu, Q., Dang, Y., Li, Y., and Quan, X. (2016) Communities stimulated with ethanol to perform direct interspecies electron transfer for syntrophic metabolism of propionate and butyrate. *Water Research* **102**: 475–484.

Zhao, Z., Zhang, Y., Yu, Q., Ma, W., Sun, J., and Quan, X. (2016) Enhanced decomposition of waste activated sludge via anodic oxidation for methane production and bioenergy recovery. *International Biodeterioration & Biodegradation* **106**: 161–169.

Zhen, G., Zheng, S., Lu, X., Zhu, X., Mei, J., Kobayashi, T., et al. (2018) A comprehensive comparison of five different carbon-based cathode materials in CO_2 electromethanogenesis: Long-term performance, cell-electrode contact behaviors and extracellular electron transfer pathways. *Bioresource Technology* **266**: 382–388.

Zinder, S.H. (1993) Physiological Ecology of Methanogens. In *Methanogenesis: Ecology, Physiology, Biochemistry & Genetics*. Chapman & Hall Microbiology Series. Ferry, J.G. (ed). Boston, MA: Springer US, pp. 128–206.

Chapter

3

Bioelectrical methane production coupled with an abiotic ammonia oxidation

3.1 Introduction

Methane is the prime component of natural gas and is widely utilized as an energy source worldwide. It is mainly produced by biological and physical actions that together contribute to 20%–80% of natural gas reserves (Rice and Claypool, 1981). Methane is physically produced through the thermal decomposition of organic matter in association with coal, gas, and oil formations (Schoell, 1988). Conversely, biological methane formation is primarily performed by methanogenic microbes (methanogens) in anaerobic environments (Whiticar *et al.*, 1986; Whiticar, 1999). Only methanogenic archaea are known to act as methanogens, and these use substrates such as acetate, formate, and hydrogen gas produced from organic matter during fermentation. Such methane fermentation occurs in nature but has also been applied as an eco-friendly wastewater treatment technology (Onodera, 2013; Townsend-Small *et al.*, 2016). The artificially produced biogas can also be utilized as an energy source after purification.

It is also possible to generate electricity from organic substances. Microbial fuel cell (MFC) technology is fascinating, and its application to wastewater treatment has been extensively studied (Logan *et al.*, 2006; Sarmin *et al.*, 2019; Wang *et al.*, 2020). Conversely, in microbial electrosynthesis systems (MESs), methane is produced by providing electricity (Rabaey and Rozendal, 2010; Eerten-Jansen *et al.*, 2012). High methane production can be expected when applying MESs to wastewater treatment because of the combination of methane fermentation using organic substances and conversion of CO_2 to methane by microbes through electricity (Clauwaert *et al.*, 2008; Clauwaert and Verstraete, 2009; Zhao *et al.*, 2016; Park *et al.*, 2018; Peng *et al.*, 2019). Ding *et al.* (2016) found 0.8 V to be the optimal applied voltage for appropriate wastewater treatment and maximum methane production using an MES.

In the MES, bioelectrical methane production is performed without organic substrates (Cheng *et al.*, 2009; Villano *et al.*, 2010; Zhen *et al.*, 2015). Cheng *et al.* (2009) found that carbon dioxide was reduced to methane at a biocathode potential of <-0.7 V (vs. Ag/AgCl). At −1.0 V (vs. Ag/AgCl), the electron capture efficiency of methane production was 96%. Two mechanisms have been proposed for biological methane production using a biocathode. First, at high applied voltages, methane may be produced by hydrogenotrophic methanogens using abiotic H_2 formed in water oxidation (Wagner *et al.*, 2009; Eerten-Jansen *et al.*, 2012). In this case, H_2 is an important intermediate for methane production. The second mechanism

is direct electrotrophic methane production. Cheng *et al.* (2009) reported that some methanogens must use electrons with CO_2 to directly produce methane, without hydrogen as an intermediary. Previous studies related to extracellular electron transfer have demonstrated that applied voltage might not be effective in promoting methane production, also suggesting a pathway without H_2 (Rotaru *et al.*, 2013; Lohner *et al.*, 2014; Holmes *et al.*, 2017; Lee *et al.*, 2017). However, there was insufficient experimental data to prove direct electrotrophic methane production. It is still unclear whether bioelectrical methane production occurs via direct and/or indirect reaction(s) in MESs.

The CO_2 reduction potential to methane $E^{0'}_{cat}$ at the biocathode is -0.24 V (vs. SHE) under the standard condition at pH = 7. When coupled with H_2O oxidation ($E^{0'}_{an}$ = 0.81 V vs SHE) at the anode, methane production in an MES occurs thermodynamically by applying more than 1.05 V under the standard condition. If, instead of H_2O oxidation, oxidation of inorganic compounds with lower potential (such as NH_4^+ oxidation to NO_3^- and N_2: $E^{0'}_{an}$ = 0.36 V and –0.29 V vs. SHE, respectively) takes place, methane can be produced at a lower applied voltage. However, many MES studies do not provide sufficient information about the oxidation reaction at the anode, with experiments conducted at relatively high voltages.

In this study, we designed an MES experiment in which no organic substrate was supplied, and NH_4^+ was added to the anode chamber to investigate whether methane production is possible even at very low applied voltages. Although the reaction of electrotrophic methane production with NH_4^+ oxidation to N_2 thermodynamically proceeds even without electricity supply, this is the first study to report the coupling to the NH_4^+ oxidative reaction. In addition, the microbial community was analyzed to identify the organisms involved in bioelectrical methane production.

3.2 Materials and methods

3.2.1 MES set-up

The MES used in this study consisted of two glass chambers with each effective volume of 70 ml, which were connected with a salt bridge of approximately 10 cm length containing 2% (w/w) agar (KF-30, Fujirika, Japan) and 20% (w/w) KCl (**Fig. 3-1**). The top of each chamber was connected to a 10 mL loss-of-resistance glass syringe to release the pressure in the chamber generated from the produced gas and facilitate gas collection.

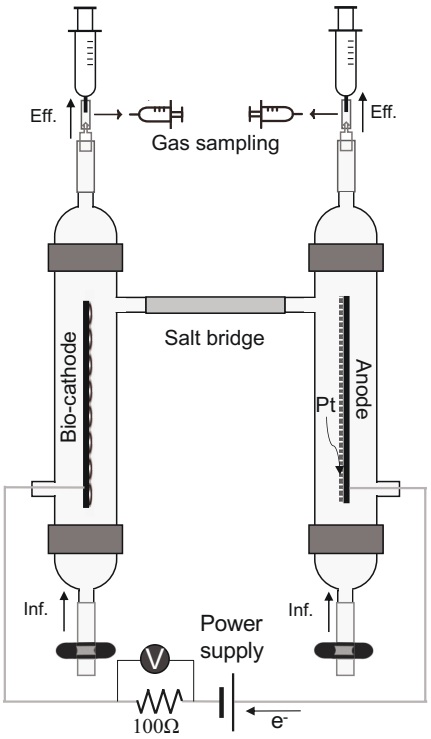

Fig. 3-1 Schematic of MES consisting of two chambers connected with a salt bridge.

Fig. 3-2 MES in operations

A 9 cm^2 electrode of carbon cloth (Toyobo Company, Japan) was installed in both chambers. The biocathode and anode electrodes were connected to a DC power supply (Array 3600 Series, T&C Technology, Japan) using a platinum wire. A 100 Ω resistor was inserted between the power supply and the biocathode electrode to estimate electric current by measuring voltage using a digital multimeter (FlePow, Levin Japan company, Japan). Even if the external resister is inserted, the effect on the actual applied voltage is negligible when the internal resistance of the MES is so high. A small amount of anaerobic sludge taken from a laboratory-scale UASB (upflow anaerobic sludge blanket) reactor was inoculated on the surface of the cathode electrode. A platinum powder (10% by weight platinum on carbon powder; E-TEK, C-1 10% Pt on Vulcan XC-72) was coated on the surface of the anode, according to previous studies (Müller and Spitzer, 1905; Nutt and Kapur, 1968; De Vooys *et al*., 2001; Bunce and Bejan, 2011; Li *et al.*, 2017).

Table 3-1 MES operational conditions

Batch no.	Duration	Voltage	pH at the end	
	(d)	(V)	Biocathode	Anode
1	3	2.0	8.1	6.7
2		1.6	8.1	7.5
3		1.4	7.9	7.6
4		2.0	7.9	7.4
5	5	2.0	8.6	7.0
6		1.6	8.7	7.0
7		1.4	8.5	7.0
8		1.2	7.9	7.3
9		1.0	7.6	7.2
10	6	0.8	7.6	7.1
11		0.6	7.6	7.3
12		0.4	7.4	7.3
13		0.1	7.7	7.6
14	5	1.4	7.6	7.2
15		3.0	9.7	6.8
16	6	1.2	7.7	7.2
17		0.8	7.4	7.3
18		0.4	7.5	7.4
19	8	1.0	7.6	7.2
20	13	0.05	7.5	7.5

3.2.2 MES operation

The MES was operated in batch processing mode at 30°C in a thermostatic chamber (**Table 3-1**). The anodic and biocathodic chambers were filled with the same medium without organic substances and deoxidized through a nitrogen purge. The medium was composed of $NaHCO_3$ (200 mg L^{-1}), NH_4Cl (190 mg L^{-1}), NaH_2PO_4 (17 mg L^{-1}), and Na_2HPO_4 (124 mg L^{-1}), as well as trace elements, including $FeSO_4 \cdot 7H_2O$ (7 mg L^{-1}), $CoCl_2 \cdot 6H_2O$ (1.7 mg L^{-1}), $ZnSO_4 \cdot 7H_2O$ (1.5 mg L^{-1}), HBO_3 (0.6 mg L^{-1}), $MnCl_2 \cdot 4H_2O$ (4.2 mg·L^{-1}), $NiCl_2 \cdot 4H_2O$ (0.4 mg L^{-1}), $CuCl_2 \cdot 2H2O$ (0.27 mg L^{-1}), and $Na_2MoO_2 \cdot 2H_2O$ (0.25 mg L^{-1}), at a pH of 7.5. The medium was completely replaced at intervals of 3, 5, 6, and 13 d, with the batch experiment repeated 20 times over 110 d of operation. Each batch duration time was determined dependent on gas production for gas sampling. Each batch experiment was performed at a constant applied voltage in the range of 0.05–3.0 V to investigate whether

methane production is possible even at low voltages. After setting up the MES, a voltage was immediately supplied to enhance microbial activity at the biocathode, and the anode was unsterilized.

3.2.3 Sampling and analyses

The volume of gas production in the respective chambers was measured using an airtight syringe. CH_4, N_2, CO_2, and H_2 concentrations were then measured using a gas chromatograph equipped with a thermal conductivity detector (GC-TCD, Shimadzu GC-8A). NH_4^+, NO_3^-, and NO_2^- concentrations in the medium were measured by ion chromatography (Shimadzu HPLC-20A) at the start and end of each batch operation. Dissolved CH_4 and N_2 concentrations were estimated using Henry's law.

3.2.4 Microbial community

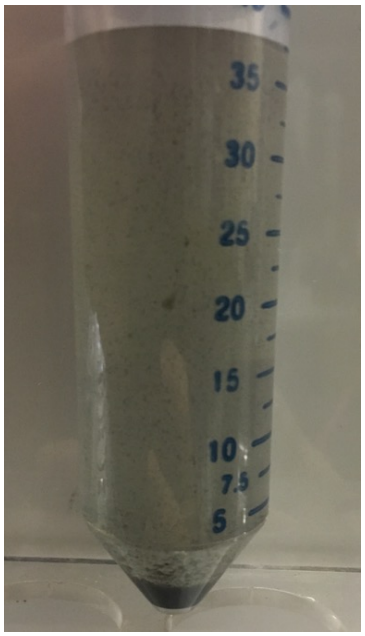

Fig. 3-3 Cathode's biomass

The sludge sample at the biocathode shown in **Fig. 3-3** was collected on day 110 of the last MES operation and washed with phosphate buffer. DNA was extracted using the FastDNA® SPIN Kit for Soil (MP Biomedicals, Solon, OH, USA), according to the manufacturer's instructions. PCR amplification of the 16S rRNA gene was performed using the primer sets 341'F (5'-CCTAHGGGRBGCAGCAG-3') and 805R (5′-GACTACHVGGGTATCTAATCC-3′) with KAFA HiFi Hotstart ReadyMix (Kapa Biosystems, USA). The PCR conditions were as follows: 3 min initial denaturation of DNA at 95 ºC, followed by 25 cycles of 30 s at 95 ºC, 30 s at 55 ºC, and 30 s at 72 ºC, with a final extension at 72 ºC for 5 min. The PCR product was purified and sequenced by the emulsion method using Illumina/Miseq (Illumina, Inc., San Diego, CA, USA) at Hokkaido System Science (Sapporo, Japan). The sequences obtained were analyzed using QIIME (v1.8.0) (Caporaso *et al.*, 2010). Operational taxonomic units (OTUs) were grouped based on a threshold value of 97% identity for DNA using the UCLUST algorithm (Edgar, 2010). These OTUs were classified using the Greengenes database (McDonald *et al.*, 2012; Werner *et al.*, 2012).

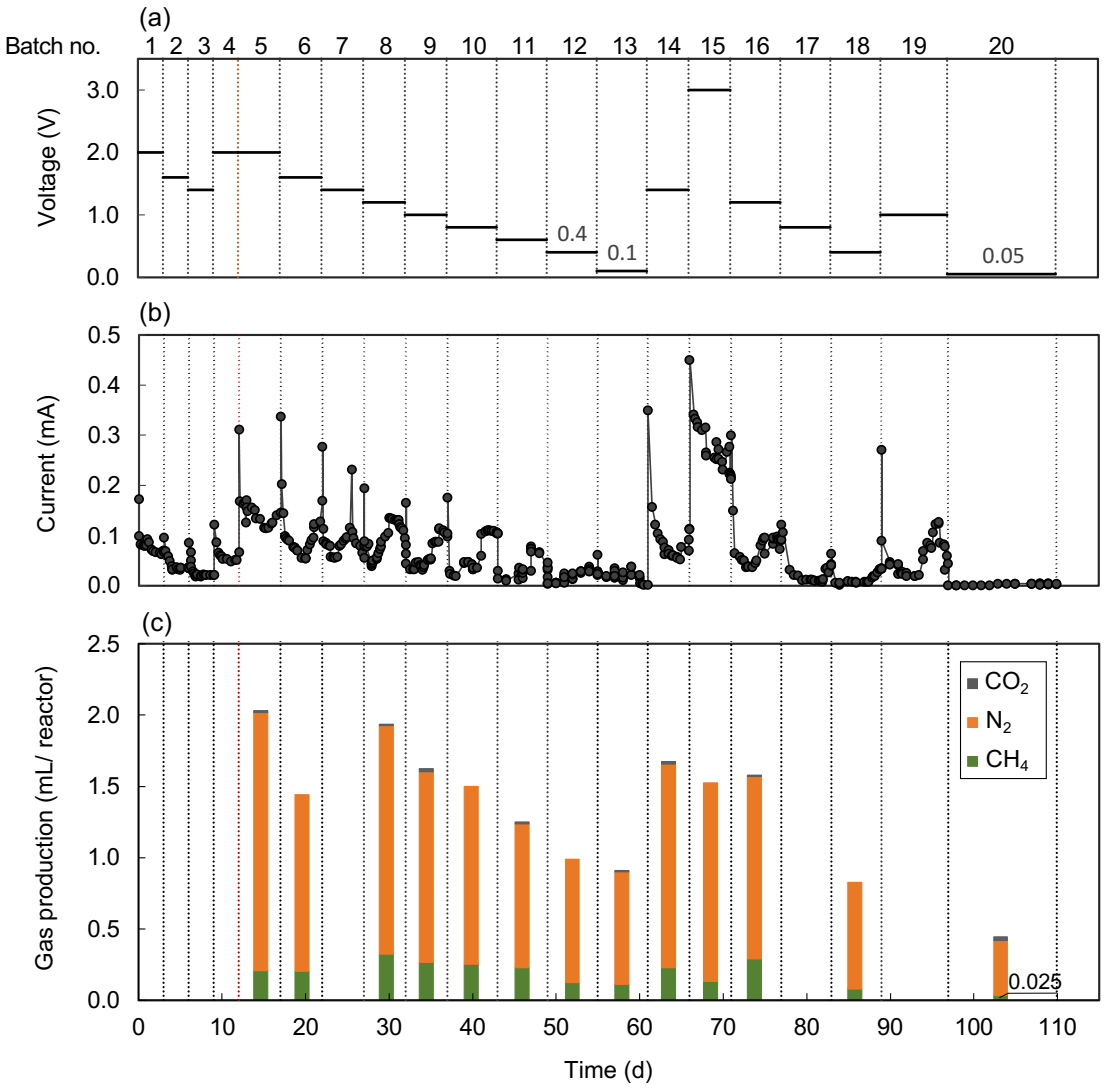

Fig. 3-4 Time courses of applied voltage (a), current (b), and gases (CH_4, N_2, and CO_2) produced (c) in batch experiments

The sequence data was deposited in the DDBJ database under DDBJ/EMBL/GenBank accession number DRA011341.

3.3 Results

3.3.1 Performance of batch experiments

In the MES batch operations, we first attempted to apply a relatively high voltage of 2.0 V over three days. Once a higher current of approximately 0.18 mA was observed, it immediately decreased to 0.09 mA and gradually declined over time, as shown in **Fig. 3-4**. However, no produced gas bubbles were visible in either the biocathode or anode chambers, despite sludge inoculation that should have enabled methane production activity. The three-

day batch experiment was then repeated with changes in bulk liquid but at lower voltages of 1.6 V and 1.4 V, resulting in current behaviors that were the same as at 2.0 V. Under these conditions, very few bubbles were observed in the biocathode chamber. For the next batch operation, where the applied voltage was returned to 2.0 V, bubbles were also observed. However, it was not possible to sample the produced gas because of its low volume.

Therefore, we changed the batch interval time from three to five days from day 12 onwards, except for some special batches. More bubbles were produced in the biocathode chamber and collected as a gas in the fifth batch operation at 2.0 V. Produced gas was approximately 2.0 mL on days 12–17 (**Fig. 3-4**). As expected, methane was detected, but its concentration was only 10.0%. The main component of the gas was N_2, with a very low concentration of CO_2. Surprisingly, the current was much higher compared with the previous batch experiment at the same voltage. It was also noted that the current decreased for approximately three days but increased thereafter. There was a significant difference between small and large gas production chambers with respect to current behavior. In control batch experiments without inoculation, methane was not detected in the range of 1.0–2.0 V, although hydrogen production was observed over 1.2 V in the cathode chamber. The methane production should be derived from inorganic carbon in the presence of microbes on the carbon cloth, the biological activity of which would be enhanced after 17 days of operation. However, no bubbles were observed in the anode chamber under any conducted conditions.

To investigate the effect of voltage on methane production, experiments were continuously performed while decreasing applied voltage step-by-step down to 0.1 V until day 60 (**Fig. 3-4**). The current tended to decrease with decreasing voltage, but its pattern of behavior was similar in each batch period. The gas containing CH_4 and N_2 was produced at any voltage, except during days 22–27, when the gas sampling failed.

Given that high N_2 concentrations of approximately 75% to 90% were detected, to reveal the source of N_2 yield by measuring ammonium, nitrate, and nitrite, we reconducted batch experiments under almost identical conditions over a range of 0.05–3.0 V on days 55–110. In the last batch operation, we also attempted methane production at a very low voltage of 0.05 V. Surprisingly, a small amount of gas containing 6.09% CH_4 was collected, even at the lowest voltage, especially over a prolonged period of 13 days. Concentrations of NH_4^+

and NO_3^- decreased in both chambers of the biocathode and anode (**Fig. 3-5**). The total nitrogen ions of the two chambers decreased in all batches, suggesting that the yield of N_2 was derived from inorganic nitrogen ions. With respect to nitrogen balance, a strong relationship was observed between the amount of consumed NH_4^+ plus NO_3^- and produced N_2 (**Fig. 3-6**). Cecconet *et al*. (2019) reported accumulation of NO_2^- and N_2O in a biocathodic denitrification process for groundwater bioremediation. However, these intermediates in denitrification were not detected in this MES experiment. No accumulation of intermediates might be caused by a slow reaction.

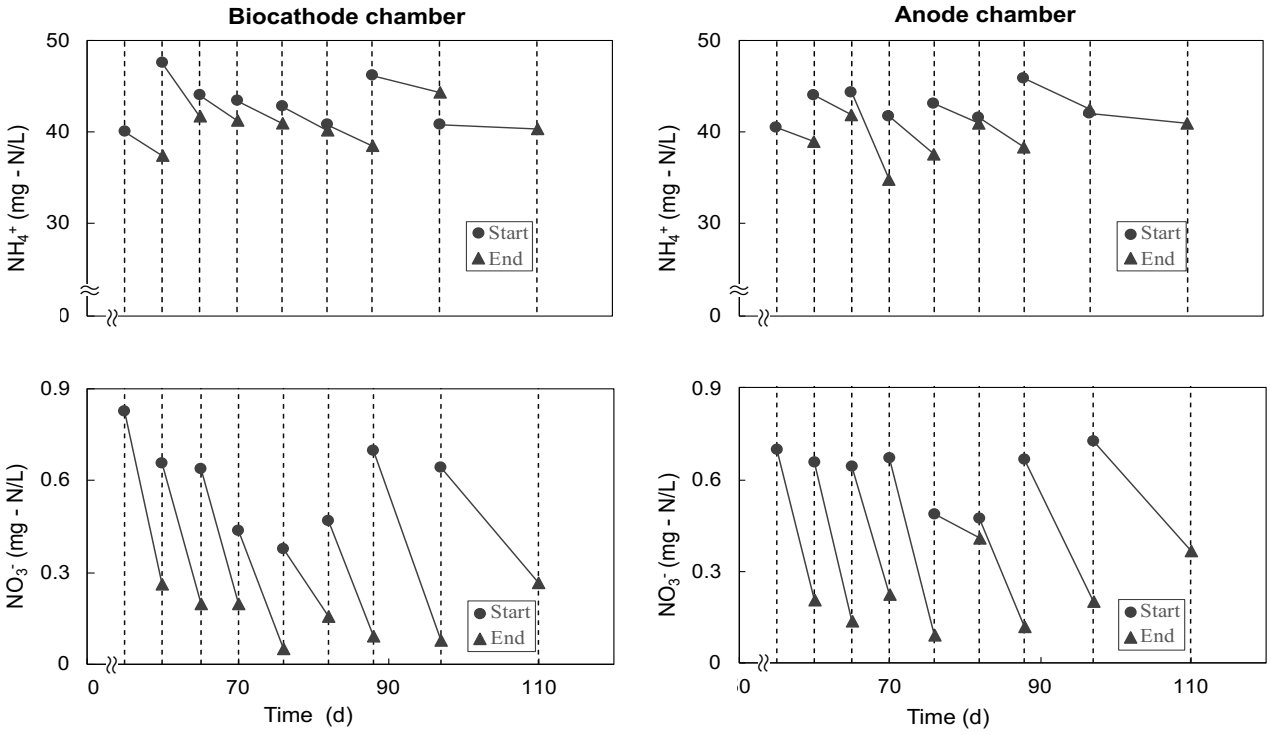

Fig. 3-5 NH_4^+–N and NO_3^-–N at the start and end of each batch operation.

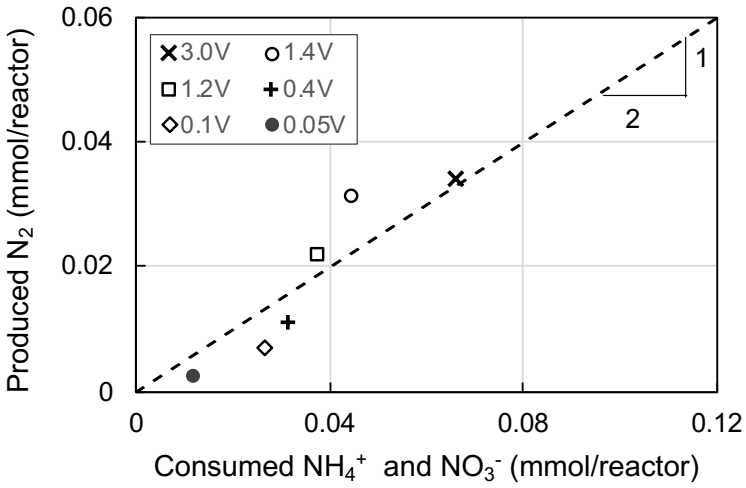

Fig. 3-6 Relationship between the produced N_2 and total amount of consumed NH_4^+ and NO_3^-.

3.3.2 Effect of voltage on gas production

Although a 100 Ω external resistor was inserted, the supplied voltage was nearly equal to the actual applied voltage between the biocathode and anode because the current versus the supplied voltage was small throughout the experiment, as shown in **Fig. 3-3**. The gas production rate was significantly dependent on the applied voltage, as shown in **Fig. 3-7**. CH_4 production tended to increase in proportion to the voltage with 0.306 mL at 1.2 V, after which it decreased to 0.128 mL at 3.0 V. These results suggest that a very high voltage does not always enhance methane production and would have a negative effect on the microbes.

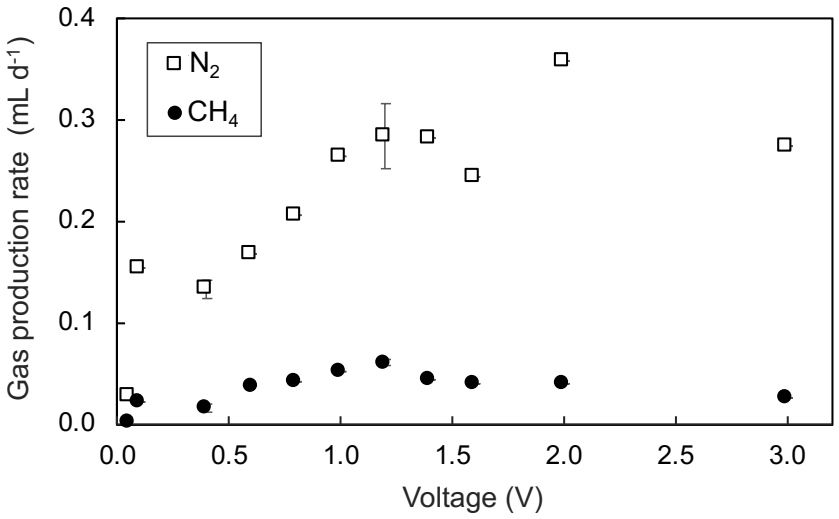

Fig. 3-7 Gas production rates at different applied voltages

The N_2 production rate was similar to that of CH_4 with respect to the effects of voltage, although large fluctuations were observed. This suggests that microbes also play a role in N_2 production. The retained microbes should grow and increase with operational time. However, these were slightly detached when bulk liquid was replaced as a result of changes in batch conditions. The number of microbes was therefore unstable, possibly contributing to fluctuations in gas production.

3.3.3 Microbial community

In the 16S rRNA gene sequencing of the biomass sample on day 110, more than 100,000 reads, including domain bacteria and archaea, were obtained, and the number of OTUs exceeded 1,200. Sequencing results revealed the presence of bacterial and archaeal communities (**Fig. 3-8**). Archaea comprised only 3.9% of the total reads.

The major families of bacteria were *Porphyromonadaceae*, *Rhodocyclaceae*, and *Geobacterceae*, contributing 26.8%, 11.4%, and 10.7%, respectively. The three families made up approximately 45% of all microbes. Of the most dominant family *Porphyromonadaceae*, approximately 50% was an obligately anaerobic genus of *Petrimonas*, while 29.8% uncultured genera were detected (Fig. 3). *Petrimonas* consists of hydrogen-producing bacteria (Lu *et al.*, 2012; Sun *et al.*, 2015; Liu *et al.*, 2016), suggesting that hydrogen is produced in the biocathode chamber. Most bacteria belonging to *Rhodocyclaceae* exhibit denitrification activity (Zhao *et al.*, 2013; Wang *et al.*, 2017). The detected predominant *Azonexus* genus, which can grow on molecular hydrogen as an electron donor (Zhao *et al.*, 2011; Liang *et al.*, 2021), plays an important role in the denitrification process to produce nitrogen gas. Only *Geobacter* was detected within the *Geobacterceae* family. The presence of electrically conductive pili or flagella on *Geobacter* species is reportedly linked to electron transfer in the MFC (Cabezas *et al.*, 2015; Yan *et al.*, 2020). In this study, *Geobacter* was likely responsible for electron transfer to yield biogas.

Regarding archaea, all OTUs were *Euryarchaeota*. Almost all detected *Euryarchaeota* were methanogens, with the dominant family (81.7%) being *Methanobacteriaceae*, a hydrogen-utilizing methanogen (**Fig. 3-8**). Two genera, namely *Methanobrevibacter* and *Methanobacterium,* were detected at concentrations of 63.8% and 36.3%, respectively (**Fig. 3-8**). These play a major role in CH_4 production in the biocathode chamber. In addition,

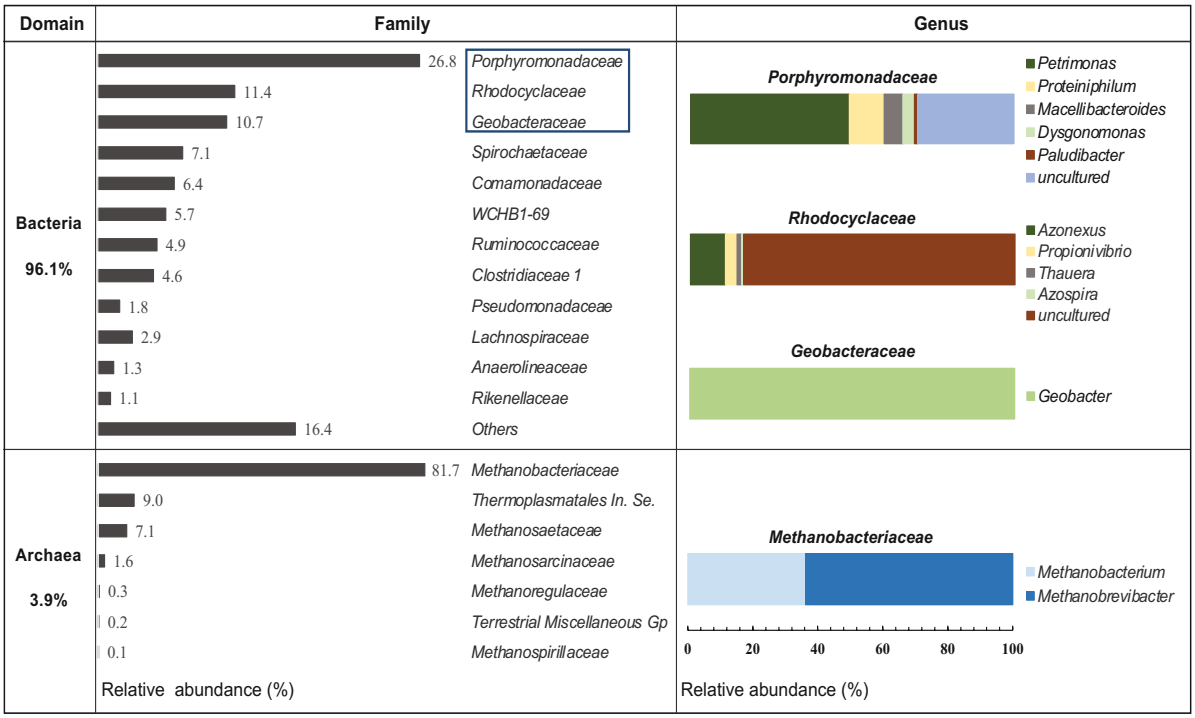

Fig. 3-8 Microbial community of biomass on day 110, based on 16S rRNA gene.

Methanosaetaceae, an obligate acetoclastic methanogen, was detected, albeit at a low concentration (7.1%); this means that acetate might be produced and converted to CH_4. However, its contribution is likely insignificant.

The biological contributors to denitrification and methane production were thus identified; the produced gas containing CH_4 and N_2 can be explained by the presence of these microbes. Thus, we demonstrated the biological production of CH_4 through the provision of electricity even at very low voltages and in the absence of organic substances in the MES.

3.4 Discussion

NH_4^+ oxidation was observed in the anode chamber, although in insignificant amounts, indicating that NH_4^+ was oxidized by donating electrons to the biocathode. Platinum is commonly accepted as the most promising catalyst in the electrochemical oxidation of ammonia (*e.g.,* De Vooys *et al*., 2001; Li *et al*., 2017). Müller and Spitzer (1905) reported that the anodic products of electrolyzing ammonia at a platinum anode were mainly NO_3^- and N_2 (25%–35%). In such over-oxidation, NO_2^- and NO_3^- products were observed over + 0.6 V (vs Ag/AgCl) (Endo *et al.*, 2005; Bunce and Bejan, 2011). NO_3^- was also reportedly

formed from NH_4^+ by catalytic oxidation with PtO_x (Fóti and Comninellis, 2004; Panizza and Cerisola, 2009). In this study, because platinum powder was coated on the surface of the anode with a carbon cloth electrode, similar reactions to electrolysis of water occurred, although neither N_2 nor NO_2^- production was observed.

The oxidation of NH_4^+ at the anode can be represented as follows:

$$1/8\ NH_4^+ + 3/8\ H_2O \rightarrow 1/8\ NO_3^- + 5/4\ H^+ + e^- \quad (3\text{-}1)$$

The produced NO_3^- was transferred to the biocathode chamber through the salt bridge by diffusion, resulting in a decrease in NO_3^- concentration in the anode chamber (**Fig. 3-5**) because of N_2 production in the biocathode chamber.

CH_4 and N_2 production (**Fig. 3-9**) in the biocathode chamber suggests that the reduction reactions of NO_3^- and CO_2 are represented, respectively, as follows:

$$1/8\ CO_2 + H^+ + e^- \rightarrow 1/8\ CH_4 + 1/4\ H_2O \quad (3\text{-}2)$$

$$1/5\ NO_3^- + 6/5\ H^+ + e^- \rightarrow 1/10\ N_2 + 3/5\ H_2O \quad (3\text{-}3)$$

Based on Faraday's laws of electrolysis, the number of donated electrons, *Ne* [mol], can be calculated from the measured current using the following equation:

$$Ne = \frac{\int Idt}{F} \quad (3\text{-}4)$$

where I is the current (A), t is the time (s), and F is the Faraday's constant (C mol^{-1})

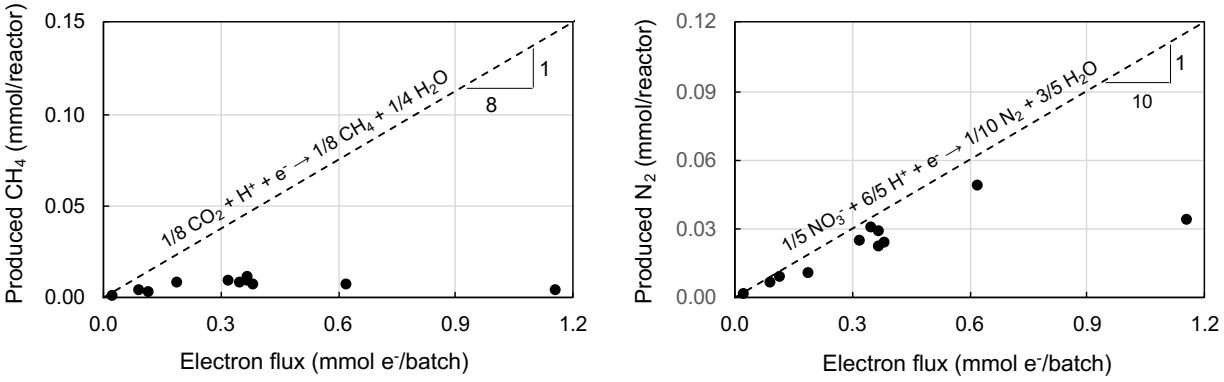

Fig. 3-9 Produced CH_4 and N_2 versus electron flux *Ne*. Circle: measured productions, dash lines: theoretical production assuming that all yield electrons *Ne* are only used for the reduction of CO_2 or NO_3^-.

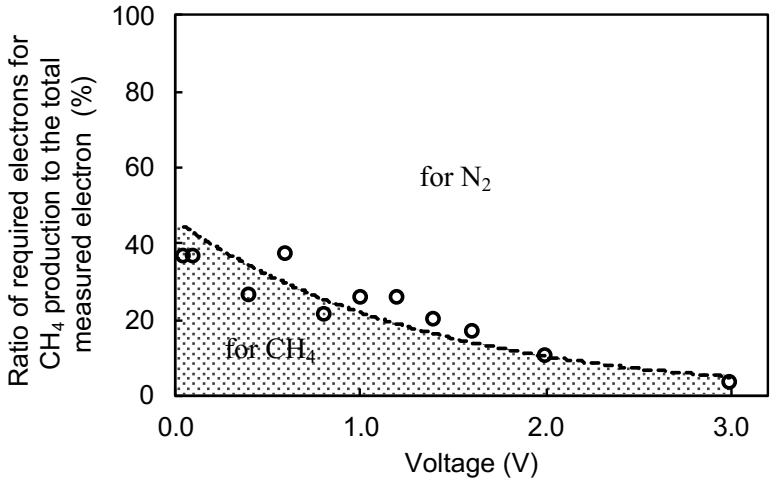

Fig. 3-10 Relationship between the ratio of required electrons for CH_4 production to total measured electrons *Ne* and applied voltage.

Assuming that all yield electrons *Ne*, calculated as per Eq. (3-4), are used for the reduction of only CO_2 or NO_3^-, the amounts of produced CH_4 and N_2 versus electron yield were calculated using Eqs. (3-2) and (3-3), respectively. The measured CH_4 production was much less than the calculated value, and the measured N_2 production was also smaller than

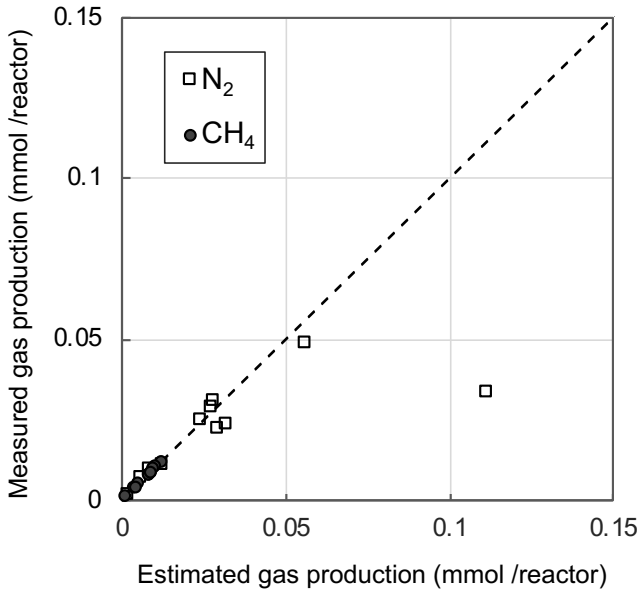

Fig. 3-11 Comparison between measured and estimated gas production. Estimation of produced CH_4 and N_2 was performed assuming that all electrons *Ne* were used for reduction of both CO_2 and NO_3^-, while electrons from the ratio in Fig. 4 were used for CH_4 production.

the theoretical value under this assumption (**Fig. 3-9**). This means that the two reductions were simultaneously performed, and *Ne* was distributed in both the reductions. The required electrons for measured CH_4 production from CO_2 reduction were estimated using Eq. (3-2), with the ratio of required electrons to total measured electrons *Ne* shown in Fig. **3-10**. Surprisingly, the electron ratio tended to decrease with an applied voltage, rather than remaining constant. At very low voltages of 0.05 V and 0.1 V, approximately 40% of the current was used for CO_2 reduction to CH_4, while only approximately 5% was utilized at 3 V. Assuming that the current to electron ratio was used for CO_2 reduction and that the remaining electrons were used for NO_3^- reduction to N_2 as per Eq. (3-3), it is possible to estimate CH_4 and N_2 production from *Ne*. **Fig. 3-11** compares the measured and estimated CH_4 and N_2 production, with the curve showing the relationship between the electron ratio and voltage in Fig. 4 used in the calculation. A good agreement was observed for both CH_4 and N_2 production, meaning that the electron balance was almost maintained in this experiment, and production of CH_4 and N_2 would theoretically be performed in the biocathode chamber according to the reduction reactions of Eqs. (3-2) and (3-3). However, at a high voltage of 3.0 V, the calculated value of produced N_2 was far greater than the measured value (**Fig. 3-11**), indicating that some electrons were used for other reductions by chemical and/or microbial reactions. If NO_3^- reduction to NH_4^+ instead of N_2, which is the reverse reaction at the anode, is performed at the biocathode at high voltages, the reversible reactions will lead to a waste of electrons yielded in the MES. As reported, a high imposing voltage has a negative effect on methanogens (Ding *et al.*, 2016) and nitrate-reducing bacteria (Li *et al.*, 2001; Ding *et al.*, 2016), and excessive voltage would not only cause inhibition of microbial activity but also induce chemical reactions.

No hydrogen was detected. However, hydrogen should be produced in the biocathode chamber because of the presence of hydrogenotrophic methanogens such as *Methanobacterium* and *Methanobrevibacter* and hydrogenotrophic denitrifiers of *Rhodocyclaceae (Azonexus)*. In addition, the hydrogen-producing bacteria *Petrimonas* was present. Previous studies on MESs have also detected hydrogenotrophic methanogens such as *Methanobrevibacter*, *Methanocorpusculum,* and *Methanoculleus sp.* (Sasaki *et al.*, 2011; Van Eerten-Jansen *et al.*, 2013; Jiang *et al.*, 2014; Siegert *et al.*, 2015). Cheng *et al.* (2019) reported that *Methanobacterium palustre* methanogens directly use electrons to produce methane without organic substances (Cheng *et al.*, 2009). However, this study does not provide sufficient evidence of electron utilization. Although *Geobacter* species are well-

known to have the ability to transfer electrons, it is surprising that the dominant genus identified in this study is *Petrimonas*, given that no literature on the electron transfer ability of this genus is available. However, *Petrimonas* can probably accept electrons to produce hydrogen, which would be provided to the detected hydrogenotrophic methanogens and denitrifiers in the absence of an organic substrate in the reactor. During the bio-electrochemical production of hydrogen, it is reasonable to assume that a very small amount of hydrogen is electrochemically formed and biologically consumed. However, this electrochemical pathway would negligibly contribute to the production because hydrogen-producing *Petrimonas* was dominant in the microbial community.

Hydrogenotrophic methanogens and denitrifiers compete for the shared substrate of H_2 produced at the biocathode. In wastewater treatments under anoxic conditions in the presence of nitrate, denitrifiers are dominant; this phenomenon can be explained by Gibbs free energy. The obtained energy in the denitrification reaction of Eq. (3-3) is much larger than that in the methane production reaction of Eq. (3-2). However, under hydrogenotrophic conditions, both methanogens and denitrifiers were enriched even though denitrification dominated throughout the experiment. At the lowest applied voltage of 0.05 V, approximately 40% of the produced H_2 was utilized for methane production by the methanogens. However, with an increase in applied voltage, the utilization ratio decreased (**Fig. 3-10**), meaning that the applied voltage affected the H_2 utilization of methanogens and denitrifiers. H_2 production and concentration should increase with increasing voltages. In general, microbes with a high affinity for substrates can consume the substrates faster than those with low affinity. The Monod constant K_m for H_2 uptake was reportedly 1 μM and 2 μM for *Methanobacterium ruminatium (Lovley and Goodwin, 1988)* and *Methanobrevibacter formicium (Schauer and Ferry, 1980),* respectively. In contrast, Smith *et al.* (1994) reported that the K_m of hydrogenotrophic denitrifiers ranged from 0.3 μM to 3.32 μM. If methanogens had lower K_m than the denitrifiers at the biocathode, indicating a higher affinity for H_2 and lower maximum H_2 uptake rate, the phenomenon of decreasing current ratio in methane production with increasing applied voltage, as shown in **Fig. 3-10**, could be explained by this difference in K_m between methanogens and denitrifiers.

Based on the above experimental results, **Fig. 3-12** proposes a scheme for the process of electronic methane production used in this study, without organic substances in the MES.

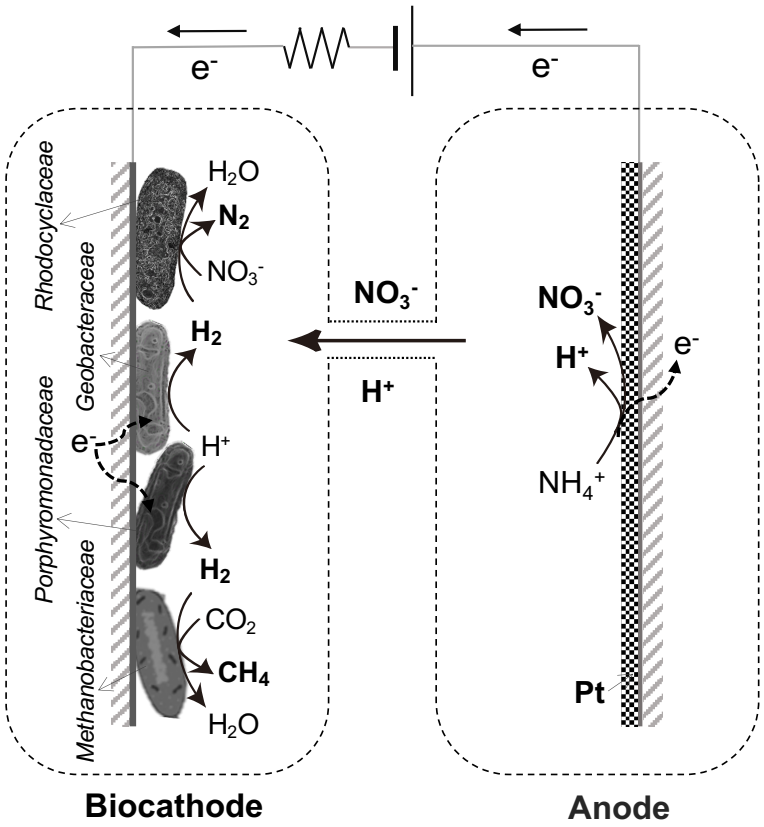

Fig. 3-12 Scheme of electronic methane and nitrogen production in MEC reactor without organic substances.

Ammonium is oxidized to nitrate by a Pt catalyst at the anode with electron release. The formed nitrate is transferred into the biocathode chamber through the salt bridge. At the biocathode, the hydrogen-producing bacteria *Petrimonas* biochemically produce H_2 by accepting electrons and protons. The produced H_2 is biologically consumed by hydrogenotrophic methanogens of *Methanobacterium* and *Methanobrevibacter* coupled with CO_2 uptake, and by hydrogenotrophic denitrifiers of *Rhodocyclaceae (Azonexus)*, with the transferred nitrate reduction resulting in the production of methane and N_2, respectively.

Consequently, the overall reaction at the anode and biocathode in the MES is as follows:

$$1/8\ CO_2 + 1/3\ NH_4^+ \rightarrow 1/8\ CH_4 + 1/6\ N_2 + 1/3\ H^+ + 1/4\ H_2O$$

$$\Delta G^{0\prime} = -3.134\ kJ\ mol^{-1}\ e^- \qquad (3\text{-}5)$$

Thermodynamically, this reaction proceeds under the standard condition even without the provision of external energy, such as electricity, because of the negative Gibbs free

energy $\Delta G^{0'}$ value. The actual condition, for example, at an applied voltage of 0.1 V was as follows: p_{CH4} = 0.36 atm, p_{N2} = 0.65 atm, p_{CO2} = 0.03 atm, $[H^+] = 15.1 \times 10^{-5}$ M, and $[NH_4^+] = 5.38 \times 10^{-3}$ M. In this case, the actual Gibbs free energy ΔG (= $\Delta G^{0'}$ + RT ln(K)) was estimated to have a value of -5.18 kJ mol^{-1} e^-, suggesting that production of methane and N_2 is to be expected. Thus, this study revealed that even in an inorganic environment, biological methane production coupled with denitrification is possible in combination with catalytic ammonium oxidation even at very low applied voltages < 0.1 V, through the three key players of hydrogenotrophic methanogens, denitrifiers, and hydrogen-producing bacteria.

3.5 Conclusion

This study investigated bioelectrical methane production from CO_2 without organic substances. Even though microbial methane production has been reported at relatively high electric voltages, it is unclear how much voltage is required and which organisms contribute to the process. Methane production using a biocathode was investigated in a microbial electrolysis cell coupled with an NH_4^+ oxidative reaction at an anode coated with platinum powder under a wide range of applied voltages and anaerobic conditions. Microbial community analysis revealed that methane production occurred simultaneously with biological denitrification at the biocathode. In denitrification, NO_3^- was produced by chemical NH_4^+ oxidation at the anode and was provided to the biocathode chamber. H_2 was produced at the biocathode by the hydrogen-producing bacteria *Petrimonas* through the acceptance of electrons and protons. The produced H_2 was biologically consumed by hydrogenotrophic methanogens of *Methanobacterium* and *Methanobrevibacter* with CO_2 uptake and by hydrogenotrophic denitrifiers of *Azonexus*. This microbial community suggests that methane is indirectly produced without the use of electrons by methanogens. It was also found that bioelectrical methane production occurred under experimental conditions even at a very low voltage of 0.05 V coupled with NH_4^+ oxidation, which was thermodynamically feasible.

References

Bunce, N.J., and Bejan, D. (2011) Mechanism of electrochemical oxidation of ammonia. *Electrochim Acta* **56**: 8085–8093.

Cabezas, A., Pommerenke, B., Boon, N., and Friedrich, M.W. (2015) Geobacter, Anaeromyxobacter and Anaerolineae populations are enriched on anodes of root exudate-driven microbial fuel cells in rice field soil. *Environ Microbiol Rep* **7**: 489–497.

Caporaso, J.G., Kuczynski, J., Stombaugh, J., Bittinger, K., Bushman, F.D., Costello, E.K., et al. (2010) QIIME allows analysis of high-throughput community sequencing data. *Nat Methods* **7**: 335–336.

Cecconet, D., Bolognesi, S., Callegari, A., and Capodaglio, A.G. (2019) Controlled sequential biocathodic denitrification for contaminated groundwater bioremediation. *Sci Total Environ* **651**: 3107–3116.

Cheng, S., Xing, D., Call, D.F., and Logan, B.E. (2009) Direct Biological Conversion of Electrical Current into Methane by Electromethanogenesis. *Environ Sci Technol* **43**: 3953–3958.

Clauwaert, P., Tolêdo, R., van der Ha, D., Crab, R., Verstraete, W., Hu, H., et al. (2008) Combining biocatalyzed electrolysis with anaerobic digestion. *Water Sci Technol* **57**: 575–579.

Clauwaert, P., and Verstraete, W. (2009) Methanogenesis in membraneless microbial electrolysis cells. *Appl Microbiol Biotechnol* **82**: 829–836.

De Vooys, A.C.A., Koper, M.T.M., Van Santen, R.A., and Van Veen, J.A.R. (2001) The role of adsorbates in the electrochemical oxidation of ammonia on noble and transition metal electrodes. *J Electroanal Chem* **506**: 127–137.

Ding, A., Yang, Y., Sun, G., and Wu, D. (2016) Impact of applied voltage on methane generation and microbial activities in an anaerobic microbial electrolysis cell (MEC). *Chem Eng J* **283**: 260–265.

Edgar, R.C. (2010) Search and clustering orders of magnitude faster than BLAST. *Bioinformatics* **26**: 2460–2461.

Eerten-Jansen, M.C.A.A.V., Heijne, A.T., Buisman, C.J.N., and Hamelers, H.V.M. (2012) Microbial electrolysis cells for production of methane from CO2: long-term performance and perspectives. *Int J Energy Res* **36**: 809–819.

Endo, K., Katayama, Y., and Miura, T. (2005) A rotating disk electrode study on the ammonia oxidation. *Electrochim Acta* **50**: 2181–2185.

Fóti, G., and Comninellis, C. (2004) Electrochemical Oxidation of Organics on Iridium Oxide and Synthetic Diamond Based Electrodes. In *Modern Aspects of Electrochemistry*. Modern Aspects of Electrochemistry. White, R.E., Conway, B.E., Vayenas, C.G., and Gamboa-Adelco, M.E. (eds). Boston, MA: Springer US, pp. 87–130.

Holmes, D.E., Shrestha, P.M., Walker, D.J.F., Dang, Y., Nevin, K.P., Woodard, T.L., and Lovley, D.R. (2017) Metatranscriptomic Evidence for Direct Interspecies Electron Transfer between Geobacter and Methanothrix Species in Methanogenic Rice Paddy Soils. *Appl Environ Microbiol* **83**: e00223–17.

Jiang, Y., Su, M., and Li, D. (2014) Removal of Sulfide and Production of Methane from Carbon Dioxide in Microbial Fuel Cells–Microbial Electrolysis Cell (MFCs–MEC) Coupled System. *Appl Biochem Biotechnol* **172**: 2720–2731.

Lee, J.-Y., Park, J.-H., and Park, H.-D. (2017) Effects of an applied voltage on direct interspecies electron transfer via conductive materials for methane production. *Waste Manag* **68**: 165–172.

Li, X.-G., Cao, H.-B., Wu, J.-C., and Yu, K.-T. (2001) Inhibition of the metabolism of nitrifying bacteria by direct electric current. *Biotechnol Lett* **23**: 705–709.

Li, Z.-F., Wang, Y., and Botte, G.G. (2017) Revisiting the electrochemical oxidation of ammonia on carbon-supported metal nanoparticle catalysts. *Electrochim Acta* **228**: 351–360.

Liang, D., He, W., Li, C., Wang, F., Crittenden, J.C., and Feng, Y. (2021) Remediation of nitrate contamination by membrane hydrogenotrophic denitrifying biofilm integrated in microbial electrolysis cell. *Water Res* **188**: 116498.

Liu, Q., Ren, Z.J., Huang, C., Liu, B., Ren, N., and Xing, D. (2016) Multiple syntrophic interactions drive biohythane production from waste sludge in microbial electrolysis cells. *Biotechnol Biofuels* **9**: 162.

Logan, B.E., Hamelers, B., Rozendal, R., Schröder, U., Keller, J., Freguia, S., et al. (2006) Microbial Fuel Cells: Methodology and Technology. *Environ Sci Technol* **40**: 5181–5192.

Lohner, S.T., Deutzmann, J.S., Logan, B.E., Leigh, J., and Spormann, A.M. (2014) Hydrogenase-independent uptake and metabolism of electrons by the archaeon Methanococcus maripaludis. *ISME J* **8**: 1673–1681.

Lovley, D.R. and Goodwin, S. (1988) Hydrogen concentrations as an indicator of the predominant terminal electron-accepting reactions in aquatic sediments. *Geochim et Cosmochim Acta* **52**: 2993–3003.

Lu, L., Xing, D., and Ren, N. (2012) Pyrosequencing reveals highly diverse microbial communities in microbial electrolysis cells involved in enhanced H2 production from waste activated sludge. *Water Res* **46**: 2425–2434.

McDonald, D., Price, M.N., Goodrich, J., Nawrocki, E.P., DeSantis, T.Z., Probst, A., et al. (2012) An improved Greengenes taxonomy with explicit ranks for ecological and evolutionary analyses of bacteria and archaea. *ISME J* **6**: 610–618.

Müller, E., and Spitzer, F. (1905) Über die Elektrolytische Oxydation des Ammoniaks und Ihre Abhängigkeit vom Anodenmaterial. *Zeitschrift für Elektrochemie und angewandte physikalische Chemie* **11**: 917–931.

Nutt, C.W., and Kapur, S. (1968) Mechanism of Oxidation of Ammonia on Platinum. *Nature* **220**: 697–698.

Onodera, I. (2013) Development of Methane Fermentation Technology for Wastewater Treatment. *Tappi J* **67**: 82–85.

Panizza, M., and Cerisola, G. (2009) Direct And Mediated Anodic Oxidation of Organic Pollutants. *Chem Rev* **109**: 6541–6569.

Park, J., Lee, B., Tian, D., and Jun, H. (2018) Bioelectrochemical enhancement of methane production from highly concentrated food waste in a combined anaerobic digester and microbial electrolysis cell. *Bioresour Technol* **247**: 226–233.

Peng, H., Zhao, Z., Xiao, H., Yang, Y., Zhao, H., and Zhang, Y. (2019) A strategy for enhancing anaerobic digestion of waste activated sludge: Driving anodic oxidation by adding nitrate into microbial electrolysis cell. *J Environ Sci* **81**: 34–42.

Rabaey, K. and Rozendal, R. (2010) Microbial electrosynthesis - Revisiting the electrical route for microbial production. *Nat Rev Microbiol* **8**: 706–716.

Rice, D.D., and Claypool, G.E. (1981) Generation, Accumulation, and Resource Potential of Biogenic Gas. *AAPG Bulletin* **65**: 5–25.

Rotaru, A.-E., Shrestha, P.M., Liu, F., Shrestha, M., Shrestha, D., Embree, M., et al. (2013) A new model for electron flow during anaerobic digestion: direct interspecies electron transfer to Methanosaeta for the reduction of carbon dioxide to methane. *Energy Environ Sci* **7**: 408–415.

Sarmin, S., Ethiraj, B., Islam, M.A., Ideris, A., Yee, C.S., and Khan, M.M.R. (2019) Bio-electrochemical power generation in petrochemical wastewater fed microbial fuel cell. *Sci Total Environ* **695**: 133820.

Sasaki, K., Morita, M., Sasaki, D., Hirano, S., Matsumoto, N., Ohmura, N., and Igarashi, Y. (2011) Methanogenic communities on the electrodes of bioelectrochemical reactors without membranes. *J Biosci Bioeng* **111**: 47–49.

Schauer, N.L., and Ferry, J.G. (1980) Metabolism of formate in Methanobacterium formicicum. *J Bacteriol* **142**: 800–807.

Schoell, M. (1988) Multiple origins of methane in the Earth. *Chemical Geology* **71**: 1–10.

Siegert, M., Li, X.-F., Yates, M.D., and Logan, B.E. (2015) The presence of hydrogenotrophic methanogens in the inoculum improves methane gas production in microbial electrolysis cells. *Front Microbiol* **5**: 778.

Smith, R.L., Ceazan, M.L., and Brooks, M.H. (1994) Autotrophic, Hydrogen-Oxidizing, Denitrifying Bacteria in Groundwater, Potential Agents for Bioremediation of Nitrate Contamination. *Appl Environ Microbiol* **60**: 1949–1955.

Sun, R., Zhou, A., Jia, J., Liang, Q., Liu, Q., Xing, D., and Ren, N. (2015) Characterization of methane production and microbial community shifts during waste activated sludge degradation in microbial electrolysis cells. *Bioresour Technol* **175**: 68–74.

Townsend-Small, A., Disbennett, D., Fernandez, J.M., Ransohoff, R.W., Mackay, R., and Bourbonniere, R.A. (2016) Quantifying emissions of methane derived from anaerobic organic matter respiration and natural gas extraction in Lake Erie. *Limnol Oceanogr* **61**: S356–S366.

Van Eerten-Jansen, M.C.A.A., Veldhoen, A.B., Plugge, C.M., Stams, A.J.M., Buisman, C.J.N., and Ter Heijne, A. (2013) Microbial Community Analysis of a Methane-Producing Biocathode in a Bioelectrochemical System. *Archaea* **2013**: 481784

Villano, M., Aulenta, F., Ciucci, C., Ferri, T., Giuliano, A., and Majone, M. (2010) Bioelectrochemical reduction of CO2 to CH4 via direct and indirect extracellular electron transfer by a hydrogenophilic methanogenic culture. *Bioresour Technol* **101**: 3085–3090.

Wagner, R.C., Regan, J.M., Oh, S.-E., Zuo, Y., and Logan, B.E. (2009) Hydrogen and methane production from swine wastewater using microbial electrolysis cells. *Water Res* **43**: 1480–1488.

Wang, W., Zhang, Y., Li, M., Wei, X., Wang, Y., Liu, L., et al. (2020) Operation mechanism of constructed wetland-microbial fuel cells for wastewater treatment and electricity generation: A review. *Bioresour Technol* **314**: 123808.

Wang, Y., Tian, H., Huang, F., Long, W., Zhang, Q., Wang, J., et al. (2017) Time-resolved analysis of a denitrifying bacterial community revealed a core microbiome responsible for the anaerobic degradation of quinoline. *Sci Rep* **7**: 14778.

Werner, J.J., Koren, O., Hugenholtz, P., DeSantis, T.Z., Walters, W.A., Caporaso, J.G., et al. (2012) Impact of training sets on classification of high-throughput bacterial 16s rRNA gene surveys. *ISME J* **6**: 94–103.

Whiticar, M.J. (1999) Carbon and hydrogen isotope systematics of bacterial formation and oxidation of methane. *Chemical Geology* **161**: 291–314.

Whiticar, M.J., Faber, E., and Schoell, M. (1986) Biogenic methane formation in marine and freshwater environments: CO2 reduction vs. acetate fermentation—Isotope evidence. *Geochim et Cosmochim Acta* **50**: 693–709.

Yan, Y., Li, T., Zhou, L., Tian, L., Yan, X., Liao, C., et al. (2020) Spatially heterogeneous propionate conversion towards electricity in bioelectrochemical systems. *J Power Sources* **449**: 227557.

Zhao, H.-P., Ontiveros-Valencia, A., Tang, Y., Kim, B., Ilhan, Z.E., Krajmalnik-Brown, R., and Rittmann, B. (2013) Using a Two-Stage Hydrogen-Based Membrane Biofilm Reactor (MBfR) to Achieve Complete Perchlorate Reduction in the Presence of Nitrate and Sulfate. *Environ Sci Technol* **47**: 1565–1572.

Zhao, H.-P., Van Ginkel, S., Tang, Y., Kang, D.-W., Rittmann, B., and Krajmalnik-Brown, R. (2011) Interactions between Perchlorate and Nitrate Reductions in the Biofilm of a Hydrogen-Based Membrane Biofilm Reactor. *Environ Sci Technol* **45**: 10155–10162.

Zhao, Z., Zhang, Y., Yu, Q., Ma, W., Sun, J., and Quan, X. (2016) Enhanced decomposition of waste activated sludge via anodic oxidation for methane production and bioenergy recovery. *Int Biodeterior Biodegradation* **106**: 161–169.

Zhen, G., Kobayashi, T., Lu, X., and Xu, K. (2015) Understanding methane bioelectrosynthesis from carbon dioxide in a two-chamber microbial electrolysis cells (MECs) containing a carbon biocathode. *Bioresour Technol* **186**: 141–148.

Chapter

4

Bioelectrical methane production coupled with an abiotic HS^- oxidation

4.1 Introduction

Methane and carbon dioxide are the most important carbon compounds in the natural carbon cycle. Methane is the final reduced state, while carbon dioxide is the most oxidized state. Therefore, methane is produced under reduced environmental conditions, both abiotic and biological. Abiotic methane production occurs only at very high temperatures, for example, deep in the ground with organic matter, such as fossils (Etiope and Whiticar, 2019; Schoell, 1983, 1980). However, biological methane is produced at ambient temperatures, and methane is released from natural sources, such as paddy fields and wetlands (Anderson *et al.*, 2016; Deppenmeier and Müller, 2008). This biological reaction is known as fermentation, and has been applied to anaerobic wastewater treatment as an eco-friendly technology (Biniaz *et al.*, 2021; Li *et al.,* 2019; Onodera, 2013; Pan *et al.*, 2017). The produced biogas, mainly composed of methane, is used as an energy source. In biological methane production, methanogens are the key players, which are classified into two groups, hydrogenotrophic and acetoclastic methanogens, that utilize H_2 + CO_2 and acetate, respectively (Conrad, 2020; Fournier and Gogarten, 2008; Xu *et al.*, 2019).

In the fermentation process, certain bacteria can transfer electrons to the electrode and other bacteria as direct interspecies electron carriers. *Geobacter* is known to possess electron transfer ability (Bond and Lovley, 2003; Lovley, 2017; Rotaru *et al*., 2013, Yoho *et al.*, 2014). In the microbial fuel cell (MFC) process, electricity is generated by the action of microbes, such as electrogenic bacteria, at the anode with degradation of organic matter (Logan *et al.,* 2006; Sarmin *et al.,* 2019). Conversely, in a microbial electrosynthesis system (MES), which is a type of modified MFC, hydrogen gas is produced at the cathode, not the anode by providing electricity (González-Pabón *et al.*, 2021; Logan *et al.*, 2008). In addition to hydrogen gas, methane is produced in the cathode chamber of the MES (Clauwaert and Verstraete, 2009; Zakaria and Dhar, 2021; Zhao *et al.,* 2016). Higher methane production can be expected in MES than in conventional methane fermentation reactors for wastewater treatment because the combination of methane production from organic substances and conversion of CO_2 to methane through electricity by microbes occurs at the cathode (Peng *et al.,* 2019)

Electronic methane production occurs in the MES even in the absence of organic substrates (Aryal *et al.,* 2017; Schlager *et al.,* 2017; Villano *et al.,* 2010; Zhen *et al*., 2018). Two mechanisms have been proposed for bioelectrotrophic methane production at the

biocathode. First, certain methanogens directly accept electrons from the electrode to generate methane with CO_2 reduction (Cheng *et al.,* 2009). Second, once H_2 is abiotically or biologically produced by proton reduction with electrons, methane is produced by hydrogenotrophic methanogens using the generated H_2 with CO_2 uptake (Villano *et al.*, 2010; Zhen *et al.*, 2018). For direct electrotrophic methane production, there is insufficient experimental data to prove the electron transfer (Cheng *et al*., 2009; Lohner *et al.,* 2014). On the contrary, indirect methane production via H_2 from electrons is possible when the applied voltage is high. Even at lower applied voltages, bioelectrotrophic H_2 production might be achieved because few bacteria, such as *Geobacter*, are known to transfer electrons (Call *et al.,* 2009). Dinh *et al.* (2021) proposed a scheme for biological methane production via bioelectrotrophic H_2 production in an MES. However, the mechanism of bioelectrotrophic methane production remains unclear.

The standard reduction potential $E^{0\prime}$ of CO_2 to methane at pH = 7 is −0.24 V (vs. standard hydrogen potential [SHE]) equivalent to −0.44 V (vs. Ag/AgCl). Cheng et al. (2009) demonstrated that bioelectrotrophic methane production occurred at a biocathode potential of < −0.7 V (vs. Ag/AgCl), and found that −1.0 V (vs. Ag/AgCl) gave an excellent result, with an electron capture efficiency of 96%. The voltage applied to produce methane in MES depends not only on the biocathode potential but also on the anode potential. When coupling of H_2O oxidation ($E^{0\prime}$ = 0.81 V vs. SHE) at the anode and CO_2 reduction at the cathode takes place in an MES, more than 1.05 V is thermodynamically required in the applied voltage under the standard condition for methane production. However, when coupled with oxidation of NH_4^+ to NO_3^- ($E^{0\prime}$ = 0.36 V vs. SHE) instead of H_2O oxidation, methane can be produced a lower applied voltage of 0.6 V. If oxidation of HS^- to SO_4^{2-} ($E^{0\prime}$ = −0.22 V vs. SHE) occurs at the anode, an MES for methane production at a very low applied voltage (0.02 V) can be theoretically established without organic substrates. However, several experiments using an MES were conducted at relatively high voltages (Gomez Vidales et al., 2019), and there is little information about the oxidation of inorganic compounds, such as NH_4^+ and HS^-, with lower potential at the anode.

To the best of our knowledge, this study is the first to investigate whether bioelectrical methane production is achieved in an MES consisting of a biocathode and an anode with oxidation of abiotic HS^- to SO_4^{2-} at low applied voltages in the absence of organic

substances. In addition, we propose a scheme of electron flow in methane production at the biocathode based on the microbial community analysis of biomass enriched on the electrode.

4.2 Materials and methods

4.2.1 MES set-up

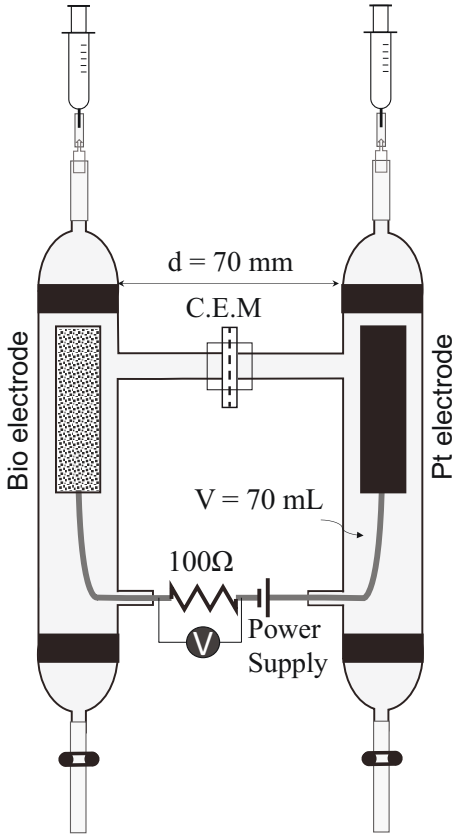

Fig. 4-1 Schematic representation of microbial electrosynthesis system consisting of two chambers connected with a cation exchange membrane (MES; abiotic anode).

The MES used in this study consisted of two glass chambers with an effective volume of 70 mL each and were connected through a cation exchange membrane (Nafion EC–NM–211, Toyo Corporation, Japan) of working area 0.5 cm^2 (**Fig. 4-1**). The top of each chamber was connected to a 10-mL loss-of-resistance glass syringe to release the pressure in the chamber generated from the produced gas and to facilitate gas collection. A carbon cloth (Toyobo Co. Ltd, Japan) with an area of 24 cm^2 was installed in both chambers as electrodes. The electrodes were connected to a DC power supply (Array 3600 Series, T&C Technology, Japan) using a titanium wire. A 100 Ω resistor was inserted beside the power supply to monitor the electric current using a data logger (GL 240 midi LOGGER, GRAPHTEC, DATAQ Instruments, Inc., USA). A small amount of anaerobic sludge collected from a laboratory-scale upflow anaerobic sludge blanket (UASB) reactor was inoculated on the surface of the electrode, which worked as a biocathode. For the anode, platinum powder (10% w/w Pt on carbon powder; E-TEK, C-1 10% Pt on Vulcan XC-72) was coated on the surface of the electrode as a catalyst, according to previous studies (De Vooys *et al.*, 2001; Li *et al.*, 2017)

The anode and biocathode chambers were filled with the same medium and deoxidized through a nitrogen purge without organic substances. The medium was composed of $NaHCO_3$ (200 mg L^{-1}), $Na_2S{\cdot}9H_2O$ (0–20 mg S L^{-1}), NH_4Cl (3–30 mg N L^{-1}), KH_2PO_4 (102 mg L^{-1}), K_2HPO_4 (305 mg L^{-1}), and trace elements, including $FeSO_4{\cdot}7H_2O$ (7 mg L^{-1}), $CoCl_2{\cdot}6H_2O$ (1.7 mg L^{-1}), $ZnSO_4{\cdot}7H_2O$ (1.5 mg L^{-1}), HBO_3 (0.6 mg L^{-1}), $MnCl_2{\cdot}4H_2O$ (4.2 mg L^{-1}), $NiCl_2{\cdot}4H_2O$ (0.4 mg L^{-1}), $CuCl_2{\cdot}2H_2O$ (0.27 mg L^{-1}), $Na_2MoO_2{\cdot}2H_2O$ (0.25 mg L^{-1}), $MgCl_2{\cdot}6H_2O$ (4.0 mg L^{-1}), $CaCl_2{\cdot}2H_2O$ (1.5 mg L^{-1}), and KCl (3.0 mg L^{-1}) at pH 7.3 (**Table 4-1**). The only difference between the biocathode and anode medium was the concentration of HS^- from day 188 onwards. N_2 gas (0.5 mL) was initially injected into both chambers to facilitate sampling of the produced gas containing methane.

4.2.2 MES operation

The MES was operated in batch processing mode at 30°C in a thermostatic chamber. The batch experiment was repeated 35 times over 293 days at intervals of 5–14 days, and the duration was determined to be dependent on the gas production rate for gas sampling. A voltage of 0.8 V was applied by setting up the MES to phase III. In phase IV, each batch experiment was performed in an applied voltage range of 0.8–0.1 V to investigate the effect of voltage on methane production, as shown in **Fig. 4-2** and **Table 4-1**. Phase III was conducted to investigate the influence of HS^- concentration.

Table 4-1 MES operational conditions

Phase	Batch no.	Batch duration (d)	Operational time (d)	Voltage (V)	NH_4^+ (mg N L^{-1})	HS^- (mg S L^{-1})	
					Cathode/Anode	Cathode	Anode
I	1–3	5–11	0–21	0.8	30	0	0
II	4–8	7	22–57	0.8	30	4	4
	9–15	5–14	58–131	0.8	15	4	4
III	16–20	8–13	132–187	0.8	15	6–20	6–20
	21–29	7	188–250	0.8	3	2–4	20–32
IV	30–35	7–10	251–293	0.1–0.8	3	4	26.7

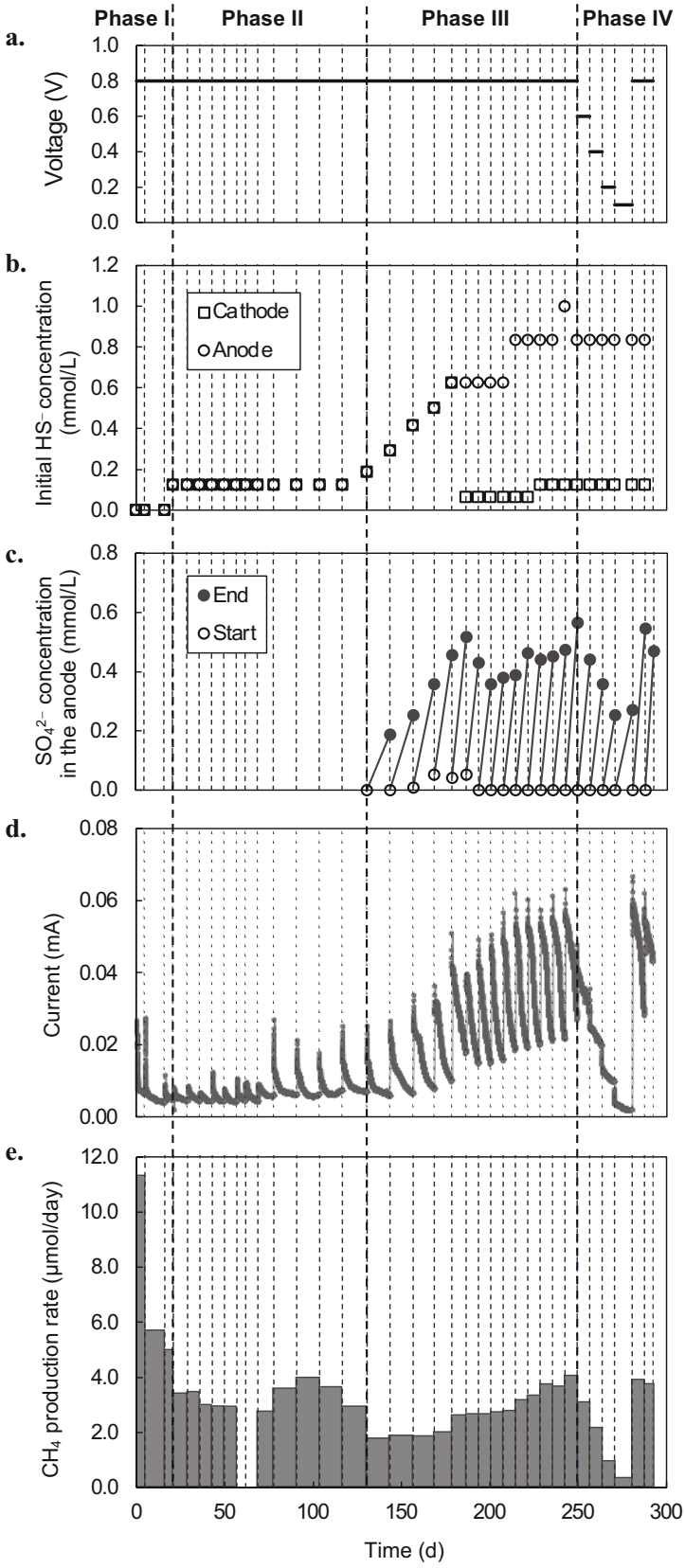

Fig. 4-2 Time courses of (a) applied voltage, (b) initial HS^- concentration, (c) SO_4^{2-} concentration in the anode, (d) current, and (e) CH_4 production rate in batch experiments.

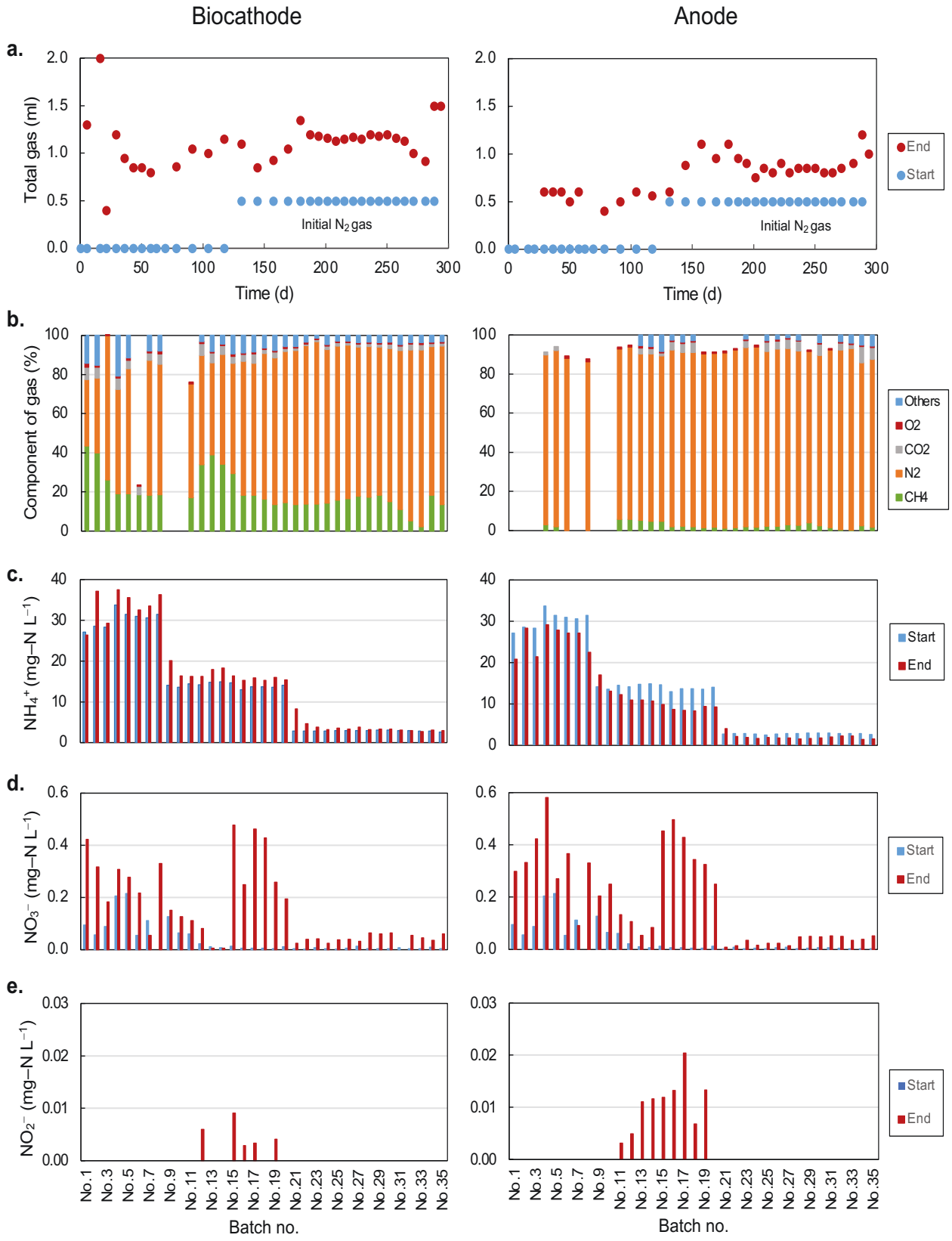

Fig. 4-3 The measured values at the start and end of each batch experiment.

4.2.3 Sampling and analyses

The volume of gas in each chamber was measured at the end of each batch operation using an airtight syringe. The gas compositions of CH_4, N_2, CO_2, and H_2 were then measured using a gas chromatograph equipped with a thermal conductivity detector (GC-TCD, Shimadzu GC-8A). Analysis of the liquid samples at the start and end of each batch was performed after filtration with 0.2-μm pore size polytetrafluoroethylene membranes. NH_4^+, NO_3^-, and NO_2^- concentrations were measured using an ion chromatograph (Shimadzu HPLC-20A). SO_4^{2-} concentration was determined by a colorimetric method using a Hach DR-2800 spectrophotometer (Hach Co., Loveland, CO, USA). The dissolved CH_4 and N_2 concentrations were estimated using Henry's law.

4.2.4 Microbial community

Microbial community analysis was performed for the biomass collected from the biocathode on the last day of the MES operation. After washing the biomass with phosphate buffer, DNA was extracted using the FastDNA® SPIN kit for soil (MP Biomedicals, Solon, OH, USA), according to the manufacturer's instructions. The DNA sample was transported to the Bioengineering Lab (Kanagawa, Japan) for performing polymerase chain reaction with the primer sets 341′F (5′-CCTAHGGGRBGCAGCAG-3′) and 805R (5′-GACTACHVGGGTATCTAATCC-3′), and sequencing using the Illumina MiSeq platform (Illumina, Inc., San Diego, CA, USA). The raw sequence data were trimmed using Cutadapt software (version 1.18) (Parada *et al.,* 2016) to remove primers from the sequence reads. Noise and low-quality sequence reads were removed using Trimmomatic (version 0.39-1) (Bolger *et al.,* 2014) when the quality per base dropped below 20 bp in the sliding window and the minimum length of the reads was below 40 bp. The clean reads were analyzed using QIIME2 (version 2020.08) (Bolyen *et al.,* 2019; Hall and Beiko, 2018). Operational taxonomic units (OTUs) were classified using the pipeline software DADA2 (Callahan *et al.,* 2016) with the SILVA (release_132) database (Pruesse *et al.,* 2012; Quast *et al.,* 2013; Yilmaz *et al.,* 2014). The sequence data were deposited in the DDBJ database under DDBJ/EMBL/GenBank accession number DRA011923.

4.3 Results

4.3.1 Performance of batch experiments

During the batch experiment, we observed an increase in the current that immediately decreased and gradually declined over time, as shown in **Fig. 4-2**. This behavior was observed for all batch experiments. In phase I, bubbles were produced, and methane was detected at a concentration of 42%–24% in the biocathode chamber (**Fig. 4-3**), even though HS^- was not added. The first batch had the highest methane production, including dissolved methane of bulk liquid estimated using Henry's law, followed by the second and third batch. These methane productions were derived from organic substances in the inoculated sludge.

In phase II, HS^- was added to the bulk liquid at 4 mg S L^{-1} to enhance methane production activity associated with an increase in current by sulfide oxidation at the Pt anode. However, no change was observed in the amount of current until batch 11. Conversely, methane production continued to decrease. This indicates that the organic substances remained in the biocathode chamber despite the reduction in the amount of organic substances. In batches 12 and 13, the current tended to increase slightly with an increase in methane production. However, methane production decreased in batches 14 and 15, which suggests that the methane in the biocathode would be produced from the resident sludge and CO_2 reduction coupled to electrons. In batches 9 and 10, the bulk liquid was purged with He gas instead of N_2 to investigate N_2 production. However, the produced gas was very low for sampling; therefore, N_2 purging was performed in the subsequent batch operations.

As a slight increase in current was observed in late phase II, the amount of HS^- added to the bulk liquid in the anode chamber was increased step by step to enhance current and methane production in phase III of batches 16–29 for operation days 132–250. Prior to batch 16, sludge deposited at the bottom of the biocathode chamber was removed because the sludge detached from the inoculated sludge on the electrode, which increased over time, thereby affecting methane production. As a result of removing the deposited sludge, methane production drastically decreased in batch 16. However, methane production steadily increased with an accompanying increase in the amount of current, as expected. The retained microbes at the biocathode are expected to grow and increase with the operational time. In addition, sulfate production also increased in the anode chamber, suggesting that oxidation of HS^- to sulfate occurred and its rate was enhanced in phase III.

Nitrate and nitrite were detected in the anode chamber, although the concentrations were very low (**Fig. 4-3**), suggesting that the oxidation of NH_4^+ to nitrate or nitrite was insignificant. For the total nitrogen of NH_4^+, nitrate, and nitrite, the change in the amount in the reactor was small between the start and end of each batch experiment (**Fig. 4-4**). These results indicate that the current was derived mainly from the oxidation of HS^- to sulfate, and the effect of NH_4^+ oxidation was insignificant.

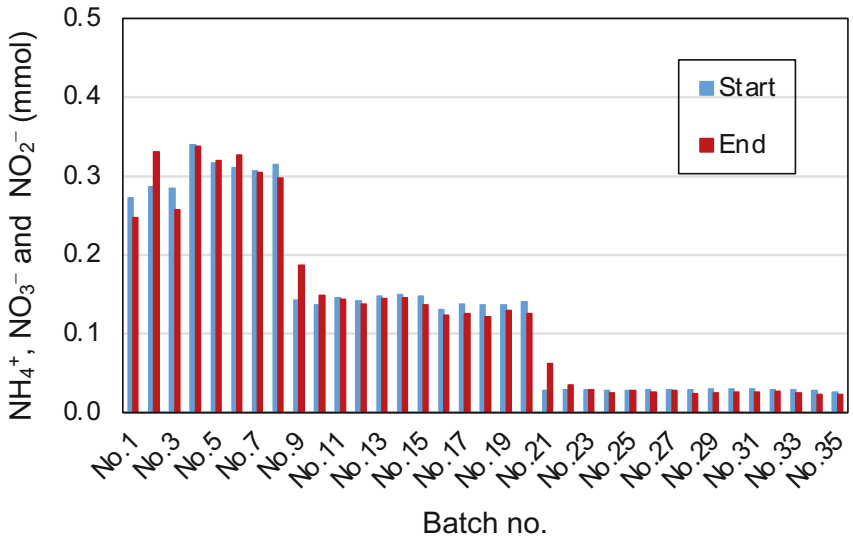

Fig. 4-4 Total amount of NH_4^+, NO_3^- and NO_2^- in both chambers at the start and end of each batch experiment.

Since high gas production was obtained in an early phase III, the batch interval time was shortened to seven days from batch 21 onwards. Moreover, the initial HS^- concentration in the biocathode liquid was also reduced to 2 mg S L^{-1} because high HS^- concentration might inhibit microbial activity at the biocathode. In addition, the NH_4^+ of the bulk liquid was reduced to 3 mg N L^{-1} because of little effect on the current. In batch 21, the amount of current declined, and sulfate production in the anode liquid decreased. These sudden changes could be caused by changing the HS^- concentration in the biocathode liquid, where sulfate was not detected.

In phase IV, we investigated the effect of voltage on methane production, although it was unclear whether the activity of microbes reached a steady state. We decreased the

applied voltage in a step-by-step manner till 0.1 V of batch 33, where the batch period was prolonged to 10 days because of the low current. The applied voltage was then returned to 0.8 V. With a decrease in the applied voltage, both the amount of current and methane production sharply declined. However, even at the lowest voltage (0.1 V), methane was produced, although the amount was very low. When the applied voltage was increased to 0.8 V, current and methane production were recovered. As a very low applied voltage caused a considerably small amount of methane production and the production at 0.8 V in batch 34 was almost the same as that in batches 27–28 of phase III, we inferred that most of the organic substance in the inoculated sludge was consumed and the microbial activity nearly reached a steady state before beginning phase IV.

Methane production rate was proportional to the applied voltage, as shown in **Fig. 4-5**. As voltage affects the electron production by chemical oxidation at the anode, the change in the current should be closely related to methane production. However, in a control batch experiment without inoculation for 20 days, methane was not detected even at the highest voltage of 0.8 V (data not shown). This suggests that microbes on the electrode are essential to produce methane, and not only would the intensity of chemical oxidation at the anode but also the biological activity directly affect the current.

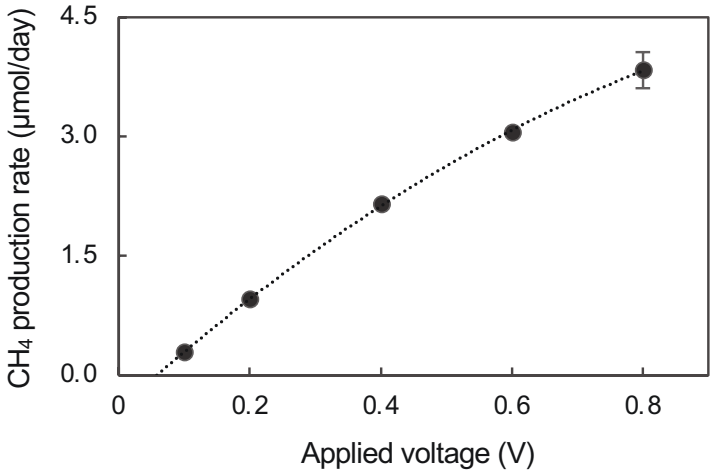

Fig. 4-5 CH_4 production rates at different applied voltages in phase III (batches 28–29) and phase IV.

4.3.2 Electrical CO_2 reduction and HS^- oxidation

Oxidation of HS^- to SO_4^{2-} occurred at the anode, and its oxidation reaction is represented as follows:

$$1/8\ HS^- + 1/2\ H_2O \rightarrow 1/8\ SO_4^{2-} + 9/8\ H^+ + e^- \quad (4\text{-}1)$$

where 1 mol of electron and 1/8 mol of SO_4^{2-} are produced from 1/8 mol of HS^-.

Based on Faraday's laws of electrolysis, the amount of donated or accepted electrons, *Ne* [mol], can be calculated from the measured current using the following equation:

$$Ne = \frac{\int Idt}{F} \quad (4\text{-}2)$$

where *I* is the current (A), t is the time (s), and *F* is Faraday's constant (C mol^{-1}).

Fig. 4-6a shows the relationship between the amount of calculated electron flux per batch operation and the amount of SO_4^{2-} produced in phases III and IV with its theoretical line based on the half reaction of Eq. (4-1). The data of phases I and II were not used in **Fig. 4-6** because organic matter in the inoculated sludge might strongly affect the electron current. Although the plots of the measured SO_4^{2-} production were not on the theoretical line, they were close to the line, and the slope was almost similar.

In contrast, at the biocathode, the electrons donated from the anode were accepted through the external circuit and were used for reduction of CO_2 to CH_4. This half-reduction reaction can be represented as follows:

$$1/8\ CO_2 + H^+ + e^- \rightarrow 1/8\ CH_4 + 1/4\ H_2O \quad (4\text{-}3)$$

where 1/8 mol of CH_4 is produced from 1 mol of electrons and 1/8 mol of CO_2.

Similarly, the relationship between the amount of calculated electron flux per batch operation and the amount of measured CH_4 production in phases III and IV is shown in **Fig. 4-6b** with its theoretical line based on the half reaction of Eq. (4-3). Similar to **Fig. 4-6a**, there was a small discrepancy between the measured CH_4 production and the theoretical values. Despite the discrepancies with a coulombic efficiency of 85.2% on average, the electron balance of the redox reaction was maintained in this MES experiment (**Fig. 4-6**). Therefore, in the MES system without organic substances, methane production can be performed by coupling CO_2 reduction at the biocathode and HS^-

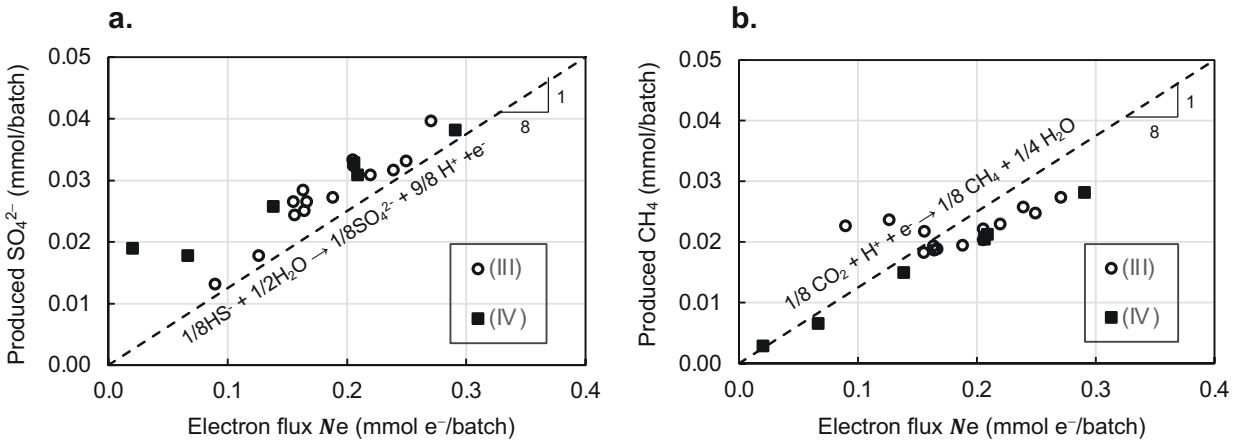

Fig. 4-6 Produced SO_4^{2-} (a) and CH_4 (b) versus electron flux *N*e. Dash lines: theoretical production based on the half reactions.

oxidation at the anode, even at relatively low applied voltages of 0.1–0.8 V. One cause of these discrepancies may be due to a current occring even without applied voltage to keep the charge balance.

4.3.3 Microbial community

In the 16S rRNA gene analysis, 237 OTUs were obtained from 31922 sequence reads. Of the total, 123 OTUs were dominant (> 0.1%). The diversity of dominant OTUs was relatively low compared to the general microbial communities of anaerobic wastewater treatment sludge. Archaea and bacteria were detected at population sizes of 37.9% and 62.1%, respectively (**Fig. 4-7**).

In archaea, all OTUs belonged to Euryarchaeota, and most of the OTUs were methanogens (**Fig. 4-7a**). The major dominant genera of methanogens were *Methanosaeta*, *Methanobacterium*, and *Methanolinea*, accounting for 65.1%, 26.3%, and 6.6% of the archaea, respectively. The highly detected *Methanosaeta* are obligate acetoclastic methanogens, suggesting that acetate is produced in the biocathode chamber. In contrast, *Methanobacterium* and *Methanolinea* are hydrogen-utilizing methanogens, and hydrogen production is expected. Only three genera of methanogens play a major role in methane production in MES.

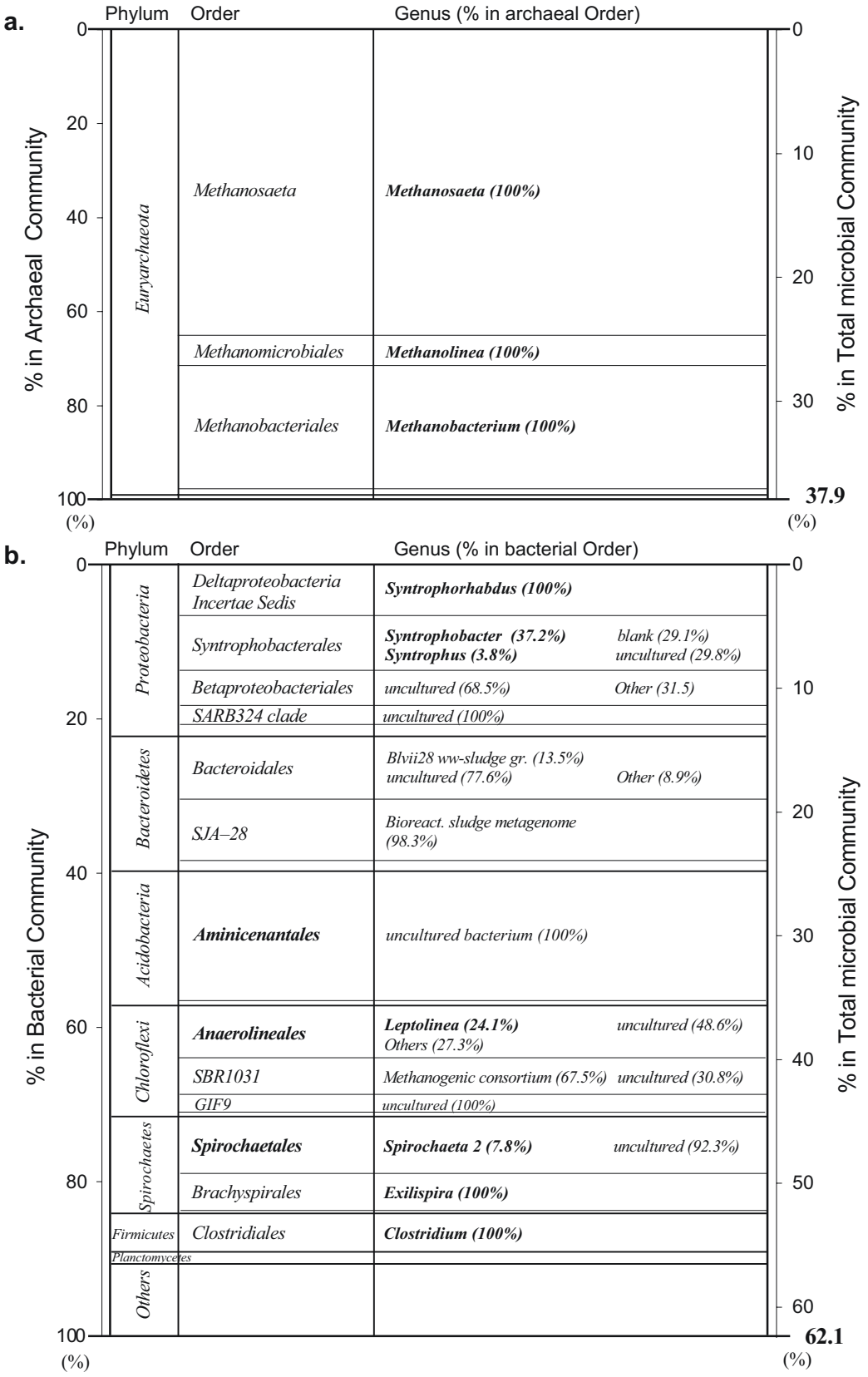

Fig. 4-7 Microbial community of biomass on day 293 based on 16S rRNA gene.

Table 4-2 Microbial community

Domain	Phylum	Class	Order	Family	Genus	(%)
Archaea	*Euryarchaeota*	*Methanomicrobia*	*Methanosarcinales*	*Methanosaetaceae*	***Methanosaeta***	**24.7**
			Methanomicrobiales	*Methanoregulaceae*	***Methanolinea***	**2.5**
		Methanobacteria	*Methanobacteriales*	*Methanobacteriaceae*	***Methanobacterium***	**10.0**
		Other	Other	Other	Other	0.4
	Other	Other	Other	Other	Other	0.3
					Total (Archaea)	37.9
Bacteria	*Proteobacteria*	*Deltaproteobacteria*	*Deltaproteobacteria Incertae Sedis*	*Syntrophorhabdaceae*	***Syntrophorhabdus***	**4.1**
			Syntrophobacterales	*Syntrophobacteraceae*	***Syntrophobacter***	**1.7**
					Blank	1.3
				Syntrophaceae	***Syntrophus***	**0.2**
					uncultured bacterium	**1.3**
			SAR324 clade	*unclutured baterium*	*uncultured bacterium*	1.4
			Other	Other	Other	0.5
		Gammaproteobacteria	*Betaproteobacteriales*	*Rhodocyclaceae*	*uncultured bacterium*	2.0
				Other	Other	0.9
			Other	Other	Other	0.4
		Other	Other	Other	Other	0.1
	Bacteroidetes	*Bacteroidia*	*Bacteroidales*	*Bacteroidetes vadinHA17*	*uncultured bacterium*	3.9
				Rikenellaceae	*Blvii28 wastewater-sludge group*	0.7
				Other	Other	0.4
			Other	Other	Other	0.6
		Ignavibacteria	*SJA-28*	*bioreactor sludge metagenome*	*bioreactor sludge metagenome*	4.9
				Other	Other	0.1
			Other	Other	Other	0.3
	Acidobacteria	*Aminicenantia*	***Aminicenantales***	***uncultured bacterium***	***uncultured bacterium***	**10.4**
		Other	Other	Other	Other	0.4
	Chloroflexi	*Anaerolineae*	*Anaerolineales*	***Anaerolineaceae***	***Leptolinea***	**1.2**
					uncultured bacterium	**2.5**
					Other	0.4
			SBR1031	*methanogenic consortium bacterium*	*methanogenic consortium bacterium*	2.1
				unclutured bacterium	*unclutured bacterium*	0.9
				Other	Other	0.1
			Other	Other	Other	0.1
		Dehalococcoidia	*GIF9*	*unclutured bacterium*	*uncultured bacterium*	1.4
			Other	Other	Other	0.2
	Spirochaetes	*Spirochaetia*	*Spirochaetales*	***Spirochaetaceae***	***Spirochaeta 2***	**0.4**
					unclutured bacterium	**4.2**
		Brachyspirae	*Brachyspirales*	***Brachyspirales Incertae Sedis***	***Exilispira***	**2.9**
		Other	Other	Other	Other	0.4
	Firmicutes	*Clostridia*	*Clostridiales*	***Clostridiaceae***	***Clostridium***	**3.0**
		Other	Other	Other	Other	0.0
	Planctomycetes	*Phycisphaerae*	*Phycisphaerae*	*unclutured bacterium*	*unclutured bacterium*	1.0
	Others (< 1%)	Other	Other	Other	Other	0.0
			Other	Other	Other	5.7
					Total (Bacteria)	62.1
					TOTAL	100%

The bacterial community mainly involved the following six phyla: *Proteobacteria*, *Bacteroidetes*, *Acidobacteria*, *Chloroflexi*, *Spirochaetes*, and *Firmicutes* that accounted for 22.3%, 17.6%, 17.5%, 14.4%, 12.6%, and 4.9%, respectively (**Fig. 4-7b**). Most OTUs were identified as uncultured bacteria. The most dominant OUTs with 17.5% at the taxonomic genus level were affiliated with *Aminicenantales*, which were found in extreme environments (Farag et al., 2014), thermophilic anaerobic digestion reactor (Yamada *et al.*, 2019), and sediment MFCs (Salgado-Dávalos *et al.,* 2021). Although no bacteria in *Aminicenantales* have been isolated, their group reportedly produces hydrogen using metagenome assembly, characterized as syntrophic bacteria (Kadnikov *et al.*, 2019). Surprisingly, in addition to *Aminicenantales*, many typical syntropies, such as *Syntrophorhabdus*, *Syntrophobacter*, *Syntrophus*, and *Leptolinea*, were detected at relatively high abundance (Qiu *et al.*, 2008). *Clostridium* and *Spirochaeta 2* accounted for 4.9% and 0.6% of the bacterial community, respectively. These are homoacetogens, which produce only acetate as its fermentation product using H_2. Although the relative abundance of homoacetogens was not significant, it would play an important role in providing acetate for the highly detected *Methanosaeta*.

Thus, methane production was achieved in MES using the above-mentioned microbial consortium. The consortium at the biocathode mainly consisted of certain dominant bacteria that produce hydrogen by accepting and utilizing electrons, homoacetogens that provide acetate, and acetoclastic and hydrogenotrophic methanogens that produce methane from acetate and hydrogen, respectively.

4.4 Discussion

Several MES studies on methane production without organic substrates have been reported (Gomez Vidales *et al.*, 2019; Schlager *et al.,* 2017; Villano *et al.,* 2010). Cheng *et al.* (2009) was the first to produce methane using an MES with *Methanobacterium* attached to an electrode at a reduction potential of less than −0.7 V (vs. Ag/AgCl). The study revealed that methanogens produced methane using electrons directly, not through abiotically produced H_2. However, evidence of direct biological methane production from electrons has not yet been reported. Zhen *et al.* (2018) reported that methane was mainly produced by hydrogenophilic methanogens using abiotic H_2 derived from water reduction at a cathode, and the direct methane production from electrons on the electrode was a very small fraction

at high negative potentials less than −0.9 V (vs. Ag/AgCl), suggesting that H_2 may be a key pathway for methane production.

In this study, hydrogenophilic methanogens, such as *Methanobacterium* and *Methanolinea,* were detected, which indicates that H_2 was produced, although it was not detected in the cathode chamber. For the electrolysis of water for H_2 production, a high applied voltage is required to achieve high negative potentials at the cathode. However, very low voltages (0.1–0.8 V) between the biocathode and anode were applied in this study, suggesting that abiotic H_2 production was difficult at such a low voltage. Moreover, in a control experiment using a plain cathode without any catalyst or microbe, neither H_2 nor methane was detected at an applied voltage of 0.8 V.

However, biological H_2 production may be possible even at low applied voltages. *Geobacter* possessing electron transfer genes are well known to be detected in MFCs, where they can directly transfer electrons to electron acceptors, such as the anode and iron compounds, as exoelectrogens (Bond and Lovley, 2003; Gao *et al.*, 2014; Ishii *et al.,* 2008; Kato *et al.,* 2013; Li *et al.,* 2018; Reguera *et al.,* 2005; Shehab *et al.,* 2013; Yan *et al.,* 2020). In addition to *Geobacter*, syntrophic bacteria are reportedly related to direct interspecies electron transfer (Cabezas *et al.,* 2015; He *et al.,* 2021; Liu *et al*., 2016; Mostafa *et al.,* 2020). Genome analysis of *Syntrophorhabdus* revealed that electron transfer genes may contribute to syntrophic H_2 and formate generation in aromatic compound metabolism (Nobu *et al.,* 2015). This finding implies that, in the absence of electron donors of organic substrates, syntrophic bacteria can accept electrons directly from the cathode associated with H_2 scavengers of hydrogenophilic methanogens. In our experiment, many OTUs affiliated with syntrophic groups, such as *Syntrophorhabdus*, *Syntrophobacter*, *Syntrophus*, *Leptolinea*, and *Aminicenantales,* were detected at very high abundance. Considering that electrons were directly accepted from the biocathode, these syntrophic-like bacteria were the most promising key players. As a result, biological H_2 production was achieved using this MES.

Although both acetoclastic and hydrogenotrophic methanogens were detected, the former was more dominant than the latter, suggesting that the methane pathway was mainly via acetate. Acetate is produced by homoacetogens, *Clostridium* and *Spirochaeta 2,* which act as scavengers of H_2 (product of syntrophic bacteria). However, the population of the detected homoacetogens was not high compared to that of acetoclastic methanogens and

thus, would be insufficient in providing acetate. Therefore, it is suggested that other homoacetogenic bacteria were involved in the MES, or there might be a different acetate production pathway. As a promising bacterial group, highly detected *Aminicennantales* can be considered. *Aminicennantales* reportedly dominated the UASB reactor, where *Methanosaeta* was predominant (Hua *et al.,* 2020; Romero *et al.,* 2020). *Aminicennantales* produce not only H_2 but also acetate in syntrophic association (Kadnikov *et al.,* 2019), suggesting the existence of a symbiotic relationship between *Aminicennantales* and *Methanosaeta* via acetate, although such a relationship has never been reported.

Based on the results of the microbial community described above, we propose a model to describe the process of electrotrophic methane production at the biocathode in this MES, as shown in **Fig. 4-8**. First, syntrophic bacteria such as *Syntrophorhabdus*, *Syntrophobacter*, *Syntrophus*, *Leptolinea*, and *Aminicenantales* accepted electrons, which were obtained from oxidation of HS^- to SO_4^{2-} at the anode, and transferred to protons for H_2 production.

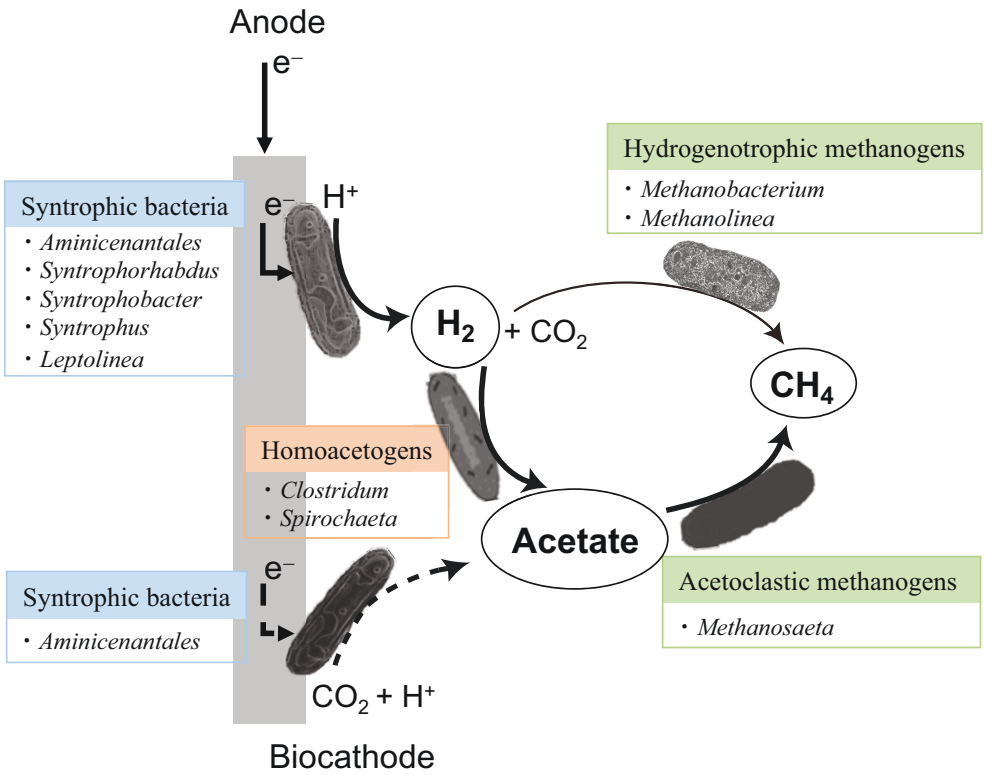

Fig. 4-8 Scheme of electronic methane production at the biocathode in microbial electrosynthesis system without organic substrates

The important aspect in this reaction is the opposite current of the MFC. In MFCs, syntrophic bacteria detected at the bioanode release electrons to the cathode, acting as an electron donor. Syntrophic bacteria are considered to possess the ability to accept and donate electron. Second, a small part of the produced H_2 was converted to CH_4 by the hydrogentrophic methanogens, *Methanobacterium* and *Methanolinea*. The H_2 was used by homoacetogens, *Clotrodium and Spirochate 2,* to produce acetate. Acetate might also be produced by the dominant *Aminicenantales*, which directly accepts electrons from the electrode with CO_2 reduction. Lastly, the highest abundance of acetoclastic methanogens of *Methanosaeta* yielded CH_4 from the produced acetate. Thus, the main pathway to produce methane using this MES was via acetate from electrons, protons, and CO_2 reductions.

The overall reaction process at the anode and biocathode in MES was as follows:

$$1/8\ CO_2 + 1/8\ HS^- \rightarrow 1/8\ CH_4 + 1/8\ SO_4^{2-} + 1/8\ H^+ \qquad (4\text{-}4)$$

$$\Delta G^{0\prime} = 2.17\ \text{kJ mol}^{-1}\ e^-$$

Under standard conditions, this reaction could not proceed. The actual Gibbs free energy ΔG ($= \Delta G^{0\prime} + RT \ln K$) value was 1.14 kJ mol^{-1} e^-, for example, at an applied voltage of 0.1 V, where $p_{CH4} = 0.027$ atm, $[SO_4^{2-}] = 0.35 \cdot 10^{-3}$ M, $[H^+]_{an.} = 1.58 \cdot 10^{-7}$ M, $p_{CO2} = 0.048$ atm, $[HS^-] = 0.323 \cdot 10^{-5}$ M, and $[H^+]_{ca.} = 4.47 \cdot 10^{-8}$ M. Even under actual conditions, the reaction cannot occur because of positive ΔG value, suggesting that an external energy is required for the reaction progress. The applied voltage (0.1 V) is equivalent to ΔG ($= E_H \cdot F$) = −9.65 $mol^{-1}e^-$. Given the count on the energy of applied voltage, in this case, the actual total Gibbs free energy was −8.51 (= −9.65 + 1.14) kJ mol^{-1} e^-, implying that production of methane is to be expected because of the negative ΔG value. Thus, this study revealed that biological methane production is possible in combination with catalytic HS^- oxidation even at a very low applied voltage (0.1 V) in an inorganic environment.

As mentioned above, a small discrepancy was observed between the measured CH_4 production and the theoretical value evaluated from the electron flux. To explain it, abiotic batch experiments without inoculation (**Table 4-3**) were conducted. Even in control batch experiments, the electron flow was disrupted, as shown in **Fig. 4-9.** The charge of the liquids was different between the cathode and anode, and its imbalance became significant by imposing voltage on the MES. To release the charge imbalance, a current was generated

Table 4-3 Abiotic batch experimental conditions

	Batch duration (day)	**Voltage** (V)	**HS^-** (mg S L^{-1})		**NH_4^+** (mg N L^{-1})	
			Cathode	Anode	Cathode	Anode
Run 1	13	0.8	9.3	9.3	15	15
Run 2	7	0.8	4	26.7	3	3

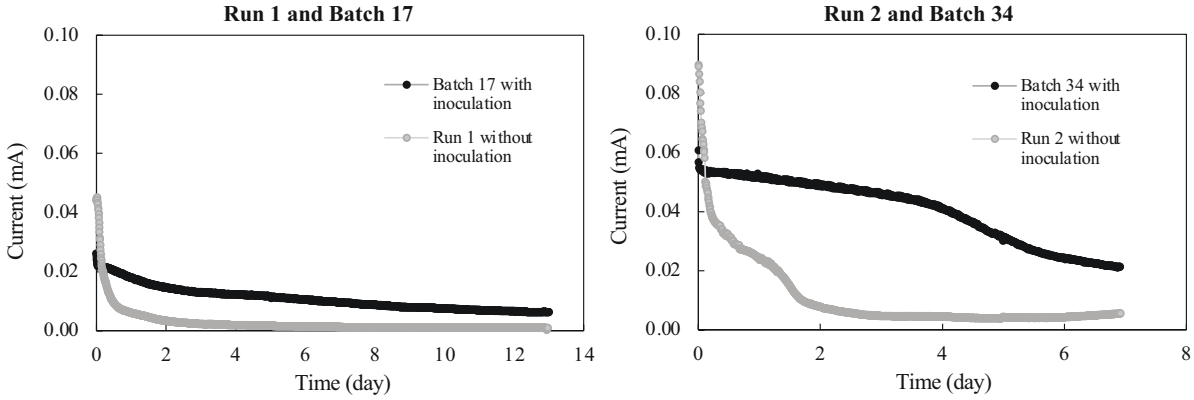

Fig. 4-9 Time courses of current in batch experiments under abiotic and biotic conditions

Table 4-4 Electron flux and the ratio of abiotic to biotic flux

	Electron flux **Without inoculation (1)** (mmol e^- $batch^{-1}$)	Electron flux **With inoculation (2)** (mmol e^- $batch^{-1}$)	**Ratio (1)/(2)** (%)	**Average** (%)
Run 1 vs. batch 17	3.0×10^{-2}	12.6×10^{-2}	23.8	23.4
Run 2 vs. batch 34	6.7×10^{-2}	29.1×10^{-2}	23.0	

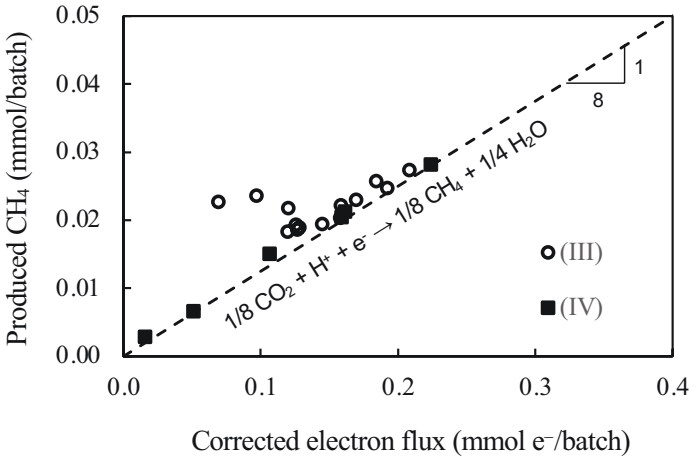

Fig. 4-10 Relationship between the produced methane and corrected electron flux to assess the influence of abiotic current.

even in the control batch experiments, and the number of electrons was related to the intensity of the voltage (**Table 4-4**). By adjusting the effect of electron flow in the control batch conditions, the measured CH_4 production was in good agreement with the corrected theoretical value, as shown in **Fig. 4-10**. Thus, the electron balance was maintained in this MES experiment.

4.5 Conclusion

This study demonstrated that bioelectrical methane production was possible in the MES without organic substrates, where abiotic HS^- oxidation to SO_4^{2-} was achieved at the Pt anode, even in a very low applied voltage range of 0.1–0.8 V. Microbial community analysis revealed that syntrophic bacteria, homoacetogens, and methanogens are key players in methane production. The most dominant microbe was *Methanosaeta,* an acetoclastic methanogen, and the main pathway to produce methane was via acetate.

References

Anderson, F.E., Bergamaschi, B., Sturtevant, C., Knox, S., Hastings, L., Windham-Myers, L., et al. (2016) Variation of energy and carbon fluxes from a restored temperate freshwater wetland and implications for carbon market verification protocols. *J Geophys Res: Biogeosci* **121**: 777–795.

Aryal, N., Ammam, F., Patil, S.A., and Pant, D. (2017) An overview of cathode materials for microbial electrosynthesis of chemicals from carbon dioxide. *Green Chem* **19**: 5748–5760.

Biniaz, P., Shirazi, N.A., Roostaie, T., and Rahimpour, M.R. (2021) 12 - Wastewater treatment: employing biomass. In *Advances in Bioenergy and Microfluidic Applications*. Rahimpour, M.R., Kamali, R., Amin Makarem, M., and Manshadi, M.K.D. (eds). Elsevier, pp. 303–327.

Bolger, A.M., Lohse, M., and Usadel, B. (2014) Trimmomatic: a flexible trimmer for Illumina sequence data. *Bioinformatics* **30**: 2114–2120.

Bolyen, E., Rideout, J.R., Dillon, M.R., Bokulich, N.A., Abnet, C.C., Al-Ghalith, G.A., et al. (2019) Reproducible, interactive, scalable and extensible microbiome data science using QIIME 2. *Nat Biotechnol* **37**: 852–857.

Bond, D.R. and Lovley, D.R. (2003) Electricity Production by *Geobacter sulfurreducens* Attached to Electrodes. *Appl Environ Microbiol* **69**: 1548–1555.

Cabezas, A., Pommerenke, B., Boon, N., and Friedrich, M.W. (2015) *Geobacter*, *Anaeromyxobacter* and *Anaerolineae* populations are enriched on anodes of root exudate-driven microbial fuel cells in rice field soil. *Environ Microbiol Rep* **7**: 489–497.

Call, D.F., Wagner, R.C., and Logan, B.E. (2009) Hydrogen Production by *Geobacter* Species and a Mixed Consortium in a Microbial Electrolysis Cell. *Appl Environ Microbiol* **75**: 7579–7587.

Callahan, B.J., McMurdie, P.J., Rosen, M.J., Han, A.W., Johnson, A.J.A., and Holmes, S.P. (2016) DADA2: High-resolution sample inference from Illumina amplicon data. *Nat Methods* **13**: 581–583.

Cheng, S., Xing, D., Call, D.F., and Logan, B.E. (2009) Direct Biological Conversion of Electrical Current into Methane by Electromethanogenesis. *Environ Sci & Technol* **43**: 3953–3958.

Clauwaert, P. and Verstraete, W. (2009) Methanogenesis in membraneless microbial electrolysis cells. *Appl Microbiol Biotechnol* **82**: 829–836.

Conrad, R. (2020) Importance of hydrogenotrophic, aceticlastic and methylotrophic methanogenesis for methane production in terrestrial, aquatic and other anoxic environments: A mini review. *Pedosphere* **30**: 25–39.

De Vooys, A.C.A., Koper, M.T.M., Van Santen, R.A., and Van Veen, J.A.R. (2001) The role of adsorbates in the electrochemical oxidation of ammonia on noble and transition metal electrodes. *J Electroanal Chem* **506**: 127–137.

Deppenmeier, U. and Müller, V. (2008) Life Close to the Thermodynamic Limit: How Methanogenic Archaea Conserve Energy. In *Bioenergetics: Energy Conservation and Conversion*. Results and Problems in Cell Differentiation. Schäfer, G. and Penefsky, H.S. (eds). Berlin, Heidelberg: Springer, pp. 123–152.

Dinh, T.T H., Kambara H., Harada Y., Matsushita S., Aoi Y., Kindaichi T., Ozaki N., Ohashi A., 2021. Bioelectrical methane production with an ammonium oxidative reaction under the no organic substance condition. *Microbes Environ* **36**: ME21007

Etiope, G. and Whiticar, M.J. (2019) Abiotic methane in continental ultramafic rock systems: Towards a genetic model. *Appl Geochem* **102**: 139–152.

Farag, I.F., Davis, J.P., Youssef, N.H., and Elshahed, M.S. (2014) Global Patterns of Abundance, Diversity and Community Structure of the *Aminicenantes* (Candidate Phylum *OP8*). *PLOS ONE* **9**: e92139.

Fournier, G.P. and Gogarten, J.P. (2008) Evolution of Acetoclastic Methanogenesis in Methanosarcina via Horizontal Gene Transfer from Cellulolytic Clostridia. *J Bacteriol* **190**: 1124–1127.

Gao, Y., Ryu, H., Santo Domingo, J.W., and Lee, H.-S. (2014) Syntrophic interactions between H2-scavenging and anode-respiring bacteria can improve current density in microbial electrochemical cells. *Bioresour Technol* **153**: 245–253.

Gomez Vidales, A., Omanovic, S., and Tartakovsky, B. (2019) Combined energy storage and methane bioelectrosynthesis from carbon dioxide in a microbial electrosynthesis system. *Bioresour Technol Rep* **8**: 100302.

González-Pabón, M.J., Cardeña, R., Cortón, E., and Buitrón, G. (2021) Hydrogen production in two-chamber MEC using a low-cost and biodegradable poly(vinyl) alcohol/chitosan membrane. *Bioresour Technol* **319**: 124168.

Hall, M. and Beiko, R.G. (2018) 16S rRNA Gene Analysis with QIIME2. *Methods Mol Biol* **1849**: 113–129.

He, C., Liu, T., Ou, H., Yuan, S., Hu, Z., and Wang, W. (2021) Coupling granular activated carbon and exogenous hydrogen to enhance anaerobic digestion of phenol via predominant syntrophic acetate oxidation and hydrogenotrophic methanogenesis pathway. *Bioresour Technol* **323**: 124576.

Hua, D., Fan, Q., Zhao, Y., Xu, H., Chen, L., and Li, Y. (2020) Comparison of methanogenic potential of wood vinegar with gradient loads in batch and continuous anaerobic digestion and microbial community analysis. *Sci Total Environ* **739**: 139943.

Ishii, S., Watanabe, K., Yabuki, S., Logan, B.E., and Sekiguchi, Y. (2008) Comparison of Electrode Reduction Activities of *Geobacter sulfurreducens* and an Enriched Consortium in an Air-Cathode Microbial Fuel Cell. *Appl Environ Microbiol* **74**: 7348–7355.

Kadnikov, V.V., Mardanov, A.V., Beletsky, A.V., Karnachuk, O.V., and Ravin, N.V. (2019) Genome of the candidate phylum *Aminicenantes* bacterium from a deep subsurface thermal aquifer revealed its fermentative saccharolytic lifestyle. *Extremophiles* **23**: 189–200.

Kato, S., Hashimoto, K., and Watanabe, K. (2013) Iron-oxide minerals affect extracellular electron-transfer paths of *Geobacter* spp. *Microbes Environ* **28**: 141–148.

Kurade, M.B., Saha, S., Salama, E.-S., Patil, S.M., Govindwar, S.P., and Jeon, B.-H. (2019) Acetoclastic methanogenesis led by *Methanosarcina* in anaerobic co-digestion of fats, oil and grease for enhanced production of methane. *Bioresour Technol* **272**: 351–359.

Li, M., Zhou, M., Tian, X., Tan, C., McDaniel, C.T., Hassett, D.J., and Gu, T. (2018) Microbial fuel cell (MFC) power performance improvement through enhanced microbial electrogenicity. *Biotechnol Adv* **36**: 1316–1327.

Li, Y., Chen, Y., and Wu, J. (2019) Enhancement of methane production in anaerobic digestion process: A review. *Appl Energy* **240**: 120–137.

Li, Z.-F., Wang, Y., and Botte, G.G. (2017) Revisiting the electrochemical oxidation of ammonia on carbon-supported metal nanoparticle catalysts. *Electrochim Acta* **228**: 351–360.

Liu, W., Cai, W., Guo, Z., Wang, L., Yang, C., Varrone, C., and Wang, A. (2016) Microbial electrolysis contribution to anaerobic digestion of waste activated sludge, leading to accelerated methane production. *Renew Energy* **91**: 334–339.

Logan, B.E., Call, D., Cheng, S., Hamelers, H.V.M., Sleutels, T.H.J.A., Jeremiasse, A.W., and Rozendal, R.A. (2008) Microbial Electrolysis Cells for High Yield Hydrogen Gas Production from Organic Matter. *Environ Sci Technol* **42**: 8630–8640.

Logan, B.E., Hamelers, B., Rozendal, R., Schröder, U., Keller, J., Freguia, S., et al. (2006) Microbial Fuel Cells: Methodology and Technology †. *Environ Sci Technol* **40**: 5181–5192.

Lohner, S.T., Deutzmann, J.S., Logan, B.E., Leigh, J., and Spormann, A.M. (2014) Hydrogenase-independent uptake and metabolism of electrons by the archaeon *Methanococcus maripaludis*. *ISME J* **8**: 1673–1681.

Lovley, D.R. (2017) Syntrophy Goes Electric: Direct Interspecies Electron Transfer. *Annu Rev Microbiol* **71**: 643–664.

Mostafa, A., Im, S., Lee, M.-K., Song, Y.-C., and Kim, D.-H. (2020) Enhanced anaerobic digestion of phenol via electrical energy input. *Chem Eng J* **389**: 124501.

Nobu, M.K., Narihiro T., Hideyuki T., Qui, Y.L., Sekiguchi, Y., Woyke, T., et al. (2015) The genome of *Syntrophorahabdus* aromaticivorans strain UI provides new insights for syntrophic aromatic compound metabolism and electron flow. Environ Microbiol **17**: 4861–4872

Onodera, I. (2013) Development of Methane Fermentation Technology for Wastewater Treatment. *Jpn Tappi J* **67**: 82–85.

Pan, X.-R., Wang, Y.-K., Li, W.-W., Wang, Y.-S., Wang, X., Cheng, Y., et al. (2017) Selective co-production of acetate and methane from wastewater during mesophilic anaerobic fermentation under acidic conditions. *Environ Sci: Water Res Technol* **3**: 720–725.

Parada, A.E., Needham, D.M., and Fuhrman, J.A. (2016) Every base matters: assessing small subunit rRNA primers for marine microbiomes with mock communities, time series and global field samples. *Environ Microbiol* **18**: 1403–1414.

Park, J., Lee, B., Tian, D., and Jun, H. (2018) Bioelectrochemical enhancement of methane production from highly concentrated food waste in a combined anaerobic digester and microbial electrolysis cell. *Bioresour Technol* **247**: 226–233.

Peng, H., Zhao, Z., Xiao, H., Yang, Y., Zhao, H., and Zhang, Y. (2019) A strategy for enhancing anaerobic digestion of waste activated sludge: Driving anodic oxidation by adding nitrate into microbial electrolysis cell. *J Environ Sci (Beijing, China)* **81**: 34–42.

Pruesse, E., Peplies, J., and Glöckner, F.O. (2012) SINA: Accurate high-throughput multiple sequence alignment of ribosomal RNA genes. *Bioinformatics* **28**: 1823–1829.

Qiu, Y.-L., Hanada, S., Ohashi, A., Harada, H., Kamagata, Y., and Sekiguchi, Y. (2008) Syntrophorhabdus aromaticivorans gen. nov., sp. nov., the First Cultured Anaerobe Capable of Degrading Phenol to Acetate in Obligate Syntrophic Associations with a Hydrogenotrophic Methanogen. *Appl Environ Microbiol* **74**: 2051–2058.

Quast, C., Pruesse, E., Yilmaz, P., Gerken, J., Schweer, T., Yarza, P., et al. (2013) The SILVA ribosomal RNA gene database project: improved data processing and web-based tools. *Nucleic Acids Res* **41**: D590-596.

Reguera, G., McCarthy, K.D., Mehta, T., Nicoll, J.S., Tuominen, M.T., and Lovley, D.R. (2005) Extracellular electron transfer via microbial nanowires. *Nature* **435**: 1098–1101.

Romero, R.M., Valenzuela, E.I., Cervantes, F.J., Garcia-Reyes, R.B., Serrano, D., and Alvarez, L.H. (2020) Improved methane production from anaerobic digestion of liquid and raw fractions of swine manure effluent using activated carbon. *J Water Process Eng* **38**: 101576.

Rotaru, A.-E., Shrestha, P.M., Liu, F., Shrestha, M., Shrestha, D., Embree, M., et al. (2013) A new model for electron flow during anaerobic digestion: direct interspecies electron transfer to Methanosaeta for the reduction of carbon dioxide to methane. *Energy Environ Sci* **7**: 408–415.

Salgado-Dávalos, V., Osorio-Avilés, S., Kamaraj, S.K., Vega-Alvarado, L., Juárez, K., Silva-Martínez, S., and Alvarez-Gallegos, A. (2021) Sediment Microbial Fuel Cell Power Boosted by Natural Chitin Degradation and Oxygen Reduction Electrocatalysts. *CLEAN – Soil, Air, Water* **49**: 2000465.

Sarmin, S., Ethiraj, B., Islam, M.A., Ideris, A., Yee, C.S., and Khan, Md.M.R. (2019) Bio-electrochemical power generation in petrochemical wastewater fed microbial fuel cell. *Sci Total Environ* **695**: 133820.

Schlager, S., Haberbauer, M., Fuchsbauer, A., Hemmelmair, C., Dumitru, L.M., Hinterberger, G., et al. (2017) Bio-Electrocatalytic Application of Microorganisms for Carbon Dioxide Reduction to Methane. *ChemSusChem* **10**: 226–233.

Schoell, M. (1983) Genetic Characterization of Natural Gases. *AAPG Bulletin* **67**: 2225–2238.

Schoell, M. (1980) The hydrogen and carbon isotopic composition of methane from natural gases of various origins. *Geochim Cosmochim Acta* **44**: 649–661.

Shehab, N., Li, D., Amy, G.L., Logan, B.E., and Saikaly, P.E. (2013) Characterization of bacterial and archaeal communities in air-cathode microbial fuel cells, open circuit and sealed-off reactors. *Appl Microbiol Biotechnol* **97**: 9885–9895.

Villano, M., Aulenta, F., Ciucci, C., Ferri, T., Giuliano, A., and Majone, M. (2010) Bioelectrochemical reduction of CO2 to CH4 via direct and indirect extracellular electron transfer by a hydrogenophilic methanogenic culture. *Bioresour Technol* **101**: 3085–3090.

Wang, W., Zhang, Y., Li, M., Wei, X., Wang, Y., Liu, L., et al. (2020) Operation mechanism of constructed wetland-microbial fuel cells for wastewater treatment and electricity generation: A review. *Bioresour Technol* **314**: 123808.

Xu, R., Xu, S., Florentino, A.P., Zhang, L., Yang, Z., and Liu, Y. (2019) Enhancing blackwater methane production by enriching hydrogenotrophic methanogens through hydrogen supplementation. *Bioresour Technol* **278**: 481–485.

Yamada, T., Hamada, M., Kurobe, M., Harada, J., Giri, S., Tsuji, H., and Daimon, H. (2019) Prokaryotic Community Structures in a Thermophilic Anaerobic Digestion Reactor Converting Poly(l-Lactic Acid) for a Long Period Revealed by 16S rRNA Gene Amplicon Sequencing. *Microbiol Resour Announc* **8**:.

Yan, Y., Li, T., Zhou, L., Tian, L., Yan, X., Liao, C., et al. (2020) Spatially heterogeneous propionate conversion towards electricity in bioelectrochemical systems. *J Power Sources* **449**: 227557.

Yilmaz, P., Parfrey, L.W., Yarza, P., Gerken, J., Pruesse, E., Quast, C., et al. (2014) The SILVA and "All-species Living Tree Project (LTP)" taxonomic frameworks. *Nucleic Acids Res* **42**: D643–D648.

Yoho, R.A., Popat, S.C., and Torres, C.I. (2014) Dynamic Potential-Dependent Electron Transport Pathway Shifts in Anode Biofilms of Geobacter sulfurreducens. *ChemSusChem* **7**: 3413–3419.

Zakaria, B.S. and Dhar, B.R. (2021) Characterization and significance of extracellular polymeric substances, reactive oxygen species, and extracellular electron transfer in methanogenic biocathode. *Sci Rep* **11**: 1–13.

Zhao, Z., Zhang, Y., Yu, Q., Ma, W., Sun, J., and Quan, X. (2016) Enhanced decomposition of waste activated sludge via anodic oxidation for methane production and bioenergy recovery. *Int Biodeterior Biodegrad* **106**: 161–169.

Zhen, G., Zheng, S., Lu, X., Zhu, X., Mei, J., Kobayashi, T., et al. (2018) A comprehensive comparison of five different carbon-based cathode materials in CO2 electromethanogenesis: Long-term performance, cell-electrode contact behaviors and extracellular electron transfer pathways. *Bioresour Technol* **266**: 382–388.

Chapter

5

Bioelectrical methane production coupled with a biotic HS^- oxidation

5.1 Introduction

Increasing competition for fossil fuels, and the need to avoid the release of carbon dioxide from the combustion of these fuels, has increased the search for new and sustainable approaches for energy production. Two new methods of bioenergy production from biomass include electricity production using microbial fuel cells (MFCs) and hydrogen production by electrohydrogenesis using microbial electrolysis cells (MECs) (Logan *et al.*, 2006, 2008). In the microbial fuel cell (MFC) process, electricity is generated by the action of microbes, such as electrogenic bacteria, at the anode with the degradation of organic matter (Sarmin *et al.*, 2019; Wang *et al.*, 2020). Conversely, in a microbial electrosynthesis system (MES), which is a type of modified MFC, hydrogen gas is produced at the cathode, not the anode by providing electricity (Logan *et al.*, 2008; González-Pabón *et al.*, 2021). In addition to hydrogen gas, methane is produced in the cathode chamber of the MES (Clauwaert and Verstraete, 2009; Zhao *et al.*, 2016; Zakaria and Dhar, 2021). Higher methane production can be expected in MES than in conventional methane fermentation reactors for wastewater treatment because the combination of methane production from organic substances and conversion of CO_2 to methane through electricity by microbes occurs at the cathode (Park *et al.*, 2018; Peng *et al.*, 2019).

Bio-electrical methane production controlled by MES is performed without organic substrates (Villano *et al.*, 2010; Aryal *et al.*, 2017; Schlager *et al.*, 2017; Zhen *et al.*, 2018). Methanogens can catalyze methane production from CO_2 via two proposed mechanisms: direct extracellular electron transfer and indirect extracellular electron transfer. With regard to the first mechanism, the ability of methanogens to produce methane from CO_2 reduction by using an electrode as a direct electron donor has been reported (Cheng *et al.*, 2009). The remainder is with intermediate production of hydrogen. Methane may be produced by methanogens using abiotic H_2 formed in water reduction coupled with CO_2 uptake. Even at lower applied voltages, bioelectrotrophic H_2 production might be achieved because few bacteria, such as *Geobacter*, are known to transfer electrons (Call *et al.*, 2009). Dinh *et al.* (2021) proposed a scheme for biological methane production via bioelectrotrophic H_2 production in an MES. However, there was insufficient experimental data to fully explore the complex interactions between microorganisms and cathode as well as interspecies. It is still unclear whether bioelectrical methane production occurs via direct and/or indirect reaction(s) in MESs.

The standard reduction potential $E^{0'}$ of CO_2 to methane at pH = 7 is −0.24 V (vs. standard hydrogen potential [SHE]) equivalent to −0.44 V (vs. Ag/AgCl). Cheng *et al.* (2009) demonstrated that bioelectrotrophic methane production occurred at a biocathode potential of < −0.7 V (vs. Ag/AgCl), and found that −1.0 V (vs. Ag/AgCl) gave an excellent result, with an electron capture efficiency of 96%. However, based on the thermodynamical calculation, the voltage applied to produce methane in MES depends not only on the biocathode potential but also on the anode potential. Several experiments using an MES were conducted at relatively high voltages to produce methane when coupling of H_2O oxidation at the anode (Zhen *et al.*, 2015; Gomez Vidales *et al.*, 2019). If instead of H_2O oxidation, oxidation of inorganic with lower potential (such as NH_4^+, HS^-) took place, whether methane can be produced even at low voltage. Our past studies demonstrated that carbon dioxide was reduced to methane even at an applied voltage of 0.05 and 0.1 V when coupling NH_4^+ and HS^- oxidation, respectively (Dinh *et al.* a,b, 2021).

One disadvantage of the method of methane production in MES even at lower applied is that a precious metal catalyst of platinum is used on the anode to catalyze NH_4^+ and HS^- oxidation. Considering the development of alternative anode catalysts, such as microbial bioanode are required. Recently, microbial bioanodes are widely known in MFC. Electricity generation is spontaneous with the oxidation of organic matter such as acetate by electrogenic bacteria on the anode. In the absence of organic matter, Sun *et al.* (2009) demonstrated that both electrochemical reactions and microbial catalysis were involved in such a complex sulfide oxidation process in the bioanode of an MFC. Not only in MFC, but the highly detected microorganism in the bioanode can mainly drive the complete anoxic conversion of ammonium to N_2 in MEC (Vilajeliu-Pons *et al.*, 2018).

In this study, a two-chamber MEC was designed, in which no organic substrate was supplied, and HS^- was added to the anode chamber, aiming to investigate whether methane production is possible even at very low applied voltages. This is the first study to report the coupling of CO_2 reduction and HS^- oxidation with the assistance of microbial catalysts, under the no substrate organic condition. In addition, a 16S rRNA gene sequencing was conducted to characterize the microbial communities in the biocathode and bioanode. From this to identify the organisms involved in bio-electrical methane production as well as sulfur oxidation.

5.2 Materials and Methods

5.2.1 MES set-up

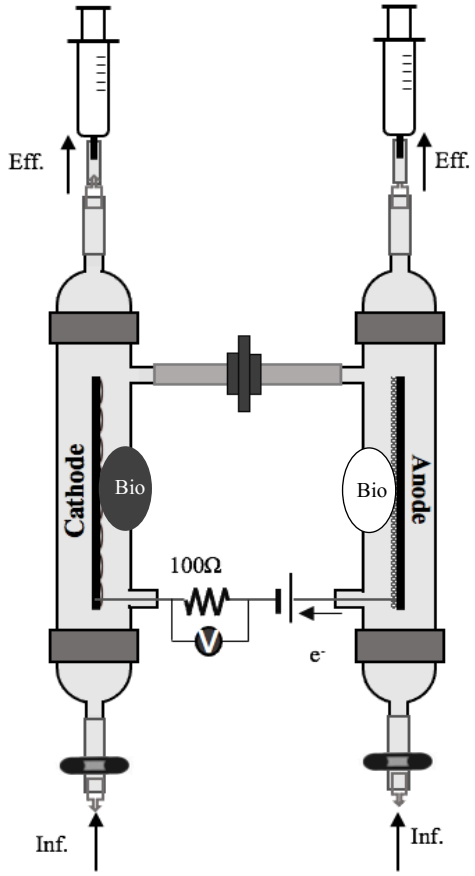

Fig. 5-1 Schematic representation of microbial electrosynthesis system consisting of two chambers connected with a cation exchange membrane (MES; biotic anode).

The MES used in this study consisted of two glass chambers with an effective volume of 70 mL each and were connected through a cation exchange membrane (CEM/Nafion EC–NM–211, Toyo Corporation, Japan) of working area 0.5 cm^2 (**Fig. 5-1**). From day 178 onwards (Batch no. 26), MES was changed by scaling up working area 3.15 cm^2 . By this way, the rate of cations transfered between cathode and anode chambers was increased, and this can speed up the rate of redox reaction in MES. The difference of CEM's working area separated our experiment into 2 parts: RUN_1 and RUN_2 (**Table 5-1**). The top of each chamber was connected to a 10-mL loss-of-resistance glass syringe to release the pressure in the chamber generated from the produced gas and to facilitate gas collection. A carbon cloth (Toyobo Co. Ltd, Japan) with an area of 24 cm^2 was installed in both chambers as electrodes. The electrodes were connected to a DC power supply (Array 3600 Series, T&C Technology, Japan) using a titanium wire. A 100 Ω resistor was inserted beside the power supply to monitor the electric current using a data logger (GL 240 midi LOGGER, GRAPHTEC, DATAQ Instruments, Inc., USA). A small amount of anaerobic sludge collected from a laboratory-scale upflow anaerobic sludge blanket (UASB) reactor was inoculated on the surface of the electrode, which worked as a biocathode. For the anode, activated sludge collected from wastewater treatment center (Higashi-shi, Hiroshima) was coated on the surface of the electrode as a bio-catalyst, according to previous studies (Sun *et al.*, 2009; Vilajeliu-Pons *et al.*, 2018)

Table 5-1 MES operational conditions

MES	Phase	Batch no.	Operational time (day)	Voltage (V)	NH_4^+ (mg N L^{-1})	HS^- (mg S L^{-1})	
					Cathode/Anode	Cathode	Anode
RUN_1 (d_1=0.5cm)	I	1–9	0–65	0.8	13.5	6.0	6.0
	II	10–15	66–107	0.8	13.5	9.3–16	9.3–16
	III	16–25	108–177	0.8	2.8	4	16–26.7
RUN_2 (d_2=2cm)	I	26–31	178–219	0.8	2.8	4	26.7–53.3
	II	32–35	220–247	0.8	2.8	4	9.3–53.3
	III	36–41	247–289	0.2–0.8	2.8	4	32

d_1, and d_2 : diameter of CEM

The anode and biocathode chambers were filled with the same medium and deoxidized through a nitrogen purge without organic substances. The medium was composed of $NaHCO_3$ (200 mg L^{-1}), $Na_2S{\cdot}9H_2O$ (0–53.3 mg S L^{-1}), NH_4Cl (3–13.5 mg N L^{-1}), KH_2PO_4 (102 mg L^{-1}), K_2HPO_4 (305 mg L^{-1}), and trace elements, including $FeSO_4{\cdot}7H_2O$ (7 mg L^{-1}), $CoCl_2{\cdot}6H_2O$ (1.7 mg L^{-1}), $ZnSO_4{\cdot}7H_2O$ (1.5 mg L^{-1}), HBO_3 (0.6 mg L^{-1}), $MnCl_2{\cdot}4H_2O$ (4.2 mg L^{-1}), $NiCl_2{\cdot}4H_2O$ (0.4 mg L^{-1}), $CuCl_2{\cdot}2H_2O$ (0.27 mg L^{-1}), $Na_2MoO_2{\cdot}2H_2O$ (0.25 mg L^{-1}), $MgCl_2{\cdot}6H_2O$ (4.0 mg L^{-1}), $CaCl_2{\cdot}2H_2O$ (1.5 mg L^{-1}), and KCl (3.0 mg L^{-1}) at pH 7.3 (**Table 5-1**). The only difference between the biocathode and anode medium was the concentration of HS^- from day 108 onwards. N_2 gas (0.5 mL) was initially injected into both chambers to facilitate sampling of the produced gas containing methane.

5.2.2 MES operation

The MES was operated in batch processing mode at 30°C in a thermostatic chamber. The batch experiment of RUN 3-1 was repeated 25 times over 177 days at interval of 7 days (batch no. 1–no.25). RUN 3-2 was continued with 16 repeated times over 112 days at at interval of 7 days (batch no. 26–no.41). A voltage of 0.8 V was applied by setting up the MES to batch no.35. In phase III of RUN_2, each batch experiment was performed in an applied voltage range of 0.8–0.2 V to investigate the effect of voltage on methane production, as shown in **Fig. 5-2** and **Table 5-1**. Phase III of RUN 3-1 and phase I, II of RUN 3-2 were conducted to investigate the influence of HS^- concentration.

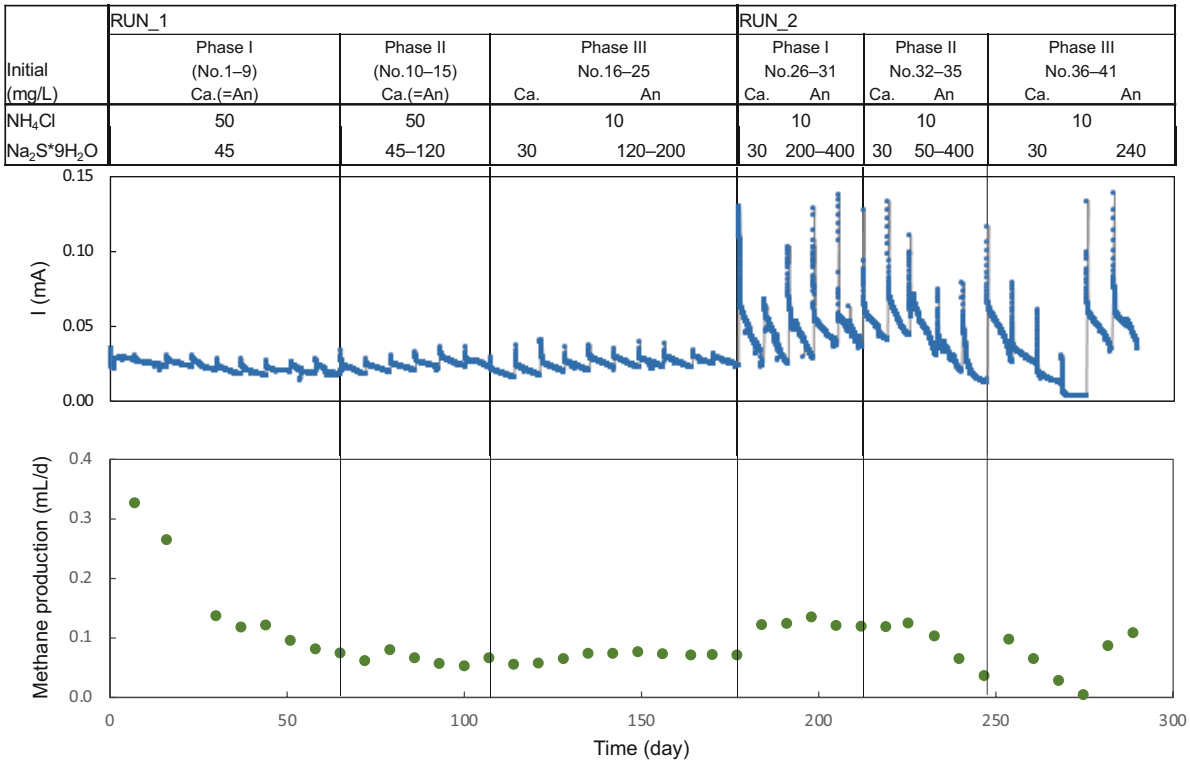

Fig. 5-2 Batch experiments of microbial electrosynthesis system including RUN 3-1 and RUN 3-2

5.2.3 Sampling and analyses

The volume of gas in each chamber was measured at the end of each batch operation using an airtight syringe. The gas compositions of CH_4, N_2, CO_2, and H_2 were then measured using a gas chromatograph equipped with a thermal conductivity detector (GC-TCD, Shimadzu GC-8A). Analysis of the liquid samples at the start and end of each batch was performed after filtration with 0.2-μm pore size polytetrafluoroethylene membranes. NH_4^+, NO_3^-, and NO_2^- concentrations were measured using an ion chromatograph (Shimadzu HPLC-20A). SO_4^{2-} concentration was determined by a colorimetric method using a Hach DR-2800 spectrophotometer (Hach Co., Loveland, CO, USA). The dissolved CH_4 and N_2 concentrations were estimated using Henry's law.

5.2.4 Microbial community

Microbial community analysis was performed for the two biomasses collected from the biocathode and bioanode on the last day of the MES operation. After washing the biomass with phosphate buffer, DNA was extracted using the FastDNA® SPIN kit for soil (MP Biomedicals, Solon, OH, USA), according to the manufacturer's instructions. The two DNA samples were transported to the Bioengineering Lab (Kanagawa, Japan) for performing polymerase chain reaction with the primer sets 341′F (5′-CCTAHGGGRBGCAGCAG-3′) and 805R (5′-GACTACHVGGGTATCTAATCC-3′), and sequencing using the Illumina MiSeq platform (Illumina, Inc., San Diego, CA, USA). The raw sequence data were trimmed using Cutadapt software (version 1.18) (Parada *et al.*, 2016) to remove primers from the sequence reads. Noise and low-quality sequence reads were removed using Trimmomatic (version 0.39-1) (Bolger *et al.*, 2014) when the quality per base dropped below 20 bp in the sliding window and the minimum length of the reads was below 40 bp. The clean reads were analyzed using QIIME2 (version 2020.08) (Hall and Beiko, 2018; Bolyen *et al.*, 2019). Operational taxonomic units (OTUs) were classified using the pipeline software DADA2 (Callahan *et al.*, 2016) with the SILVA (release_132) database (Pruesse *et al.*, 2012; Quast *et al.*, 2013; Yilmaz *et al.*, 2014).

5.3 Results

The experimental results were divided into two parts. The first part showed the results of the reactor has the same size as the one described in chapter 4. The second part was the results of the improved reactor.

5.3.1 Performance of batch experiments (RUN 3-1)

From the first batch of the experiment, the initial applied voltage was set up to 0.8V for 7 days batch. After closing the circuit, the electric current reached nearly 0.042 mA, then dropped to 0.022 mA for half of the day but gradually increased 0.027 mA and got stable until the end of the batch (**Fig. 5-3**). The next batches of phase I was then repeated with changes in a bulk liquid, resulting in the current behaviors that were the same as the first batch's one. However, the value of current was gradually lower than the previous batch, and reached steady state from batch 7. Comparing with the performance of batch experiment described in the chapter 4, under the same conditions only bio-catalyst instead of Pt-catalyst in the anode, the electric current was much higher (about 3 times) even at steady state.

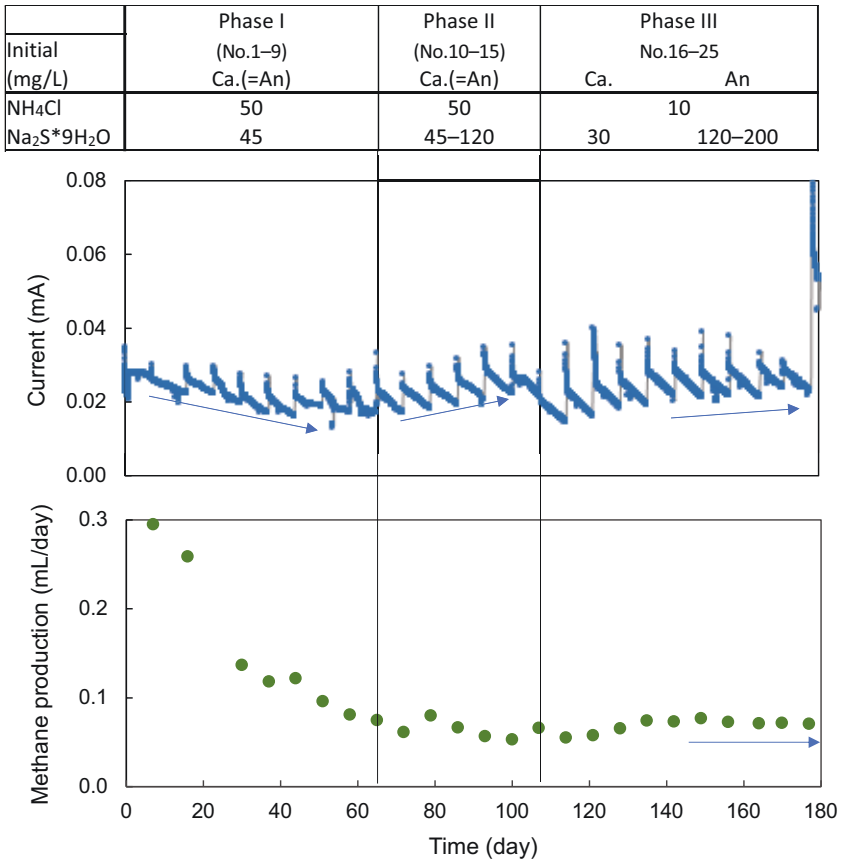

Fig 5.3 Time course of curent and methane production in RUN 3-1

Furthermore, NH_4^+ concentration in the end of the batch experiment was higher than the ones in the start. Therefore, the decomposition of organic matter from the inoculated sludge in the anode may be the reason to explain why the current had a high value in the first batch, and a part of NH_4^+ detected was the product of this decomposition. Indeed, for the next batches, since the organic matters from sludge was gradually depleted, the current tends to decrease, and the amount of NH_4^+ concentration in the end of each batch experiment also deceased.

The first batch had the highest methane production, including dissolved methane of bulk liquid estimated using Henry's law. During the next batches, methane was also detected but tend to decrease with respect to current behavior (**Fig. 5-3**). Thus, together with the explanation from Chapter 4 under the same conditions, a part of these methane productions was derived from organic matter in sludge inoculated the biocathode. The remained part may be through CO_2 reduction due to the high generated electricity in MES from the decomposition of organic matter inoculared in the anode.

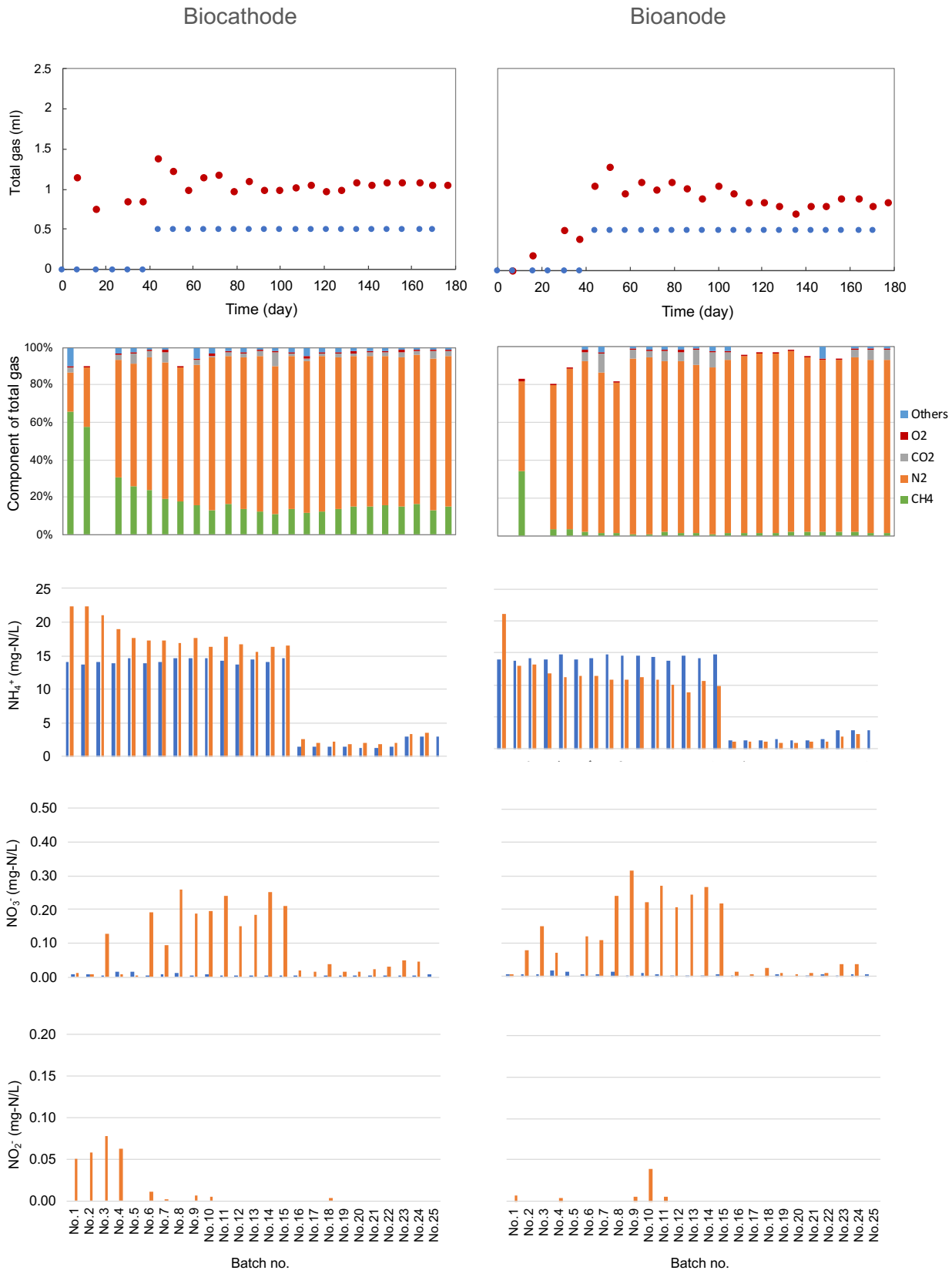

Fig. 5-4 The measure values (gas companents, NH_4^+ ,NO_3^- and NO_2^- concentration) of RUN 3.1

In summary, the organic matter of innoculated in the electrodes has impact on methane production as well as electricity production in phase I.

As a steady state of current was observed in late phase I, the amount of HS^- addition to the bulk liquid in the anode chamber was increased step by step to enhance current and methane production in Phase II of batches 10 to 15 for the operation day 66 to 107. Under these conditions, the methane production with Pt-catalyst in the anode (**Chapter 4**) steadily increased with accompanying increase in the amount of current as expected. However, here the results showed that there was only slightly increasing of current and methane in the next batches. Regarding the oxidation reaction in the anode, nitrate and nitrite were detected in the anode chamber although the concentrations were very small (**Fig. 5-4**), suggesting that NH_4^+ oxidation to nitrate or nitrite was insignificant. Conversely, sulfate production also increased in the anode chamber at a higher rate, indicating the current was derived from mainly oxidation of HS^- to sulfate, and the effect of NH_4^+ oxidation was insignificant.

In phase III, since the high HS^- concentration might inhibit microbial activity for methane production on the biocathode from batch No. 16, the substrate was separately added into the cathode and anode chambers. We decreased the initial concentration of HS^- in the cathode chambers to 2–4 mg S/L (**Fig. 5-3**). In addition, NH_4^+ of the bulk liquid was reduced to 2.8 mg N L^{-1} because of little effect on current. During the first batch of phase III, by deducting the initial concentration of HS^-, it decreased the migration of protons and cations into cathode chambers through a membrane to maintain electroneutrality when oxidations occurred in anode chambers. This may be the reason to explaine why the electrical current and the amount of produced SO_4^{2-} in anode chambers would be less than the results of batch No. 15. Although initial HS^- concentration in the anode was continued to increase every batch, sulfate production was observed not to increase. This result linked to the current and produced methane were almost stable.

Both of phase II and phase III, the results showed that the oxidation of HS^- had effect on the curent and methane production. Although, the current reached steady state after totally eliminating the organic matter in the inoculated sludge was relatively high, there had no tendency of increasing current and methane like when using Pt-catalyst in the anode (**Chapter 4**) (**Fig. 5-5**).

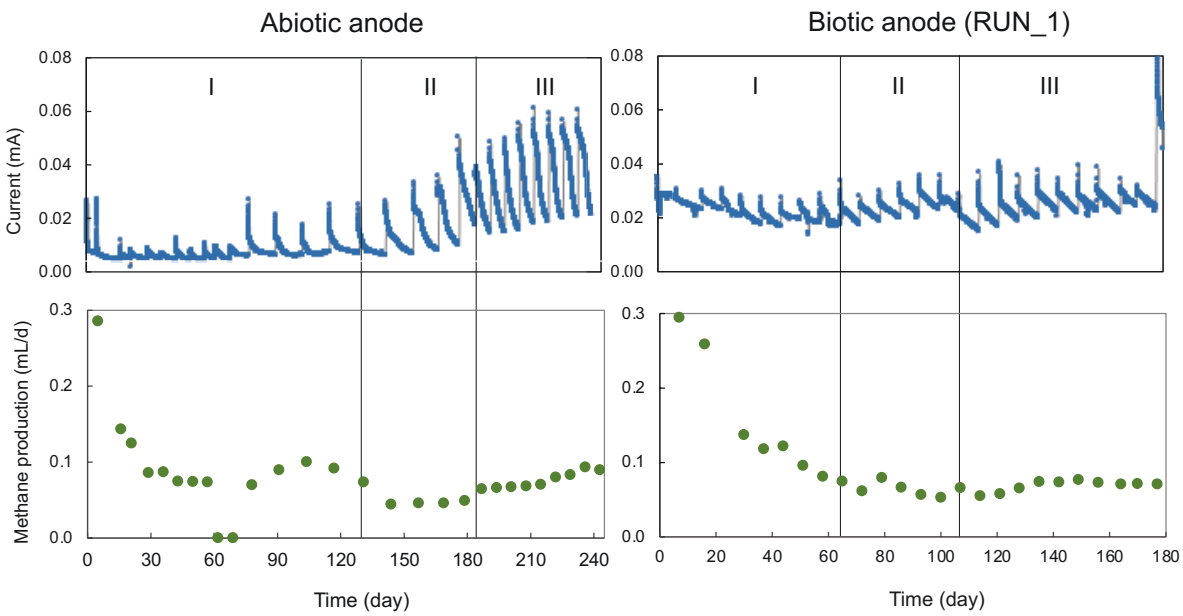

Fig. 5-5 Comparison with the current and methane production of batch experiments using Pt-catalyst (abiotic anode)

In this case, the oxidation of HS^- to sulfate is dependent on bio-electrochemical process of the inoculated sludge in the anode. Thus, this issue will be clearly discussed latter based on the microbial analysis in the bioanode.

5.3.2 Performance of batch experiments (RUN 3-2)

Increasing the initial HS^- concentration step by step in the anode didn't enhance current and methane production as expected. One of the reasons is that the rate of transferring cations between cathode and anode chamber may be the rate-limiting step, affecting the overall rate of a redox reaction in MES. To fix this problem, CEM's working area connected with both chambers was increased. After completing the improved MES, the batch experiment was continued to conduct, namely RUN 3-2.

As expected, the current and methane production were about two times higher compared with the batches of RUN 3-1 under the same conditions of HS^- concentration. To investigate the effect of HS^- concentration on methane as well as current production, batch experiments were continuously performed while increasing and decreasing HS^- concentration step-by-step. In phase I, HS^- concentration was increased in range of 26.7–53.3 mg-S/L.

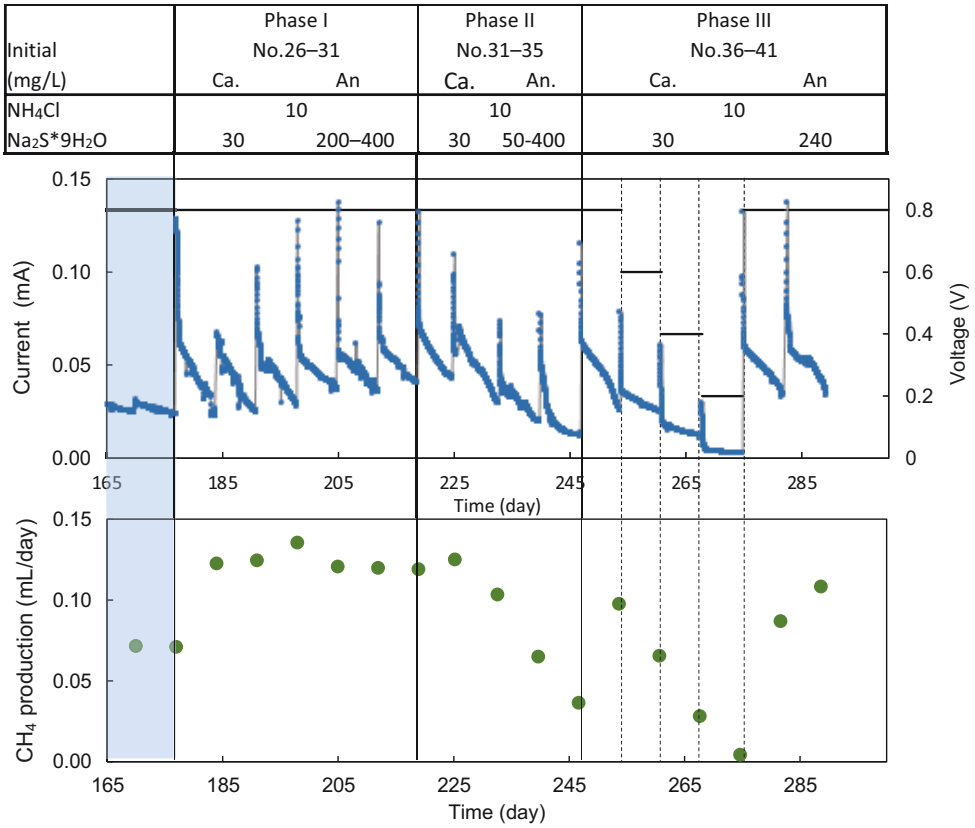

Fig. 5-6 Time course of curent and methane production in RUN 3-2

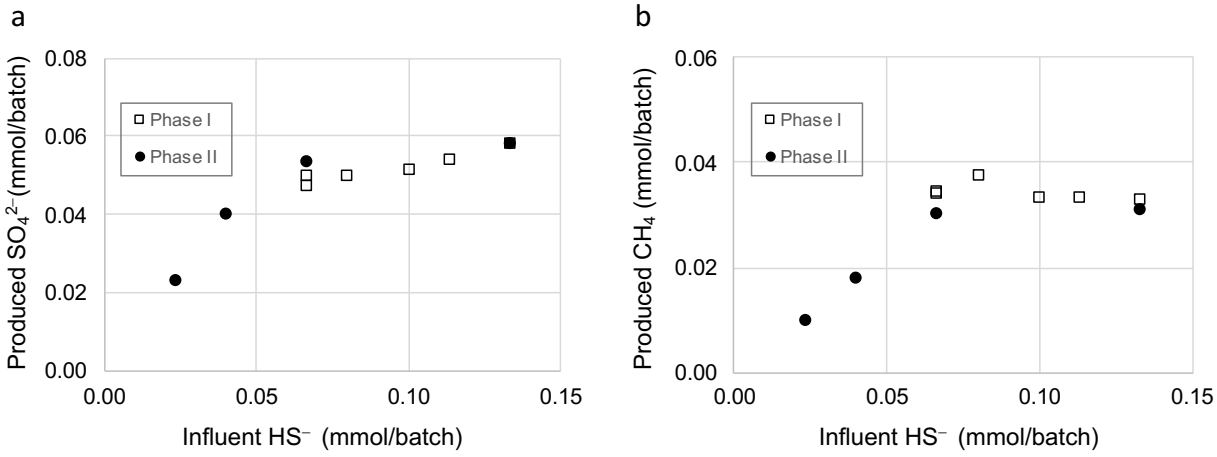

Fig. 5-7 Relationship between the produced SO_4^{2-} (a), CH_4 (b) and influent HS^-

The results showed that there was no increase in the current and methane production (Fig. **5-6**). Conversely, when decreasing HS^- concentration from 53.5 to 9.3 mg-S/L, we observed a significant decrease in the current and methane production. In addition**, Fig. 5-7a** also indicated that sulfate production was almost constant at high HS^- concentration in phase I, and tended to decease when decreasing HS- concentration in phase II.

In phase III, we investigate the effect of applied voltage on methane and sulfate production, although it was unclear whether the activity of microbes reached a steady state. A step-by-step decrease in the applied voltage was conducted until 0.2 V of bach 39, and then the applied voltage was returned back to 0.8 V. With decreasing the applied voltage, both of the amount of current and the methane production were sharply declined. However, even at the lowest voltage of 0.2 V, methane production occurred although the amount was very small. When the applied voltage was increased to 0.8 V, the current and the methane production were recovered. As a very low applied voltage caused a significantly small amount of methane production and methane productions at 0.8 V were almost the same value, it is supposed that the most of organic substance in the inoculated sludge was consumed and the microbial activity nearly reached a steady state before Phase III.

The methane production was proportional to the applied voltage, as shown in **Fig. 5-8**. As the voltage will affect electron production by chemical oxidation on the anode, the change of the current should be related closely to the methane production. Sulfate production was also proportional to the applied voltage. However, the results also showed that sulfate production could be detected even if no applied voltage. It suggests that there should be amount of HS- to ensure the anoxic environment inside of MES. In sumary, sulfate production rate was similar to that of CH_4 with respect to the effect of volatage. Together with methane was not detected even at the highest voltage of 0.8V (data not shown), suggesting that microbes on the biocathode and bioanode are essential to produce methane and sulfate, respectively.

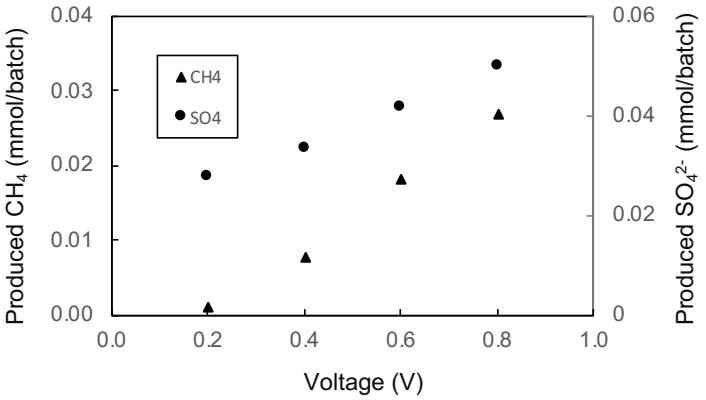

Fig. 5-8 Produced CH_4 and SO_4^{2-} at different applied voltage in phase III (RUN 3.2)

5.3.3 Electrical CO_2 reduction and HS^- oxidation

Oxidation of HS^- to SO_4^{2-} occurred at the anode, and its oxidation reaction is represented as follows:

$$1/8\ HS^- + 1/2\ H_2O \rightarrow 1/8\ SO_4^{2-} + 9/8\ H^+ + e^- \qquad (5\text{-}1)$$

where 1 mol of electron and 1/8 mol of SO_4^{2-} were produced from 1/8 mol of HS^-.

Based on Faraday's laws of electrolysis, the amount of donated or accepted electrons, *Ne* [mol], can be calculated from the measured current using the following equation:

$$Ne = \frac{\int I dt}{F} \qquad (5\text{-}2)$$

where *I* is the current (A), t is the time (s), and *F* is Faraday's constant (C mol^{-1}).

Fig. 5-9a shows the relationship between the amount of calculated electron flux per batch operation and the amount of SO_4^{2-} produced in phase II and III of RUN 3.1 and phases I, II and III of RUN 3.2 with its theoretical line based on the half reaction of Eq. (5-1). The data of phases I of RUN 3.1 were not used in **Fig. 5-9**, because organic matter in the inoculated sludge might strongly affect the electron current. In phase II and III of RUN 3.2, the plots of the measured SO_4^{2-} production were close to the theoretical line. However, all batches of RUN_2, the produced SO_4^{2-} was little far from the theorical line. These results may be due to the impacts of MES penetrated oxygen on HS^- oxidation. RUN 3.2 with increasing working area of CEM gave good results in methane and current production, but the amount of penetrated oxygen was higher compared with RUN 3.1.

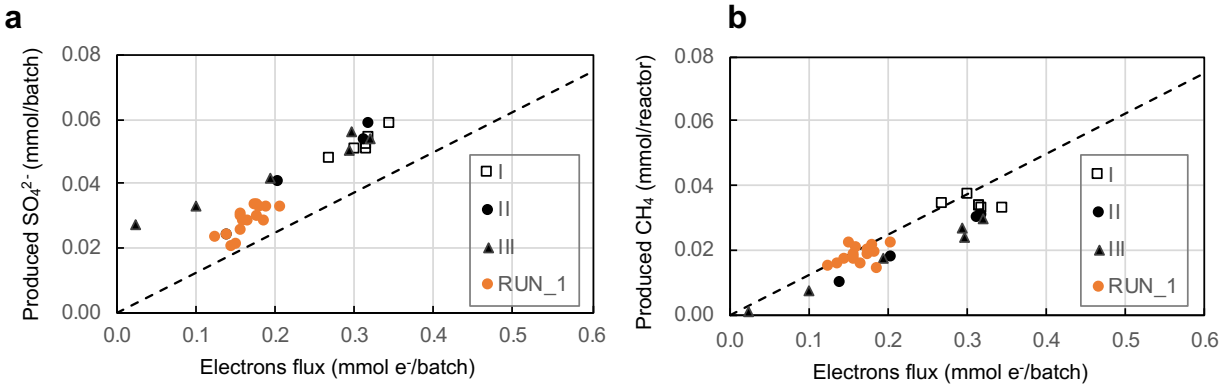

Fig. 5-9 Produced SO42- and CH4 versus electron flux *N*e. Dash line: theorical production based on the half reactions.

In contrast, at the biocathode, the electrons donated from the anode were accepted through the external circuit and were used for reduction of CO_2 to CH_4. This half-reduction reaction can be represented as follows:

$$1/8\ CO_2 + H^+ + e^- \rightarrow 1/8\ CH_4 + 1/4\ H_2O \qquad (5\text{-}3)$$

where 1/8 mol of CH_4 is produced from 1 mol of electrons and 1/8 mol of CO_2.

Similarly, the relationship between the amount of calculated electron flux per batch operation and the amount of measured CH_4 production in phases II and II of RUN 3.1, and all batches of RUN 3.2 with its theoretical line based on the half reaction of Eq. (5-3) was shown in **Fig. 5-9b**. Similar to **Fig. 5-9a,** there was a small discrepancy between the measured CH_4 production and the theoretical values. Despite the discrepancies, the electron balance of the redox reaction was maintained in this MES experiment (**Fig. 5-9**). Therefore, in the MES system without organic substances, methane production can be performed by coupling CO_2 reduction at the biocathode and HS^- oxidation at the anode, even at relatively low applied voltages of 0.2–0.8 V.

5.3.4 Microbial community

Biocathode

In chapter 4, the microbial community was analyzed to identify the organism involved in bio-electrical methane production at the biocathode. Similarly, here microbial community analysis was also performed for the biomass sample collected on the last day of the MES operation. In the 16S rRNA gene analysis, 240 OTUs were obtained from 32071 sequence reads. Sequencing results revealed the presence of bacterial and archaeal communities at population sizes of 59.9 and 40.1%, respectively. These results are relatively similar to those in chapter 4 (bacteria: 62.1% and archaea: 37.9%). To more clarify this similarity, the comparisons between two biomass samples' microbial communities were shown **Fig. 5-10**. Particularly, **Table 5-2** indicated that in not only archaeal but also bacterial community, the rates of the presence of the same OTUs in two biomass sample were quite similar. This means that the process of methane production here may be explained based on the complex interactions between microorganisms and biocathode as well as interspecies like as described in chapter 4. In addition, the formation and growth of two biomass samples-

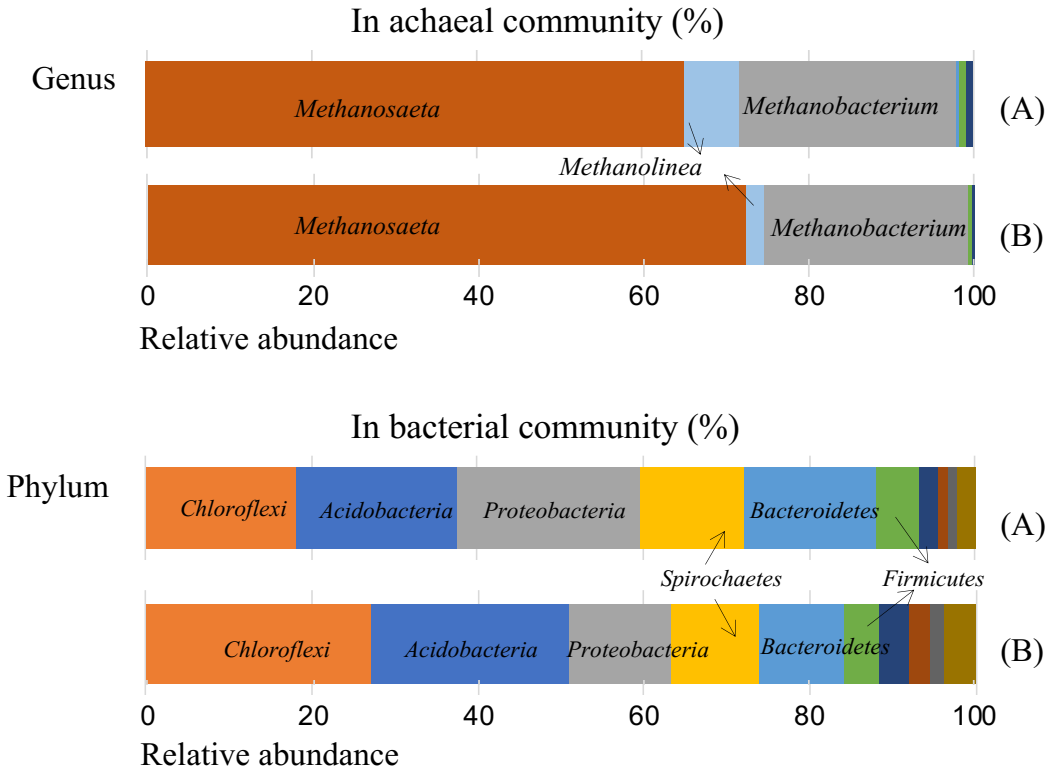

Fig. 5-10 Comparison between two microbial comunities (A) and (B) based on 16S rRNA gene. (A) : microbial community developed at the biocathode in chapter 4
(B) : microbial community developed at the biocathode in chapter 5

Table 5-2 The rate of the same OTUs in two microbial comunities

In archaeal community (%)

>0.1% and <1%
>1% and <10%
> 5%

OTU	(A)	(B)	Phyum	Class	Order	Family	Genus	Speice
525733a7bb0	65.1	72.3	D_1__Euryarchaeota	D_2__Methanomicrobia	D_3__Methanosarcinales	D_4__Methanosaetaceae	D_5__Methanosaeta	0
7db592fcddb	6.6	2.1	D_1__Euryarchaeota	D_2__Methanomicrobia	D_3__Methanomicrobiales	D_4__Methanoregulaceae	D_5__Methanolinea	D_6__uncultured Methanolinea sp.
e03cfb210a7	26.3	24.8	D_1__Euryarchaeota	D_2__Methanobacteria	D_3__Methanobacteriales	D_4__Methanobacteriaceae	D_5__Methanobacterium	D_6__uncultured archaeon
eccd2f6d8eb	0.0	0.0	D_1__Euryarchaeota	D_2__Methanomicrobia	D_3__Methanomicrobiales	D_4__Methanospirillaceae	D_5__Methanospirillum	D_6__uncultured Methanospirillum sp.
343e159c40c	0.2	0.0	D_1__Euryarchaeota	D_2__Thermoplasmata	D_3__Methanomassiliicocca	D_4__Methanomassiliicoccacea	D_5__Methanomassiliicoccus	D_6__uncultured archaeon
2f8a828b850	0.9	0.4	D_1__Asgardaeota	D_2__Odinarchaeia	D_3__uncultured sediment a	D_4__uncultured sediment arch	D_5__uncultured sediment archa	D_6__uncultured sediment archaeon
319fc463e8b	0.8	0.3	D_1__Crenarchaeota	D_2__Verstraetearchaeia	D_3__Methanomethyliales	D_4__Methanomethyliaceae	D_5__Candidatus Methanomethy	D_6__uncultured archaeon
	100.0	**100.0**						

In bacterial community (%)

<1%
>1% and <5%
> 5%

OTU	RUN 1	RUN 2	Phyum	Class	Order	Family	Genus	Speice
e11210e262e	2.4	3.2	D_1__Chloroflexi	D_2__Anaerolineae	D_3__Anaerolineales	D_4__Anaerolineaceae	0	0
1a5392b1167	6.5	10.3	D_1__Chloroflexi	D_2__Anaerolineae	D_3__SBR1031	0	0	0
8f286046edc	2.2	1.7	D_1__Chloroflexi	D_2__Dehalococcoidia	D_3__GIF9	0	0	0
ca2719b29c6	0.0	0.1	D_1__Chloroflexi	D_2__Anaerolineae	D_3__Anaerolineales	D_4__Anaerolineaceae	D_5__Anaerolinea	0
868d962bc9c	0.1	0.1	D_1__Chloroflexi	D_2__Anaerolineae	D_3__Anaerolineales	D_4__Anaerolineaceae	D_5__Bellilinea	0
30fd6bcbede	2.4	3.1	D_1__Chloroflexi	D_2__Anaerolineae	D_3__Anaerolineales	D_4__Anaerolineaceae	D_5__Leptolinea	D_6__uncultured Anaerolineaceae bacterium
f989049ab5e	0.3	0.4	D_1__Chloroflexi	D_2__Anaerolineae	D_3__Anaerolineales	D_4__Anaerolineaceae	D_5__Pelolinea	D_6__uncultured bacterium
69dbea62c23	3.9	7.7	D_1__Chloroflexi	D_2__Anaerolineae	D_3__RBG-13-54-9	D_4__uncultured bacterium	D_5__uncultured bacterium	0
c9d79f0ce61	0.1	0.3	D_1__Chloroflexi	D_2__Anaerolineae	D_3__uncultured	D_4__uncultured bacterium	D_5__uncultured bacterium	D_6__uncultured bacterium
46276ea40c9	0.2	0.1	D_1__Chloroflexi	D_2__Dehalococcoidia	D_3__FS117-23B-02	D_4__uncultured bacterium	D_5__uncultured bacterium	D_6__uncultured bacterium
d0aa04c0fe7	0.2	0.2	D_1__Acidobacteria	D_2__Acidobacteriia	D_3__Solibacterales	D_4__Solibacteraceae (Subgrou	D_5__Bryobacter	D_6__uncultured bacterium
b083a786f7d	0.0	0.2	D_1__Acidobacteria	D_2__Acidobacteriia	D_3__Solibacterales	D_4__Solibacteraceae (Subgrou	D_5__Candidatus Solibacter	D_6__uncultured bacterium
dd203d0bd67	0.4	0.0	D_1__Acidobacteria	D_2__Thermoanaerobaculi	D_3__Thermoanaerobacula	D_4__Thermoanaerobaculacea	D_5__TPD-58	D_6__uncultured bacterium
eb963ecf7b0	18.7	23.6	D_1__Acidobacteria	D_2__Aminicenantia	D_3__Aminicenantales	D_4__uncultured bacterium	D_5__uncultured bacterium	D_6__uncultured bacterium
90323be3b34	2.1	1.5	D_1__Proteobacteria	D_2__Deltaproteobacteria	D_3__Syntrophobacterales	D_4__Syntrophobacteraceae	0	0
9c7b38fc8ea	0.1	0.0	D_1__Proteobacteria	D_2__Gammaproteobacter	D_3__Betaproteobacteriales	D_4__Burkholderiaceae	0	0
da51258d85c	0.4	0.0	D_1__Proteobacteria	D_2__Gammaproteobacter	D_3__Betaproteobacteriales	D_4__Rhodocyclaceae	0	0
7b9f9b0d845	0.0	0.1	D_1__Proteobacteria	D_2__Gammaproteobacter	D_3__Betaproteobacteriales	D_4__Chromobacteriaceae	D_5__Aquitalea	D_6__Anopheles coluzzii
132a9c7a929	0.9	1.5	D_1__Proteobacteria	D_2__Gammaproteobacter	D_3__Betaproteobacteriales	D_4__Rhodocyclaceae	D_5__Azonexus	D_6__uncultured bacterium
4d4093e2fc1	0.1	0.0	D_1__Proteobacteria	D_2__Alphaproteobacteria	D_3__Caulobacterales	D_4__Caulobacteraceae	D_5__Caulobacter	0
e838793891f	0.1	0.1	D_1__Proteobacteria	D_2__Gammaproteobacter	D_3__Coxiellales	D_4__Coxiellaceae	D_5__Coxiella	D_6__uncultured bacterium
e0fcddfbd901	0.1	0.1	D_1__Proteobacteria	D_2__Gammaproteobacter	D_3__Betaproteobacteriales	D_4__Burkholderiaceae	D_5__Curvibacter	0
e698c5a9c79	0.1	0.3	D_1__Proteobacteria	D_2__Deltaproteobacteria	D_3__Syntrophobacterales	D_4__Syntrophaceae	D_5__Desulfomonile	D_6__uncultured bacterium
419691bba3b	0.2	0.2	D_1__Proteobacteria	D_2__Deltaproteobacteria	D_3__Desulfovibrionales	D_4__Desulfovibrionaceae	D_5__Desulfovibrio	D_6__Desulfovibrio aminophilus DSM 12254
593f78ba8fb	0.3	0.2	D_1__Proteobacteria	D_2__Deltaproteobacteria	D_3__Desulfobacterales	D_4__Desulfobulbaceae	D_5__Dissulfurimicrobium	D_6__uncultured bacterium
2328245a645	0.4	0.0	D_1__Proteobacteria	D_2__Gammaproteobacter	D_3__Betaproteobacteriales	D_4__Sulfuricellaceae	D_5__Ferritrophicum	D_6__uncultured bacterium
48edacdbc86	0.5	0.0	D_1__Proteobacteria	D_2__Gammaproteobacter	D_3__Methylococcales	D_4__Methylococcaceae	D_5__Methylococcus	D_6__uncultured bacterium
f08b4108149	0.0	0.2	D_1__Proteobacteria	D_2__Alphaproteobacteria	D_3__Rhizobiales	D_4__Beijerinckiaceae	D_5__Methylocystis	D_6__uncultured bacterium
4008aea3f91	0.3	0.0	D_1__Proteobacteria	D_2__Deltaproteobacteria	D_3__Syntrophobacterales	D_4__Syntrophaceae	D_5__Smithella	D_6__uncultured bacterium
8190f75bc88	2.7	1.2	D_1__Proteobacteria	D_2__Deltaproteobacteria	D_3__Syntrophobacterales	D_4__Syntrophobacteraceae	D_5__Syntrophobacter	D_6__uncultured bacterium
e8fd6af7b33	7.2	3.3	D_1__Proteobacteria	D_2__Deltaproteobacteria	D_3__Deltaproteobacteria I	D_4__Syntrophorhabdaceae	D_5__Syntrophorhabdus	0
34bbf10919b	0.7	0.4	D_1__Proteobacteria	D_2__Gammaproteobacter	D_3__Betaproteobacteriales	D_4__Hydrogenophilaceae	D_5__uncultured	0
c71666befa1	0.0	0.2	D_1__Proteobacteria	D_2__Gammaproteobacter	D_3__Betaproteobacteriales	D_4__Rhodocyclaceae	D_5__uncultured	0
4525dd9ded1	1.7	1.4	D_1__Proteobacteria	D_2__Deltaproteobacteria	D_3__Syntrophobacterales	D_4__Syntrophaceae	D_5__uncultured	D_6__uncultured bacterium
b7817f268dd	1.9	0.3	D_1__Proteobacteria	D_2__Gammaproteobacter	D_3__Betaproteobacteriales	D_4__Rhodocyclaceae	D_5__uncultured	D_6__uncultured bacterium
4512acf5433	0.0	0.3	D_1__Proteobacteria	D_2__Deltaproteobacteria	D_3__Myxococcales	D_4__bacteriap25	D_5__uncultured bacterium	D_6__uncultured bacterium
920907fe92c	2.3	0.9	D_1__Proteobacteria	D_2__Deltaproteobacteria	D_3__SAR324 clade(Marine	D_4__uncultured bacterium	D_5__uncultured bacterium	D_6__uncultured bacterium
97aa91283a7	0.1	0.0	D_1__Proteobacteria	D_2__Deltaproteobacteria	D_3__Sva0485	D_4__uncultured delta proteoba	D_5__uncultured delta proteobac	D_6__uncultured delta proteobacterium
69625ed540b	5.0	3.8	D_1__Spirochaetes	D_2__Brachyspirae	D_3__Brachyspirales	D_4__Brachyspirales Incertae S	D_5__Exilispira	0
44710009c69	0.4	0.8	D_1__Spirochaetes	D_2__Leptospirae	D_3__Leptospirales	D_4__Leptospiraceae	D_5__RBG-16-49-21	D_6__uncultured bacterium
a10c868441c	0.8	1.1	D_1__Spirochaetes	D_2__Spirochaetia	D_3__Spirochaetales	D_4__Spirochaetaceae	D_5__Spirochaeta 2	D_6__uncultured bacterium
e5f71e06cea	0.1	0.1	D_1__Spirochaetes	D_2__Spirochaetia	D_3__Spirochaetales	D_4__Spirochaetaceae	D_5__uncultured	D_6__bioreactor sludge metagenome
0a58b0be925	0.2	0.2	D_1__Spirochaetes	D_2__Leptospirae	D_3__Leptospirales	D_4__Leptospiraceae	D_5__uncultured	D_6__uncultured bacterium
d4579c242e9	6.0	4.6	D_1__Spirochaetes	D_2__Spirochaetia	D_3__Spirochaetales	D_4__Spirochaetaceae	D_5__uncultured	D_6__uncultured bacterium
5afcc84d014	5.9	3.8	D_1__Bacteroidetes	D_2__Bacteroidia	D_3__Bacteroidales	D_4__Bacteroidetes vadinHA17	0	0
c52ade5f72d	0.4	0.2	D_1__Bacteroidetes	D_2__Ignavibacteria	D_3__OPB56	0	0	0
d805ce6beee	0.2	0.2	D_1__Bacteroidetes	D_2__Bacteroidia	D_3__Sphingobacteriales	D_4__Lentimicrobiaceae	D_5__bacterium sp. OF1	D_6__bacterium sp. OF1
ceb4478107b	6.8	4.2	D_1__Bacteroidetes	D_2__Ignavibacteria	D_3__SJA-28	D_4__bioreactor sludge metage	D_5__bioreactor sludge metagen	D_6__bioreactor sludge metagenome
cbefa2450d5	1.1	0.3	D_1__Bacteroidetes	D_2__Bacteroidia	D_3__Bacteroidales	D_4__Rikenellaceae	D_5__Blvii28 wastewater-sludge	D_6__uncultured bacterium
28afc8453c4	0.6	1.6	D_1__Bacteroidetes	D_2__Bacteroidia	D_3__Bacteroidales	D_4__SB-5	D_5__uncultured bacterium	D_6__uncultured bacterium
241ef302bb6	0.5	0.2	D_1__Bacteroidetes	D_2__Bacteroidia	D_3__Sphingobacteriales	D_4__KD1-131	D_5__uncultured bacterium	D_6__uncultured bacterium
ce8855b7801	0.3	0.1	D_1__Bacteroidetes	D_2__Bacteroidia	D_3__Sphingobacteriales	D_4__Lentimicrobiaceae	D_5__uncultured bacterium	D_6__uncultured bacterium
c8c27991fc4	5.3	4.0	D_1__Firmicutes	D_2__Clostridia	D_3__Clostridiales	D_4__Clostridiaceae 1	D_5__Clostridium sensu stricto 13	0
52cfb791787	0.1	0.2	D_1__Firmicutes	D_2__Clostridia	D_3__Clostridiales	D_4__Gracilibacteraceae	D_5__Lutispora	D_6__Clostridium
f99d6b26553	0.0	0.1	D_1__Firmicutes	D_2__Clostridia	D_3__Clostridiales	D_4__Clostridiales vadinBB60 g	D_5__uncultured bacterium	D_6__uncultured bacterium
92c37990d6f	1.9	2.8	D_1__Caldisericа	D_2__Caldisericia	D_3__Caldisericales	D_4__Caldisericaceae	D_5__Caldisericum	0
2208019a71c	0.3	0.6	D_1__Caldisericа	D_2__Caldisericia	D_3__Caldisericales	D_4__TTA-B1	D_5__uncultured bacterium	D_6__uncultured bacterium
616a99d3ed4	0.1	0.0	D_1__Planctomycetes	D_2__Phycisphaerae	D_3__Phycisphaerales	D_4__Phycisphaeraceae	D_5__uncultured	D_6__uncultured bacterium
e031da9cf26	0.6	1.0	D_1__Planctomycetes	D_2__Phycisphaerae	D_3__mle1-8	D_4__uncultured bacterium	D_5__uncultured bacterium	D_6__uncultured bacterium
d19b3e83ca5	0.3	0.5	D_1__Planctomycetes	D_2__Phycisphaerae	D_3__Pla1 lineage	D_4__uncultured bacterium	D_5__uncultured bacterium	D_6__uncultured bacterium
5feb76e75db	0.4	0.9	D_1__Planctomycetes	D_2__Phycisphaerae	D_3__S-70	D_4__uncultured bacterium	D_5__uncultured bacterium	D_6__uncultured bacterium
10af08f96b6	1.0	1.7	D_1__Atribacteria	D_2__Caldatribacteriia	D_3__Caldatribacteriales	D_4__Caldatribacteriaceae	D_5__Candidatus Caldatribacteri	D_6__uncultured bacterium
0c01e573a98	0.3	0.2	D_1__Synergistetes	D_2__Synergistia	D_3__Synergistales	D_4__Synergistaceae	D_5__JGI-0000079-D21	D_6__uncultured bacterium
1a3b68cd97e	0.3	2.5	D_1__TA06	D_2__uncultured bacterium	D_3__uncultured bacterium	D_4__uncultured bacterium UA	D_5__uncultured bacterium UASB	D_6__uncultured bacterium UASB_TL20
3891749a3ac	0.2	0.3	D_1__uncultured	D_2__uncultured bacterium	D_3__uncultured bacterium	D_4__uncultured bacterium	D_5__uncultured bacterium	D_6__uncultured bacterium
629612876 78	1.3	0.9	D_1__Verrucomicrobia	D_2__Verrucomicrobiae	D_3__Pedosphaerales	D_4__Pedosphaeraceae	D_5__uncultured bacterium	D_6__uncultured bacterium
	100.0	**100.0**						

at biocathodes had the same characteristics (e.g. the same type of inoculated sludge, same substrates). Therefore, the similarity of these two microbial communities is meaningful in verifying the correctness of the experimental results obtained in chapter 4 as well as here.

Bioanode

In the 16S rRNA gene sequencing of biomass sample on day 289, 32496 reads, the number of OTUs exceed 250. Sequencing results revealed the presence of bacterial and archaeal communities (**Fig. 5-11**). Differing from the microbial communities on biocathode, bacteria were predominant on bioanode at rate up to 98.3%, while archaea comprised only 1.7%.

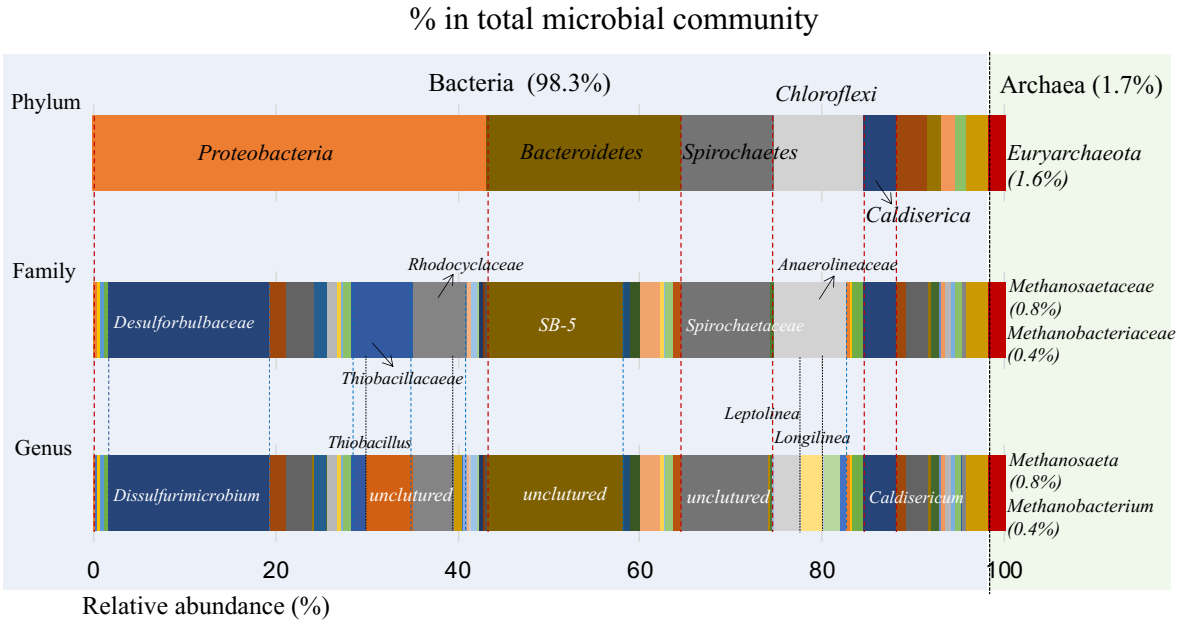

Fig. 5-11 Microbial community of biomass sample on the bioanode based on 16S rRNA gene

The bacterial community mainly involved the following six phyla: *Proteobacteria, Bacteroidetes*, *Spirochaetes, Chloroflexi, Caldiserica and Epsilonbacteraeota* that account for 43.9%, 21.7%, 10.5%, 9.9%, 3.7% and 3.4%, respectively. Of the most dominant of phyla *Proteobacteria*, genus of *Dissulfurimicrobium* were detected at highest concentration of 17.7%. They were known as a thermophilic, anerobic, chemolithoautrophic bacterium, and able to grow by disproportionation of sulfur element, thiosulfate and sulfide, namely sulfur disproportionation microorganism (SDM) (Slobodkin *et al.*, 2016). Also as members of phyla *Proteobacteria*, *Rhodocyclaceae* and *Thiobacillacaeae* accounted for 6.7% and

6.0%, respectively. Most genera of them have been also model organisms for sulfur oxidation (SOM) (TAKANO *et al.*, 1997, Bell *et al.*, 2020) **(Table 5-2).** The second most OTUs with 15.0% at taxonomic genus level were affiliated with *SB-5* of *Bacteroidetes*. Although no genera in *SB-5* have been isolated, phylogenetically, *SB-5* appear to fall within the *Cytophaga* groups and *Cytophagales* of the *Bacteroidetes* (Phelps *et al.*, 1998), where *SB-5*'s closely relative is *SB-1* (**Fig. 5-12**). *Spirochaetaceae and Anaerolineaceae* were detected at relatively high abundance, exhibiting the capability of sulifide oxidation (Bell *et al.*, 2020; Dubinina *et al.*). Conversely, sulfur reduction microorganisms (SRM) such as *Caldisericum (3.7%), Syntrophobacter* (3.0%) and *Desulfatirhabdium* (2.0%) were identified in the microbial community. These microbes together with methanogens such as *Methanosaeta* and *Methanobacterium* with very low concentration, may be play a role as an electron acceptor.

The biological contributors such as SDM and SOM to HS^- oxidation at the bioathode were detected at high concentration. The products of HS^- oxidation may be identified depending on the characteristics of each microbe (e.g. enzyme) referenced by the comprehensive information (**Table 5-3**). Base on the interactions between these dominant microbes and bio-anode, as well as interspecies, thus may explain the process of oxidizing sulfur and releasing electrons.

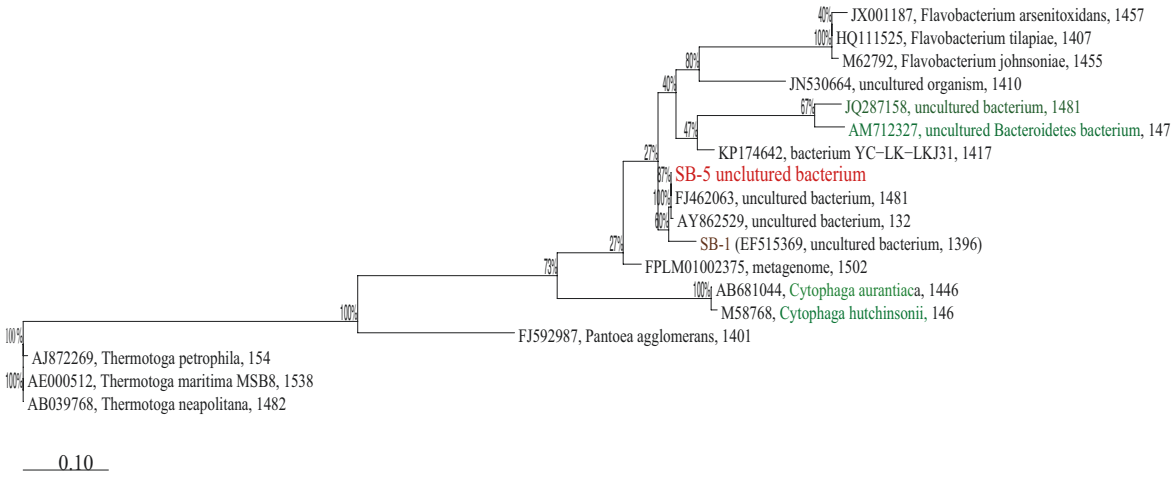

Fig. 5-12 Phylogenetic tree based on 16S rRNA gene showing the position of *SB-5* sequences (red) among members of the order Bacteroidales including some of the *Sulfiphilic Bacteroidetes* (green) (Sylvan *et al.*, 2013). The scale bar represents 10 nucleotide substitutions per 100.

5.4 Discussion

The most dominant sulfur-associated microbial species observed in the sulfur-oxidizing anode of this MES were *Dissulfurimicrobium hydrothermale* Sh 68T, which are known for sulfur disproportionation. Like as *D. hydrothermale, Desulfobulbus propionacus* DSM 2032T are also sulfur-disproportionation microorganisms (Slobodkin and Slobodkina, 2019). In most marine sediment fuel cells, *Geobacter sulfurreducens* and D. *propionacus* was also consistently enriched on the anode (D. E. Holmes *et al.*, 2004). Particularly, Dawn E. Holmes *et al.* (2004) demonstrated the ability of *D. propionacus* to transfer electrons directly to an electron during sulfur oxidation. The comparison of *D. propionacus* with *D. hydrothermale* indicated that they have 87.55 % sequence similarity (Slobodkin *et al.*, 2016). Therefore, the enrichment of *D. hydrothermale* on the surface of anode could be explained by their ability to grow with the bioanode as an electron acceptor like as *D. propionacus*. Since a relatively high current was maintained in this MES, most of the released electrons from sulfur oxidation to produce SO_4^{2-} by these most dominant microbes were transfer to anode. The small remaining one could be used in sulfur reduction to produce sulfide due to the ability of their sulfur disproportionation.

Sulfur compounds of intermediate oxidation states (sulfur cycle intermediates, SCI) such as S^0, $S_2O_3^{2-}$, SO_3^{2-} weren't measured in this study. However, SCI should be produced in the bioanode because of the presence of the dominant SDM such as *Dissulfurimicrobium* and *Desulfomonile*. The production of S^0 and adhesion to the bioanode affects on further oxidizing sulfur, or if not so the produced S^0 is able to be further oxidized to $S_2O_3^{2-}$. Thus, SCIs at liquid states such as $S_2O_3^{2-}$, SO_3^{2-} were the predominant products in this MES. Sulfide oxidation to $S_2O_3^{2-}$, SO_3^{2-} is performed by heterotrophic bacteria using sulfide: quinone oxidoreductase (sqr) and persulfide (PDO) (Xia *et al.*, 2017; Hou *et al.*, 2018). Genome analysis of the *Anaerolineaceae* family revealed the presence of *sqr* at high concentrations (Bell *et al.*, 2020). In addition, the high abundance of *Anaerolineaceae* and *Caldisericum* (filamentous bacteria) were predicted to be the keystones in the anodic microbial networks of SMFC (Wang *et al.*, 2021). These findings that that the detected most genera of *Anaerolineaceae* can catalyze to produce $S_2O_3^{2-}$, SO_3^{2-} from sulfide. The electrons were released to bioanode through the interactions between *Anaerolineaceae* and *Caldisericum*.

The population of the detected *Anaerolineaceae* was not high compared to that of *Dissulfurimicrobium* and *Desulfomonile* and thus, would be insufficient in providing SCI, suggesting that other microbes were involved in this process at the bioanode. As a promising bacterial group, highly detected *SB-5* can be considered. The *SB-5* and *SB-1* group of *Bacteroidetes* was previously detected in a benzene degrading, sulfate-reducing consortium (Phelps *et al.*, 1998). However, the bioanode stimulation as an electron acceptor to promote the bioremediation of chlorinated organic compounds, resulted in substantially increased abundance of *SB-1* (Yu *et al.*, 2016). Therefore, in the absence of electron donors of organic substrates such as benzene, the enrichment of *SB-5* was involved in the interactions with the bioanode through sulfide oxidation. Continue to consider the family of *Spirochaetaceae* – also a group of bacteria that present in a high abundance. Aerotolerant *Spirochaetes* species can non-enzymatically oxidize sulfide to S^0 (Dubinina *et al.*). Particularly, with the addition of magnetite, the structure and activity of microbial community changed markedly, the relative abundance of not only electroactive microorganism but also *Spirochaetes* increased (Jung *et al.*, 2020). This suggests that the oxidation of sulfide to S^0 by *Spirochaetes species* may occur without oxygen if alternative electron-accepting processes, possibly through interspecies electron transfer, are available. Although speculative, it is worth considering the possibility of family *Spirochaetaceae* to oxidize sulfide to S^0 with a bioanode serving as electron acceptor.

As described above, there are two main steps in the process of oxidizing HS^- to produce SO_4^{2-}. Firstly, the bacteria such as SB-5 and *Spirochaetaceae* may utilize HS^- to produce SCI. The produced SCI was further oxidized to completely produce SO_4^{2-} with the assistance of SDR as microbial catalysis. Beside of this main process, the presence of *Rhodocyclaceae Thiobacillus* and *Sulfuricurvum* could propose another Sox pathway, albeit at a lower concentration. This Sox pathway, a multienzyme system that oxidizes the sulfur compound stepwise, finally producing sulfate (Dahl *et al.*, 2008), is also a prominent form of sulfide oxidation. Most genera of *Rhodocyclaceae*, *Thiobacillus* all harbored genes for the oxidation of reduced sulfur compounds catalyzed by the Sox pathway (Friedrich *et al.*, 2001; Bell *et al.*, 2020; Kodama and Watanabe). Furthermore, *Rhodobacter* of the *Rhodocyclaceae* family was enriched in the bioanode of MFC (Sun *et al.*, 2009).

Electrons released from the processes of HS^- oxidation at the bioanode were involved in electricity generation and drove the CO_2 reduction to produce methane at the biocathode. However, the increasing trend of the current was lower compared with the case of using the abiotic anode (Pt-catalyst) when increasing HS^- concentration. Thus, bioanode was the main electron acceptor but not the only one. Indeed, as explained above, a small part of electrons could be used in sulfur reduction via the detection SDM as well as SDM. In addition, Jung *et al.* (2020) proposed an electro-synthesis association that couples the oxidation of sulfide and the reduction of CO_2. The detection of methanogen in this study, albeit at very low concentration, also could support this electro-synthesis association in which methanogen played as an electron acceptor.

Fig. 5-13 presents the possible pathways for the bio-electrical sulfide oxidation at the bioanode of this MES. There are three processes of HS^- oxidation with the assistance of microbial catalyst: (i) HS^- was oxidized to SCI by SOM such *as SB-5*, *Anaerolineaceae* and *Spirochaetes;* (ii) *SCI* was oxidized to SO_4^{2-} by SDM; and (iii) HS^- was oxidized to SO_4^{2-} by SOM such as *Rhodocyclaceae*, *Thiobacillacaeae*. Based on the high detection of the related microbes, the (i) and (ii) processed were predominant. Most of these microbes were also capable of direct electron transfer to bioanode during sulfur oxidation. The few remained organism interacted with other interspecies such as methanogens and SRM at lower concentration. Electrons are released to the anode and flow through an external electrical circuit to the biocathode. At the biocathode, methane was produced through CO_2 reduction using microorganism as catalyst. Similarly, microbial community at the biocathode was also analyzed to identify the organisms involved in bio-electrical methane production. As describes in section 5.3.4, the microbial community at the biocathode here was similar to that in the MES using abiotic anode (**Chapter 4**). Thus, the possible pathways for bio-electrical methane production at the biocathode can be referenced in the scheme mentioned in chapter 4. Finally, the oxidation of HS^- at the bioanode and the reduction of CO_2 at the biocathode were summarized in **Fig. 5-14**. This study revealed that biological methane production is possible in combination with HS^- oxidation using bio-catalyst at very low applied voltage (0.2 V) in an organic environment.

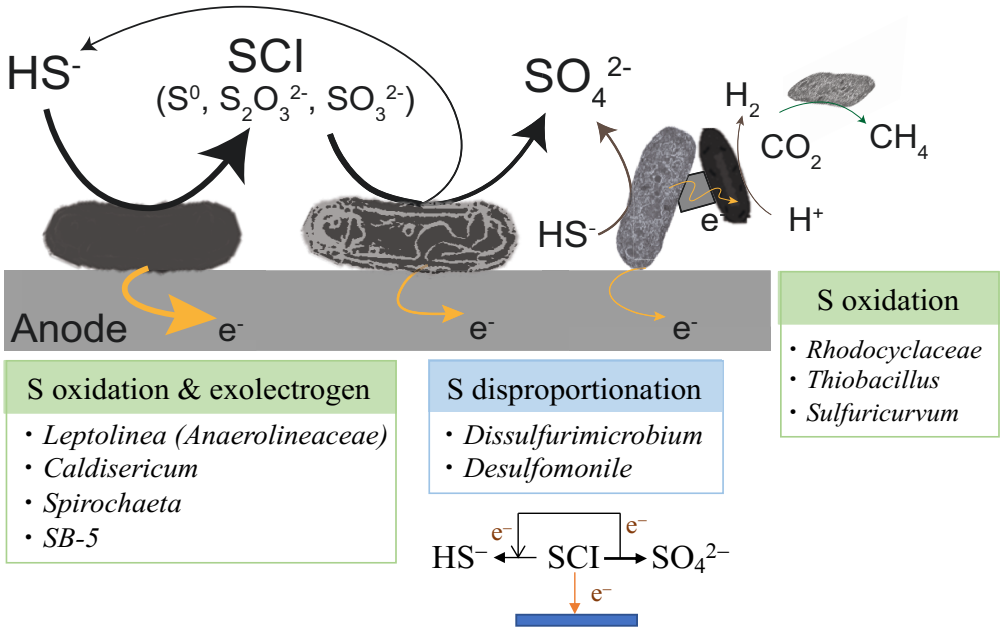

Fig. 5-13 Proposed pathways of the sulfide oxidation at the bioanode

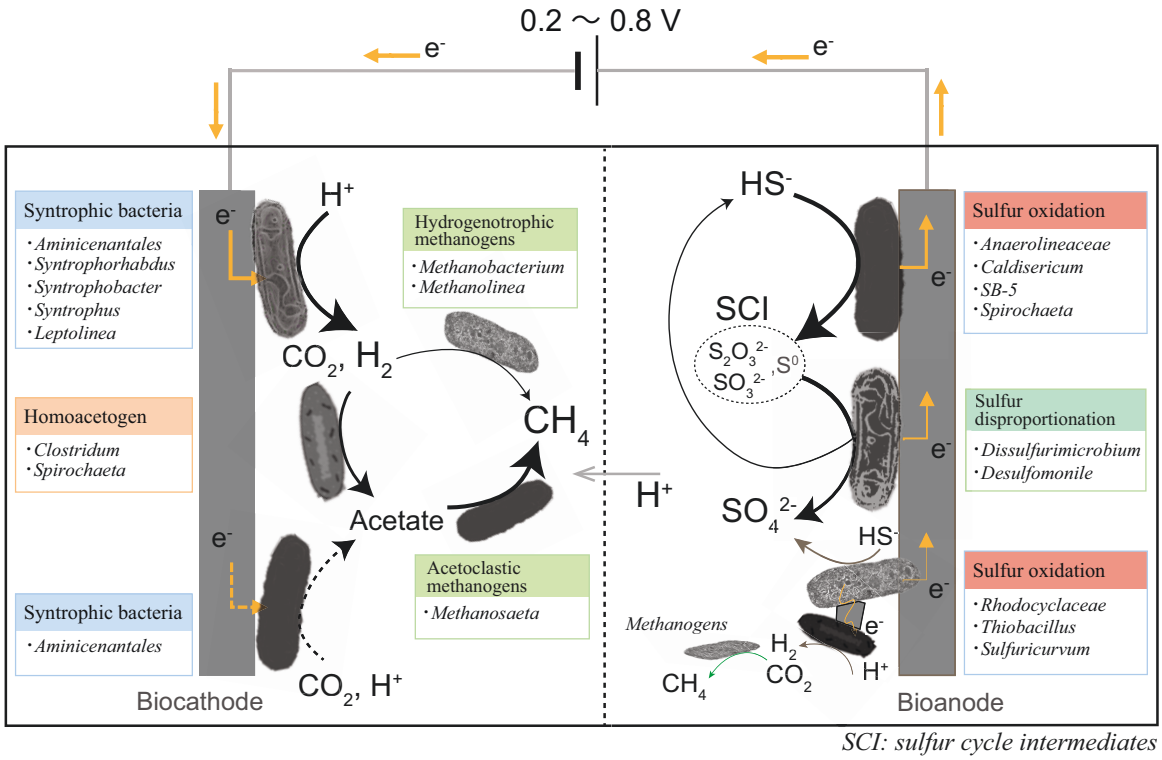

Fig. 5-14 Coupling of CO_2 reduction at the biocathode and sulfur oxidation at the bioanode with the assistance of microbial catalyst in microbial electrosynthesis system

5.5 Conclusion

Biological methane production occured in a very low range of applied voltage 0.2–0.8 V, in which HS^- oxidation took place by sulfur bacteria. The analysis of two microbial communities revealed the processes of methane production and sulfur oxidation at the biocathode and bioanode, respectively. In the biocathode, syntrophic bacteria, homoacetogens, and mathenogens were key players in the methane production. In the bioanode, sulfur-disproportionation and sulfur-oxidation microorganisms were involved such a complex sulfide oxidation.

References

Aryal, N., Ammam, F., Patil, S.A., and Pant, D. (2017) An overview of cathode materials for microbial electrosynthesis of chemicals from carbon dioxide. *Green Chem* **19**: 5748–5760.

Bell, E., Lamminmäki, T., Alneberg, J., Andersson, A.F., Qian, C., Xiong, W., et al. (2020) Active sulfur cycling in the terrestrial deep subsurface. *ISME J* **14**: 1260–1272.

Bolger, A.M., Lohse, M., and Usadel, B. (2014) Trimmomatic: a flexible trimmer for Illumina sequence data. *Bioinformatics* **30**: 2114–2120.

Bolyen, E., Rideout, J.R., Dillon, M.R., Bokulich, N.A., Abnet, C.C., Al-Ghalith, G.A., et al. (2019) Reproducible, interactive, scalable and extensible microbiome data science using QIIME 2. *Nat Biotechnol* **37**: 852–857.

Call, D.F., Wagner, R.C., and Logan, B.E. (2009) Hydrogen Production by Geobacter Species and a Mixed Consortium in a Microbial Electrolysis Cell. *Appl Environ Microbiol* **75**: 7579–7587.

Callahan, B.J., McMurdie, P.J., Rosen, M.J., Han, A.W., Johnson, A.J.A., and Holmes, S.P. (2016) DADA2: High-resolution sample inference from Illumina amplicon data. *Nat Methods* **13**: 581–583.

Cheng, S., Xing, D., Call, D.F., and Logan, B.E. (2009) Direct Biological Conversion of Electrical Current into Methane by Electromethanogenesis. *Environmental Science & Technology* **43**: 3953–3958.

Clauwaert, P. and Verstraete, W. (2009) Methanogenesis in membraneless microbial electrolysis cells. *Appl Microbiol Biotechnol* **82**: 829–836.

Dahl, C., Friedrich, C., and Kletzin, A. (2008) Sulfur Oxidation in Prokaryotes. In *eLS*. American Cancer Society.

Dinh, T.T Ha, Kambara H., Harada Y., Matsushita S., Aoi Y., Kindaichi T., Ozaki N., Ohashi A. (2021) Bioelectrical methane production with an ammonium oxidative reaction under the no organic substance condition. *Microbes and Environ* **36**:ME21007.

Dinh, T.T Ha, Kambara H., Harada Y., Matsushita S., Aoi Y., Kindaichi T., Ozaki N., Ohashi A., 2021. Biological methane production with sulfur oxidation in micorbial electrosynthesis system without organic substrate. *Journal of Environmental Sciences*. In press

Dubinina, G., Grabovich, M., Leshcheva, N., Rainey, F.A., and Gavrish, E. 2011 Spirochaetaperfilievii sp. nov., an oxygen-tolerant, sulfide-oxidizing, sulfur- and thiosulfate-reducing spirochaete isolated from a saline spring. *International Journal of Systematic and Evolutionary Microbiology* **61**: 110–117.

Friedrich, C.G., Rother, D., Bardischewsky, F., Quentmeier, A., and Fischer, J. (2001) Oxidation of Reduced Inorganic Sulfur Compounds by Bacteria: Emergence of a Common Mechanism? *Appl Environ Microbiol* **67**: 2873–2882.

Gomez Vidales, A., Omanovic, S., and Tartakovsky, B. (2019) Combined energy storage and methane bioelectrosynthesis from carbon dioxide in a microbial electrosynthesis system. *Bioresource Technology Reports* **8**: 100302.

González-Pabón, M.J., Cardeña, R., Cortón, E., and Buitrón, G. (2021) Hydrogen production in two-chamber MEC using a low-cost and biodegradable poly(vinyl) alcohol/chitosan membrane. *Bioresource Technology* **319**: 124168.

Hall, M. and Beiko, R.G. (2018) 16S rRNA Gene Analysis with QIIME2. *Methods Mol Biol* **1849**: 113–129.

Holmes, Dawn E., Bond, D.R., and Lovley, D.R. (2004) Electron Transfer by *Desulfobulbus propionicus* to Fe(III) and Graphite Electrodes. *Appl Environ Microbiol* **70**: 1234–1237.

Holmes, D. E., Bond, D.R., O'Neil, R.A., Reimers, C.E., Tender, L.R., and Lovley, D.R. (2004) Microbial communities associated with electrodes harvesting electricity from a variety of aquatic sediments. *Microb Ecol* **48**: 178–190.

Hou, N., Xia, Y., Wang, X., Liu, Huaiwei, Liu, Honglei, and Xun, L. (2018) H2S biotreatment with sulfide-oxidizing heterotrophic bacteria. *Biodegradation* **29**: 511–524.

Jung, H., Baek, G., and Lee, C. (2020) Magnetite-assisted in situ microbial oxidation of H2S to S0 during anaerobic digestion: A new potential for sulfide control. *Chemical Engineering Journal* **397**: 124982.

Kodama, Y. and Watanabe, K. 2004 Sulfuricurvum kujiense gen. nov., sp. nov., a facultatively anaerobic, chemolithoautotrophic, sulfur-oxidizing bacterium isolated from an underground crude-oil storage cavity. *International Journal of Systematic and Evolutionary Microbiology* **54**: 2297–2300.

Lin, S., Mackey, H.R., Hao, T., Guo, G., van Loosdrecht, M.C.M., and Chen, G. (2018) Biological sulfur oxidation in wastewater treatment: A review of emerging opportunities. *Water Research* **143**: 399–415.

Logan, B.E., Call, D., Cheng, S., Hamelers, H.V.M., Sleutels, T.H.J.A., Jeremiasse, A.W., and Rozendal, R.A. (2008) Microbial Electrolysis Cells for High Yield Hydrogen Gas Production from Organic Matter. *Environ Sci Technol* **42**: 8630–8640.

Logan, B.E., Hamelers, B., Rozendal, R., Schröder, U., Keller, J., Freguia, S., et al. (2006a) Microbial Fuel Cells: Methodology and Technology. *Environ Sci Technol* **40**: 5181–5192.

Logan, B.E., Hamelers, B., Rozendal, R., Schröder, U., Keller, J., Freguia, S., et al. (2006b) Microbial Fuel Cells: Methodology and Technology †. *Environ Sci Technol* **40**: 5181–5192.

Nakamura, R., Takashima, T., Kato, S., Takai, K., Yamamoto, M., and Hashimoto, K. (2010) Electrical Current Generation across a Black Smoker Chimney. *Angewandte Chemie International Edition* **49**: 7692–7694.

Ooka, H., McGlynn, S.E., and Nakamura, R. (2019) Electrochemistry at Deep-Sea Hydrothermal Vents: Utilization of the Thermodynamic Driving Force towards the Autotrophic Origin of Life. *ChemElectroChem* **6**: 1316–1323.

Parada, A.E., Needham, D.M., and Fuhrman, J.A. (2016) Every base matters: assessing small subunit rRNA primers for marine microbiomes with mock communities, time series and global field samples. *Environmental Microbiology* **18**: 1403–1414.

Park, J., Lee, B., Tian, D., and Jun, H. (2018) Bioelectrochemical enhancement of methane production from highly concentrated food waste in a combined anaerobic digester and microbial electrolysis cell. *Bioresource Technology* **247**: 226–233.

Peng, H., Zhao, Z., Xiao, H., Yang, Y., Zhao, H., and Zhang, Y. (2019) A strategy for enhancing anaerobic digestion of waste activated sludge: Driving anodic oxidation by adding nitrate into microbial electrolysis cell. *Journal of Environmental Sciences* **81**: 34–42.

Phelps, C.D., Kerkhof, L.J., and Young, L.Y. (1998) Molecular characterization of a sulfate-reducing consortium which mineralizes benzene. *FEMS Microbiology Ecology* **27**: 269–279.

Pruesse, E., Peplies, J., and Glöckner, F.O. (2012) SINA: Accurate high-throughput multiple sequence alignment of ribosomal RNA genes. *Bioinformatics* **28**: 1823–1829.

Quast, C., Pruesse, E., Yilmaz, P., Gerken, J., Schweer, T., Yarza, P., et al. (2013) The SILVA ribosomal RNA gene database project: improved data processing and web-based tools. *Nucleic Acids Res* **41**: D590-596.

Sarmin, S., Ethiraj, B., Islam, M.A., Ideris, A., Yee, C.S., and Khan, Md.M.R. (2019) Bio-electrochemical power generation in petrochemical wastewater fed microbial fuel cell. *Science of The Total Environment* **695**: 133820.

Schlager, S., Haberbauer, M., Fuchsbauer, A., Hemmelmair, C., Dumitru, L.M., Hinterberger, G., et al. (2017) Bio-Electrocatalytic Application of Microorganisms for Carbon Dioxide Reduction to Methane. *ChemSusChem* **10**: 226–233.

Slobodkin, A.I. and Slobodkina, G.B. (2019) Diversity of Sulfur-Disproportionating Microorganisms. *Microbiology* **88**: 509–522.

Slobodkin, A.I., Slobodkina, G.B., Panteleeva, A.N., Chernyh, N.A., Novikov, A.A., and Bonch-Osmolovskaya, E.A. (2016) Dissulfurimicrobium hydrothermale gen. nov., sp. nov., a thermophilic, autotrophic, sulfur-disproportionating deltaproteobacterium isolated from a hydrothermal pond. *Int J Syst Evol Microbiol* **66**: 1022–1026.

Sun, M., Mu, Z.-X., Chen, Y.-P., Sheng, G.-P., Liu, X.-W., Chen, Y.-Z., et al. (2009) Microbe-Assisted Sulfide Oxidation in the Anode of a Microbial Fuel Cell. *Environ Sci Technol* **43**: 3372–3377.

Sylvan, J.B., Sia, T.Y., Haddad, A.G., Briscoe, L.J., Toner, B.M., Girguis, P.R., and Edwards, K.J. (2013) Low Temperature Geomicrobiology Follows Host Rock Composition Along a Geochemical Gradient in Lau Basin. *Front Microbiol* **4**:.

TAKANO, B., KOSHIDA, M., FUJIWARA, Y., SUGIMORI, K., and TAKAYANAGI, S. (1997) Influence of sulfur-oxidizing bacteria on the budget of sulfate in Yugama crater lake, Kusatsu-Shirane volcano, Japan. *Biogeochemistry* **38**: 227–253.

Vilajeliu-Pons, A., Koch, C., Balaguer, M.D., Colprim, J., Harnisch, F., and Puig, S. (2018) Microbial electricity driven anoxic ammonium removal. *Water Research* **130**: 168–175.

Villano, M., Aulenta, F., Ciucci, C., Ferri, T., Giuliano, A., and Majone, M. (2010) Bioelectrochemical reduction of CO2 to CH4 via direct and indirect extracellular electron transfer by a hydrogenophilic methanogenic culture. *Bioresource Technology* **101**: 3085–3090.

Wallrabenstein, C. Syntrophobacter pfennigii sp. nov. : new syntrophically propionate-oxidizing anaerobe growing in pure culture with propionate and sulfate. 7.

Wang, B., Zhang, H., Yang, Y., and Xu, M. (2021) Diffusion and filamentous bacteria jointly govern the spatiotemporal process of sulfide removal in sediment microbial fuel cells. *Chemical Engineering Journal* **405**: 126680.

Wang, W., Zhang, Y., Li, M., Wei, X., Wang, Y., Liu, L., et al. (2020) Operation mechanism of constructed wetland-microbial fuel cells for wastewater treatment and electricity generation: A review. *Bioresource Technology* **314**: 123808.

Wasmund, K., Mußmann, M., and Loy, A. (2017) The life sulfuric: microbial ecology of sulfur cycling in marine sediments. *Environmental Microbiology Reports* **9**: 323–344.

Xia, Y., Lü, C., Hou, N., Xin, Y., Liu, J., Liu, H., and Xun, L. (2017) Sulfide production and oxidation by heterotrophic bacteria under aerobic conditions. *The ISME Journal* **11**: 2754–2766.

Yilmaz, P., Parfrey, L.W., Yarza, P., Gerken, J., Pruesse, E., Quast, C., et al. (2014) The SILVA and "All-species Living Tree Project (LTP)" taxonomic frameworks. *Nucleic Acids Research* **42**: D643–D648.

Yu, H., Feng, C., Liu, X., Yi, X., Ren, Y., and Wei, C. (2016) Enhanced anaerobic dechlorination of polychlorinated biphenyl in sediments by bioanode stimulation. *Environmental Pollution* **211**: 81–89.

Zakaria, B.S. and Dhar, B.R. (2021) Characterization and significance of extracellular polymeric substances, reactive oxygen species, and extracellular electron transfer in methanogenic biocathode. *Sci Rep* **11**: 1–13.

Zhao, Z., Zhang, Y., Yu, Q., Ma, W., Sun, J., and Quan, X. (2016) Enhanced decomposition of waste activated sludge via anodic oxidation for methane production and bioenergy recovery. *International Biodeterioration & Biodegradation* **106**: 161–169.

Zhen, G., Kobayashi, T., Lu, X., and Xu, K. (2015) Understanding methane bioelectrosynthesis from carbon dioxide in a two-chamber microbial electrolysis cells (MECs) containing a carbon biocathode. *Bioresource Technology* **186**: 141–148.

Zhen, G., Zheng, S., Lu, X., Zhu, X., Mei, J., Kobayashi, T., et al. (2018) A comprehensive comparison of five different carbon-based cathode materials in CO2 electromethanogenesis: Long-term performance, cell-electrode contact behaviors and extracellular electron transfer pathways. *Bioresource Technology* **266**: 382–388.

Chapter

6

General conclusions, future recommendations

6.1 Conclusions

Methane was produced in a microbial electrosynthesis system (MES) under the no organic substrate condition. However, a relatively high applied voltage is required for bioelectrical reactions (Gomez Vidales *et al.*, 2019). In this study, we demonstrated that bioelectrical methane production at the biocathode was achieved even at low voltage (0.05, 0.1 V) when coupled with the oxidation of inorganic compounds such as NH_4^+ and HS^- at the anode. The results of microbial community analysis indicated the roles of the microorganisms, which are abundant on the electrodes, in methane production. Combined with the feasibility of small thermoelectricity generation through the natural minerals that can function as thermoelectric materials (Ang *et al.*, 2015), the main findings of this study suggest the possible pathway of bio-electrical methane production in natural environments.

The more detailed results corresponding to different experimental conditions are described as follows:

6.1.1 Bioelectrical methane production coupled with an abiotic ammonia oxidation

In **Chapter 3**, bioelectrical methane production was possible even at a very low voltage of 0.05 V in the MES without organic substrates, when coupling of NH_4^+ oxidation at the anode coated with platinum (Pt) powder. Microbial community analysis revealed that methane production that methane production occurred simultaneously with biological denitrification at the biocathode. In denitrification, NO_3^- was produced by chemical NH_4^+ oxidation at the anode and was provided to the biocathode chamber via the salt bridge . H_2 was produced at the biocathode by the hydrogen-producing bacteria *Petrimonas* through the acceptance of electrons and protons. The produced H_2 was biologically consumed by hydrogenotrophic methanogens of *Methanobacterium* and *Methanobrevibacter* with CO_2 uptake and by hydrogenotrophic denitrifiers of *Azonexus.* This microbial community suggests that methane is indirectly produced without the use of electrons by methanogens.

6.1.2 Bioelectrical methane production coupled with an abiotic sulfur oxidation

Chapter 4 found that bio-electrical methane production occurred in the biocathode even in a very low applied of 0.1–0.8 V, where abiotic HS^- oxidation to SO_4^{2-} was achieved at the Pt anode. By using a cation exchange membrane placed between the biocathode and anode chamber, differing from the results of **Chapter 3**, only methane gas was detected on the

biocathode chamber. Based on the microbial community analysis of biomass enriched on the biocathode, the scheme of electron flow in methane production was proposed. First, electrotrophic H_2 was produced by syntrophic bacteria, such as *Syntrophorhabdus*, *Syntrophobacter*, *Syntrophus*, *Leptolinea*, and *Aminicenantales*, with direct acceptance of electrons at the biocathode. Subsequently, most of the produced H_2 was converted to acetate by homoacetogens, such as *Clotrodium* and *Spirochate 2*. In conclusion, majority of the methane was indirectly produced by a high population of acetoclastic methanogens, namely *Methanosaeta,* via acetate. Further, hydrogenotrophic methanogens, including *Methanobacterium* and *Methanolinea,* produced methane via H_2.

6.1.3 Bioelectrical methane production coupled with a biotic sulfur oxidation

In **Chapter 5**, the microbial anode was used as an alternative anode catalyst for sulfur oxidation. As expected, methane was also detected on the biocathode chamber in a low applied voltage range of 0.2–0.8 V. The microbial community of biomass collected from biocathode is the same as in **Chapter 4**. This means that not only the most probable pathways for methane production can be explained like in chapter 4, but also the correctness of the results under the same experimental conditions was verified. Similarly, a microbial community on the bioanode was also analyzed to identify the process of the bio-electrical sulfide oxidation. There are three processes of HS^- oxidation with the assistance of microbial catalyst: (i) HS^- was oxidized to sulfur cycle intermediate (SCI) by sulfur-oxidation microorganisms (SOM) such *as SB-5*, *Anaerolineaceae* and *Spirochaetes;* (ii) *SCI* was oxidized to SO_4^{2-} by also sulfur-disproportionation microorganisms (SDM); and (iii) HS^- was oxidized to SO_4^{2-} by SOM such as *Rhodocyclaceae*, *Thiobacillacaeae*. Based on the high detection of the related microbes, the (i) and (ii) processed were predominant. Most of these microbes were also capable of direct electron transfer to bioanode during sulfur oxidation. However, the few remained organism interacted with other interspecies such as methanogens and SRM at lower concentration. In summary, the microbial communities on the biocathode and bioanode were detailed analyzed with useful information from many researches. From this, the processes of methane production and sulfur oxidation in MES were obtained.

6.2 Future work recomendations

The results of RUN 1, RUN 2 and RUN 3 demonstrated that biological methane production in an MES was possible even at a very low voltage (0.05, 0.1 V), when coupling with low potential inorganic compounds such as HS^- or NH_4^+. In addition, the scheme for the process of bio-electrical methane production was proposed, based on the detailed analysis of microbial community with useful information from other studies. To bring the experimental results closer to the phenomena of biological methane production using thermoelectricity in nature, we continue to develop two MES as shown in **Fig. 6.1**. These MESs will be set-up with larger volume to investigate whether biological methane production is possible when coupling of biological ammonia and/or HS^- oxidation at very low voltage. The electric power applied to the MESs is due to the Seeback effect, which converts temperature gradients to electricity (Kher, 2015; Sonal Renge *et al.*, 2017). For instance, to theoretically produce an applied voltage of 0.02 V, the parallel wire of Alumel and Chromel with different Seeback coefficients is used, and exposed to the high temperature (T_1= 450°C) and the low temperature (T_2=30°C). The medium and inoculated sludge were derived from not only the freshwater but also the seawater environments.

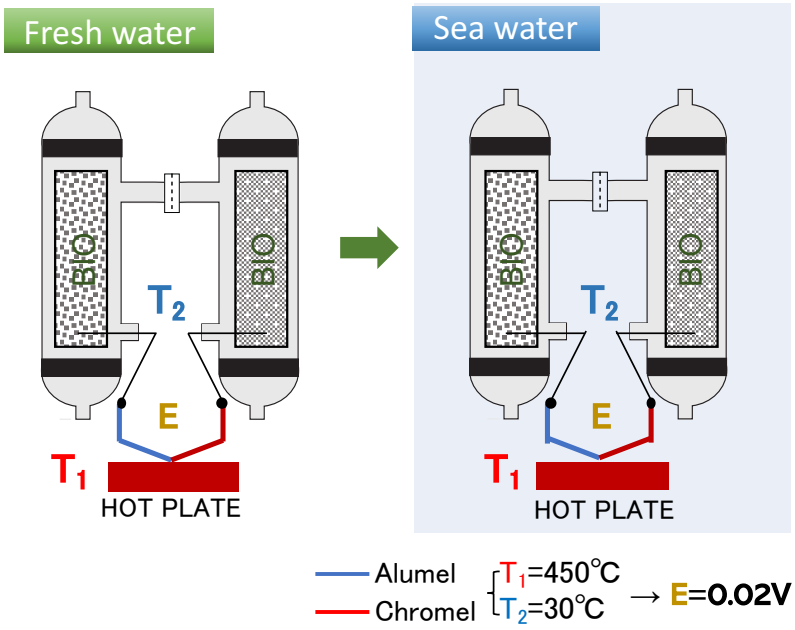

Fig. 6-1 Two MESs in batch processing mode for the future work

MES in this study was operated in batch mode. One of the disadvantages of this method is that microorganisms were peeled off from the electrodes since the fresh medium was

rapidly replenished after each run. This means that sufficient reproducibility of the experiment could not be obtained. The influence of organic matter derived from the inoculated sludge could not also be completely ignored. Therefore, operating MES in continuous mode can solve the above problems. During MES continuous operation, the deposited sludge may flow out and the influence of organic matter can be ignored. However, the flow rate must be slowed down as much as possible. For instance, it is necessary to keep the flow rate which has the same as in this study. It is one of the important factors to promote the development of a proper design MES operated in continuous mode.

The microbial community analysis of this study could only obtain the results after the operation of the MES. However, the results of microbial community analysis of the inoculated sludge are also required to explain such as the redox in MES that occurred. Therefore, when performing the same operation in the future, it is necessary to perform the microbial community analysis of the biomasses before and after the MES operation and then give explanations based on the comparison of their microbial communities.

References

Kher, M. (2015) Thermoelectric Effect? An Alternative Energy Source. *International Journal of Engineering Research* **3**: 3.

Sonal Renge, Yashika Barhaiya, Shikhar Pant, Shubham Sharma, and Shri Ramdeobaba College Of Engineering And Management, Nagpur (2017) A Review on Generation of Electricity using Peltier Module. *IJERT* **V6**: IJERTV6IS010308.

Appendix A. Publications arising from this dissertation

Peer-reviewed journals

1. *"Bioelectrical Methane Production with an Ammonium Oxidative Reaction under the No Organic Substance Condition"*, **Ha T.T Dinh**, H. Kambara, Y. Harada, S. Matsushita, Y. Aoi, T. Kindaichi, N. Ozaki, and A. Ohashi. *Microbes and Environments* 36 (2), ME21007 (IF 2.912)

2. *"Biological Methane Production coupled with Sulfur Oxidation in Microbial Electrosynthesis System without Organic Substrates"*, **Ha T.T Dinh**, H. Kambara,, S. Matsushita, Y. Aoi, T. Kindaichi, N. Ozaki, and A. Ohashi. *Journal of Environmental Sciences* , In press (IF= 5.565)

Conferences

1. **Thi Thu Ha Dinh**, Yoshiki Harada, Yoshiteru Aoi, Tomonori Kindaichi, Noriasu Ozaki, and Akiyoshi Ohashi. Methane production by using Microbial electrolysis Cell under low voltage. The 18th International Conference on Civil and Environmental Engineering. Busan, Korea, October 27-30, 2019. (Invited Speaking)

2. **Thi Thu Ha Dinh**, Yoshiteru Aoi, Tomonori Kindaichi, Noriasu Ozaki, and Akiyoshi Ohashi, Microbial methane production by using electricity. The 54th Annual Conference of Japan Society on Water Environment. Iwate, Japan March 16-18th, 2020. (Completely submitted the paper for oral presentation, but the conference has been cancelled due to the rapid spread of the coronavirus infection)